IAEA TECDOC SERIES

IAEA-TECDOC-1975

Spent Fuel Performance Assessment and Research

Final Report of a Coordinated Research Project (SPAR-IV)

IAEA
International Atomic Energy Agency

SPENT FUEL PERFORMANCE ASSESSMENT AND RESEARCH

The following States are Members of the International Atomic Energy Agency:

AFGHANISTAN
ALBANIA
ALGERIA
ANGOLA
ANTIGUA AND BARBUDA
ARGENTINA
ARMENIA
AUSTRALIA
AUSTRIA
AZERBAIJAN
BAHAMAS
BAHRAIN
BANGLADESH
BARBADOS
BELARUS
BELGIUM
BELIZE
BENIN
BOLIVIA, PLURINATIONAL STATE OF
BOSNIA AND HERZEGOVINA
BOTSWANA
BRAZIL
BRUNEI DARUSSALAM
BULGARIA
BURKINA FASO
BURUNDI
CAMBODIA
CAMEROON
CANADA
CENTRAL AFRICAN REPUBLIC
CHAD
CHILE
CHINA
COLOMBIA
COMOROS
CONGO
COSTA RICA
CÔTE D'IVOIRE
CROATIA
CUBA
CYPRUS
CZECH REPUBLIC
DEMOCRATIC REPUBLIC OF THE CONGO
DENMARK
DJIBOUTI
DOMINICA
DOMINICAN REPUBLIC
ECUADOR
EGYPT
EL SALVADOR
ERITREA
ESTONIA
ESWATINI
ETHIOPIA
FIJI
FINLAND
FRANCE
GABON
GEORGIA
GERMANY
GHANA
GREECE
GRENADA
GUATEMALA
GUYANA
HAITI
HOLY SEE
HONDURAS
HUNGARY
ICELAND
INDIA
INDONESIA
IRAN, ISLAMIC REPUBLIC OF
IRAQ
IRELAND
ISRAEL
ITALY
JAMAICA
JAPAN
JORDAN
KAZAKHSTAN
KENYA
KOREA, REPUBLIC OF
KUWAIT
KYRGYZSTAN
LAO PEOPLE'S DEMOCRATIC REPUBLIC
LATVIA
LEBANON
LESOTHO
LIBERIA
LIBYA
LIECHTENSTEIN
LITHUANIA
LUXEMBOURG
MADAGASCAR
MALAWI
MALAYSIA
MALI
MALTA
MARSHALL ISLANDS
MAURITANIA
MAURITIUS
MEXICO
MONACO
MONGOLIA
MONTENEGRO
MOROCCO
MOZAMBIQUE
MYANMAR
NAMIBIA
NEPAL
NETHERLANDS
NEW ZEALAND
NICARAGUA
NIGER
NIGERIA
NORTH MACEDONIA
NORWAY
OMAN
PAKISTAN
PALAU
PANAMA
PAPUA NEW GUINEA
PARAGUAY
PERU
PHILIPPINES
POLAND
PORTUGAL
QATAR
REPUBLIC OF MOLDOVA
ROMANIA
RUSSIAN FEDERATION
RWANDA
SAINT LUCIA
SAINT VINCENT AND THE GRENADINES
SAMOA
SAN MARINO
SAUDI ARABIA
SENEGAL
SERBIA
SEYCHELLES
SIERRA LEONE
SINGAPORE
SLOVAKIA
SLOVENIA
SOUTH AFRICA
SPAIN
SRI LANKA
SUDAN
SWEDEN
SWITZERLAND
SYRIAN ARAB REPUBLIC
TAJIKISTAN
THAILAND
TOGO
TRINIDAD AND TOBAGO
TUNISIA
TURKEY
TURKMENISTAN
UGANDA
UKRAINE
UNITED ARAB EMIRATES
UNITED KINGDOM OF GREAT BRITAIN AND NORTHERN IRELAND
UNITED REPUBLIC OF TANZANIA
UNITED STATES OF AMERICA
URUGUAY
UZBEKISTAN
VANUATU
VENEZUELA, BOLIVARIAN REPUBLIC OF
VIET NAM
YEMEN
ZAMBIA
ZIMBABWE

The Agency's Statute was approved on 23 October 1956 by the Conference on the Statute of the IAEA held at United Nations Headquarters, New York; it entered into force on 29 July 1957. The Headquarters of the Agency are situated in Vienna. Its principal objective is "to accelerate and enlarge the contribution of atomic energy to peace, health and prosperity throughout the world''.

IAEA-TECDOC-1975

SPENT FUEL PERFORMANCE ASSESSMENT AND RESEARCH

FINAL REPORT OF A COORDINATED RESEARCH PROJECT (SPAR-IV)

INTERNATIONAL ATOMIC ENERGY AGENCY
VIENNA, 2021

COPYRIGHT NOTICE

For further information on this publication, please contact:

Nuclear Fuel Cycle and Materials Section
International Atomic Energy Agency
Vienna International Centre
PO Box 100
1400 Vienna, Austria
Email: Official.Mail@iaea.org

Printed by the IAEA in Austria
September 2021

IAEA Library Cataloguing in Publication Data

Names: International Atomic Energy Agency.
Title: Spent fuel performance assessment and research : final report of a coordinated research project (SPAR-IV) / International Atomic Energy Agency.
Description: Vienna : International Atomic Energy Agency, 2021. | Series: IAEA TECDOC series, ISSN 1011–4289 ; no. 1975 | Includes bibliographical references.
Identifiers: IAEAL 21-01443 | ISBN 978-92-0-128221-7 (paperback : alk. paper) |
ISBN 978-92-0-128121-0 (pdf)
Subjects: LCSH: Radioactive waste disposal — Management. | Spent reactor fuels — Storage. | Radioactive wastes — Storage.

FOREWORD

At the end of 2020, there were 443 nuclear power plants in operation and 52 reactors under construction. To date over 400 000 tonnes of heavy metal (tHM) of spent fuel has been discharged from reactors and approximately 275 000 tHM is currently stored at various storage facilities. Although wet storage at nuclear power plant sites still dominates, the amount of spent fuel being transferred to dry storage technologies has increased significantly since 2005. For example, approximately 35% of the total fuel inventory in the United States of America is now in dry storage.

Although the licensing for the construction of geological disposal facilities is under way in Finland, France and Sweden — the first of which in Finland is not expected to be available until 2025 — for most Member States with major nuclear programmes such facilities are not expected for several decades. Spent fuel is currently accumulating at around 7000 tHM per year worldwide. The net result is that the duration of spent fuel storage has increased beyond what was originally foreseen. In order to demonstrate the safety of both spent fuel and the storage system, a good understanding of the processes that can cause deterioration is required.

To address this, the IAEA initiated the fourth phase of the Coordinated Research Project on Spent Fuel Performance Assessment and Research in 2015. The project's aim is to evaluate the performance of fuel and materials under wet and dry storage and to assess the impact of interim storage on associated spent fuel management activities (such as handling and transport). This has been achieved through evaluating surveillance and monitoring programmes of spent fuel and storage facilities; collecting and exchanging relevant experience of spent fuel storage and the impact on associated spent fuel management activities; facilitating the transfer of knowledge by documenting the technical basis for spent fuel storage; creating synergy among research projects of participating Member States; and developing the capability to assess the impact of potential deterioration mechanisms on spent fuel and storage components.

This publication is based on results obtained in the participating Member States during the project reporting period from June 2016 to June 2020. This publication provides an overview of the technical issues relating to spent fuel wet and dry storage and summarizes the objectives and major findings of the research carried out as part of the coordinated research project.

The IAEA is grateful for the contributions of the project participants and consultants who contributed to the drafting and review of this publication, in particular those who participated in each of the four phases of the project: F. Takats (Hungary) as Chair, P. Standring (United Kingdom) and A. Machiels (United States of America). The IAEA officer responsible for this publication was L. McManniman of the Division of Nuclear Fuel Cycle and Waste Technology.

EDITORIAL NOTE

This publication has been prepared from the original material as submitted by the contributors and has not been edited by the editorial staff of the IAEA. The views expressed remain the responsibility of the contributors and do not necessarily represent the views of the IAEA or its Member States.

Neither the IAEA nor its Member States assume any responsibility for consequences which may arise from the use of this publication. This publication does not address questions of responsibility, legal or otherwise, for acts or omissions on the part of any person.

The use of particular designations of countries or territories does not imply any judgement by the publisher, the IAEA, as to the legal status of such countries or territories, of their authorities and institutions or of the delimitation of their boundaries.

The mention of names of specific companies or products (whether or not indicated as registered) does not imply any intention to infringe proprietary rights, nor should it be construed as an endorsement or recommendation on the part of the IAEA.

The authors are responsible for having obtained the necessary permission for the IAEA to reproduce, translate or use material from sources already protected by copyrights.

The IAEA has no responsibility for the persistence or accuracy of URLs for external or third party Internet web sites referred to in this publication and does not guarantee that any content on such web sites is, or will remain, accurate or appropriate.

CONTENTS

1. INTRODUCTION

1.1. BACKGROUND

Regardless of whether a Member State adopts an open or closed nuclear fuel cycle policy, storage is a necessary interim step, with the necessary duration of storage related to the adopted fuel cycle policy. For those Member States opting for an open nuclear fuel cycle policy, there are currently no geological disposal facilities available for spent fuel. The first facility of its kind is planned to be operational in Finland in 2025, but it will take several decades before geological disposal facilities are operational in the majority of Member States with nuclear power programmes. For those Member States adopting a closed nuclear fuel cycle policy, the period of storage prior to reprocessing needs only be relatively short in comparison. However, the resulting spent fuels manufactured from reprocessing products are likely to require several decades of storage prior to further recycling or disposal.

The drive to increase efficiency by nuclear power plant (NPP) operators has resulted in the increase of average discharge burnups. This has the effect of reducing the overall amount of spent fuel generated for a given electrical output, but increases the demand on the performance of spent fuel storage systems. Some of the consequences of increased burnup include higher decay heats, increased cladding corrosion and higher fission gas release. The latter has implications for the fuel cladding in terms of stress and potential for defects. Increased decay heat also has implications for reprocessing and disposal, especially in geological repository systems with constraining thermal limits. This results in an increased requirement for decay storage on the surface to ensure that the thermal loadings on engineered and natural barriers are not exceeded; in some cases, the fuel may need in excess of 100 years cooling prior to disposal.

Higher burnups also have implications for zirconium alloy clad fuels as a result of increased hydrogen pickup in the cladding. Fuel drying operations and transportation represent two of the stages where hydride reorientation may occur, changing the mechanical properties of the cladding and in some cases, reducing its ductility. Research into hydriding and its effects have been common research topics throughout the SPAR Phases, and work continues into the fourth phase.

The International Atomic Energy Agency (IAEA) Spent Fuel Performance Assessment and Research (SPAR) Coordinated Research Project (CRP) is one vehicle where research and development is being discussed and reported by Member States to improve the understanding of both spent fuel and storage system behaviour over the long term.

This publication builds on a previous phase of the SPAR CRP identified as SPAR-III. In turn, the SPAR CRPs are a continuation of the previous BEFAST-I to III (BEhaviour of spent Fuel Assemblies in STorage) CRPs.

Three research coordination meetings were held during the course of the SPAR-IV CRP: the first in August 2016 in Vienna, Austria; the second in April 2018 in Seoul, Republic of Korea; and the third in October 2019 in Buenos Aires, Argentina.

1.2. OBJECTIVES

The overall objectives of the SPAR-IV CRP were to develop a technical knowledge base on long term storage of power reactor spent fuel through the evaluation of operating experience and research by participating Member States, and to extrapolate predictions of spent fuel behaviour over long periods of time. Specific research objectives included:

- Fuel and materials performance evaluation under wet and dry storage, and assessment of impact of storage on associated spent fuel management activities (such as handling and transport);

- Collection and exchange of relevant experience of spent fuel storage and the impact on associated spent fuel management activities;

- Collection of information on credible degradation mechanisms in wet and dry storage;

- Development of capability to assess the impact of potential deterioration mechanisms on spent fuel and storage components;

- Facilitation of transfer of knowledge and creation of a synergy among research projects of the participating Member States.

1.3. SCOPE

The scope of the SPAR-IV CRP focused on the long term storage of spent nuclear fuel from commercial power reactors. Whilst information may be related to the storage of experimental and research reactor fuel, there may be specificities that limit the applicability of the findings reported.

This publication, along with those previously published [1–6], provides the technical knowledge base for the long term storage of spent fuel from NPPs; i.e. the overall objective of the BEFAST and SPAR CRPs.

A summary publication describing 30 years of research in the BEFAST/SPAR programmes was issued as a TECDOC in 2019 [7].

1.4. STRUCTURE

This publication has been structured to enable quick reference to be made to the following information, as provided by the CRP participants:

- Information on spent fuel storage experience of the participating countries;

- Information and research activities relevant to wet storage;

- Information and research activities relevant to dry storage;

- Information on areas of topical interest;

- A summary of CRP research activities.

2. HISTORY OF THE BEFAST AND SPAR COORDINATED RESEARCH PROGRAMMES

The first phase of the BEFAST project (1981–1986) involved 12 organizations from 11 countries: Austria, Canada, Czechoslovakia (CSSR), Finland, Federal Republic of Germany (FRG), German Democratic Republic (GDR), Hungary, Japan, Sweden, United States of America (USA), and Union of Soviet Socialist Republics (USSR). A subsequent programme, 'BEFAST-II, Behaviour of Spent Fuel and Storage Facility Components during Long-term Storage' implemented during the years 1986–1991, involved organizations from 12 countries: Argentina, Canada, , Finland, FRG, GDR, Hungary, Italy, Republic of Korea, Japan, United Kingdom (UK), USA, and USSR. BEFAST-III, implemented during the years 1991–1996 involved 15 organizations from 12 countries: Canada, Finland, France, Germany, Hungary, Japan, Republic of Korea, Russian Federation, Slovakia, Spain, UK, and USA. There was also an observer from Sweden.

During the three BEFAST Coordinated Research Projects, the participating countries contributed their R&D results on fundamental questions of spent fuel storage. The reports from the BEFAST CRPs have been published as IAEA TECDOCs [1–3].

Towards the end of the BEFAST-III project, it became apparent that the R&D component of the project was decreasing steadily; more emphasis was being placed on the operation and implementation of storage technology. The storage technology (particularly dry storage) was undergoing a rapid evolution: new fuel and material design changes were coming on stream and target fuel burnups were steadily increasing. With the increased burnup came higher fission gas and fission product inventories, increased sheath (cladding) strains and increased cladding oxidation and hydriding. Because of all of the new parameters that surfaced during the course of BEFAST-III, a subsequent project was proposed to address the effects of these new parameters on long term storage and to determine their consequences for disposal.

The first phase of the IAEA Spent Fuel Performance Assessment and Research (SPAR) CRP (1997–2002) involved 11 organizations from 10 countries: Canada (2), France, Germany, Hungary, Japan, Republic of Korea, Russian Federation, Spain, Sweden, UK, and USA. Sweden participated in the project as an observer [4]. The second phase of the IAEA Spent Fuel Performance Assessment and Research (SPAR-II) CRP (2004–2008) involved the European Commission as well as 13 other organizations from 12 countries: Argentina, Canada, France, Germany, Hungary, Japan (2), Republic of Korea (only for a limited period), Slovakia, Spain, Sweden, UK, and USA. Sweden and the UK participated in the project as active observers [5].

The third phase of the IAEA spent fuel performance assessment and research (SPAR-III) CRP (2009–2014) involved the European Commission as well as 12 other organizations from 10 countries: Argentina, France, Germany, Hungary, Japan (2), Republic of Korea, Slovakia, Spain, Switzerland, and USA (2). Switzerland and the UK participated in the programme as active observers [6].

The fourth phase of the IAEA Spent Fuel Performance Assessment and Research (SPAR-IV) CRP (2015–2020) has involved 13 organizations from 10 countries: Argentina (2), France, Hungary, Republic of Korea, Slovakia, Spain, Switzerland, UK (2), Ukraine and USA (2). Organizations from Germany (2), Switzerland, USA (2), and the European Commission participated in the programme as active observers.

The major topics for both wet and dry storage during all seven CRPs are summarized in Table 1. It provides a record of the shift in emphasis between the various phases of the project between 1981 and 2020.

TABLE 1: RESEARCH SUBJECTS IN THE CRPS

	B-I	B-II	B-III	SPAR I	SPAR-II	SPAR-III	SPAR-IV
Long term behaviour							
Material aspects	X			X	X	X	X
Degradation mechanisms and models	X	X		X	X	X	X
Validation		X	X	X	X	X	X
Surveillance							
Monitoring			X	X	X	X	X
Fuel conditions		X	X	X	X	X	X
Different reactor types		X	X	X	X	X	X
Facilities and operation							
Capacity enhancement		X					
Changing modes Wet – Dry		X	X	X	X		X
Handling of heavily damaged fuel		X	X		X		
System performance	X	X	X	X	X		X

A complementary CRP 'Demonstrating performance of spent fuel and related storage system components during very long term storage' (DEMO) ran from 2013 to 2016 [8]. This CRP, funded by the Peaceful Uses Initiative (PUI), was mainly focused on dry storage conditions and looked to supplement the technical bases from management licenses for spent light water reactor (LWR) fuel.

3. EXPERIENCE AND STATUS OF NATIONAL SPENT FUEL MANAGEMENT STRATEGIES AND PROGRAMMES OF SPAR PARTICIPANTS

3.1. ARGENTINA

There are three operational NPPs in Argentina. The first one, Atucha-1 (CNA-1), a SIEMENS-KWU pressurized heavy water reactor (PHWR) prototype, has been in operation since 1974. Embalse (CNE) is a Canada deuterium uranium (CANDU) 600 pressure tube type Canadian reactor that started operations in 1984. Atucha-2 (CNA-2) is a Siemens design NPP, a larger version of CNA-1 that entered commercial operation in May 2016.

In 2010, an agreement was signed to refurbish the Embalse plant, increasing its power by around 7% and extending its operational lifetime by 30 years. The reactor was shut down for the main work in January 2016; it was upgraded and returned to service in January 2019.

CNA-1 originally operated with natural uranium fuel, but this was gradually increased to slightly enriched uranium (0.85% U-235) between 1995 and 2000. This modification enabled an increase in burnup by almost a factor of two to 11.3 GWd/tU, reducing the frequency of refuelling at full power from 1.29 to 0.72 fuel elements per day and, subsequently, significantly reducing the number of spent fuel assemblies (SFAs) generated. The fuel element is composed of 36 fuel rods and has a total length of ~6 m. The spent fuel elements are initially stored in pools (two houses), with a dry storage facility (ASECQ-CNA) under construction at the site. It will consist of a vault in a new building annexed to House I.

At CNA-2, spent fuel is wet stored, pending definition of a dry storage alternative.

At CNE, the fuel bundles are composed of 37 fuel rods of 0.5 m length (standard CANDU fuel bundles). SFAs are initially stored in a pool of Atomic Energy of Canada Limited (AECL) design with the capacity to store 45 144 spent fuel bundles, equivalent to approximately the quantity generated over ten years at maximum power. Dry storage at the site was implemented in 1993 to cope with the spent fuel storage demand up to the end of the operative life of CNE.

In Argentina, responsibility for the spent fuel from NPPs is with the operating organization until permanent shutdown of the plant. Post shutdown, the responsibility will be transferred to the Government, through the National Atomic Energy Commission (CNEA).

3.1.1. Wet storage experience

3.1.1.1. Atucha

The CNA-1 pool differs from most AR pools in that it has two levels, with the deeper level, or level one, the first to be filled. The fuel is stored suspended vertically from a fixing. The fixings of the Atucha-2 at-reactor (AR) pool are a modification to the original design, allowing for the pool storage capacity to be increased. There are two types of fixings:

- Singles have 28 hangers, with six SFAs suspended from each one; each single capacity fixing can accommodate up to 168 SFAs;
- Doubles have 56 hangers, each with five fuel assemblies suspended. Each double fixing can accommodate up to 280 SFAs.

At CNA-2, spent fuel is transferred to the pools, which have a storage capacity equivalent to ten years of normal operation.

3.1.1.2. Embalse

The spent fuel bundles remain in wet storage for at least six years to allow for cooling and radioactive decay. The AR storage facility is based on a standard CANDU NPP design.

3.1.2. Dry storage experience

There are two away from reactor (AFR) dry storage facilities for spent fuel in Argentina. The first one is located at the site of Embalse NPP (ASECQ-CNE) and has operated since the early 1990s. The other is currently under construction at the site of the Atucha 1 NPP (ASECQ-CNA-1).

The ASECQ-CNA-1 dry storage facility consists of a concrete building inside which up to 2754 SFAs can be accommodated in 306 vertically suspended units, each containing nine assemblies. The facility is designed for an operational life of at least 80 years, and a programme is currently running in order to ensure that the structural components will not suffer any degradation that would hamper the safety functions during this time.

The ASECQ-CNE dry storage facility consists an array of concrete silos (canisters) with a carbon steel lining. Inside each silo, nine steel, sealed baskets are stacked, each one containing 60 bundles. The facility was intended to hold spent fuel for a period of a few decades, but as a decision has not yet been taken regarding final disposition, an extension of storage time will be required. Considering that CNE is undergoing a life extension process, the storage facility is expected to be operating for a period close to at least a century.

The ASECQ-CNE dry storage facility has been in service for ~30 years and the operating organization had established an ageing management programme (AMP), which was renewed after the decision regarding the NPP life extension. The surveillance plan includes monitoring of the condition of the silo, steel liner, and concrete structure. To supplement this ongoing monitoring programme, there is periodic measurement of aerosols, noble gas content and internal moisture of selected silos. Additionally, there is external monitoring of the silos using thermoluminescent dosimeters to detect any changes in radiological conditions. To date, no abnormalities have been observed.

3.2. FRANCE

Management of spent fuel from NPPs in France is based on a recycling strategy. Most of the spent fuel produced comes from the operation of the 58 pressurized water reactors[1] (PWRs) operated by the French utility Électricité de France (EDF). This fleet includes 34 NPPs of 900 MW(e), 20 NPPs of 1300 MW(e) and 4 NPPs of 1450 MW(e) located across 19 nuclear power generation sites. Construction of the European pressurized water reactor (EPR) (1650 MW(e)) at the Flamanville site is in its final stage.

The fresh fuel used in these reactors consist of either uranium oxide (UOX), slightly enriched natural uranium (ENU), or uranium and plutonium mixed oxide (MOX) that are fabricated in the Orano MELOX plant. The plutonium used is derived from the reprocessing of spent ENU fuels in Orano's recycling facilities at La Hague. MOX fuels are used in 22 of the 900 MW(e) reactors. The fuel used in France may also consist of recycled uranium oxide (enriched reprocessed uranium, or ERU) from ENU fuel reprocessing. However, this type of fuel, which is licensed in the four units of the Cruas NPP, has not been used since 2013. EDF plans to resume its use in the next few years.

[1] As of October 2019.

By adopting a recycling strategy, spent fuels (ENU, MOX and ERU) arising from NPPs are not intended for direct disposal. The long-term industrial management of spent MOX and ERU fuel currently favoured by EDF is recycling in fast neutron reactors; spent MOX and ERU fuel is currently in wet storage awaiting recycling.

This choice was confirmed in France by a law relating to the sustainable management of radioactive materials and waste that establishes the guidelines to be respected by the national radioactive materials and waste management plan [9]. This management plan states that:

> "*reduction of the quantity and toxicity of radioactive waste is sought in particular by the treatment of spent fuel and by treating and conditioning radioactive wastes*" [9].

After unloading from the reactors and storage in the AR pools, spent fuel is transported to the Orano recycling facility at La Hague, where it is stored in one of the four pools currently in operation. The minimum cooling time in AR pools to allow for sufficient decay heat reduction to meet transportation limits is approximately 18 months for spent ENU and ERU fuel, and about 30 months for spent MOX fuel. According to transport licenses currently in force in France, the maximum thermal power of a SFA that can be transported on public roads is 6 kW; in practice it is dependent on the transport packaging model used.

The analysis of the nuclear fuel cycle operation (manufacture, use in reactor and subsequent recycling) is regularly undertaken by the Autorité de Sûreté Nucléair (ASN) and reviewed by the Institut de Radioprotection et de Sûreté Nucléair (IRSN). The particular objective of this analysis, is to ensure the adequacy of the storage and treatment capacities of radioactive materials and waste. The assessments carried out in this context by EDF in 2016 concluded that existing spent fuel pool (SFP) storage capacity may be saturated by 2030.

In 2017, EDF submitted the safety options file to ASN for a new centralized storage pool system to increase spent fuel storage capacity. The storage pool is designed for 21 000 fuel assemblies, corresponding to 10 000 tHM, and for 100 years operation. In December 2018, IRSN issued their review and questions on the EDF pool storage project. In principle, the design and safety options were found to be satisfactory. The report includes comments, some remarks and request for additional justification, for example regarding pool containment inspection and repair in the long term. EDF plans to submit the application for authorization in 2022 to construct this facility, with a target to commence commissioning by 2034.

3.2.1. Wet storage experience

Wet storage is the selected option for all commercial spent fuel storage facilities in France. The safety records covering the last 40 years of operations are very good, with no degradation or rupture of spent fuel in pools having been observed.

Two main wet storage concepts are used in France:

- Storage of fuel in racks assembled and placed at the bottom of the pool in a vertical position. In this case, for the radiation protection of operators, the height of the water should take into account the handling of the fuel above the racks. This design is the one used in EDF's NPP pools;

- Storage of fuels in baskets in vertical position. The filling of the baskets is carried out in a pit, deeper than the storage areas (to ensure radiation protection during the handling of fuel). The storage areas are of reduced depth because only the baskets are handled at low height above the bottom of the pool (no handling over stored fuel). This design is used at Orano's La Hague facility.

3.2.2. Dry storage experience

Currently there is no dry storage of spent fuel from power reactors in France.

3.3. GERMANY

Germany has transitioned from its original closed cycle policy to an open cycle following the moratorium on reprocessing passed by the German government in 2002. From 2005 on, transportation to reprocessing was no longer permitted, leading to the necessity of AFR on reactor site (AFR-RS) storage. After the Fukushima accident, a nuclear phase out decision was taken in 2011 that included the immediate shutdown of six NPPs; for the remaining NPPs shutdown dates were put into the German Atomic Energy Act [10].

There are in total 29 NPPs in Germany (20 PWR, 9 BWR) of which 22 (15 PWR, 5 BWR) are under decommissioning, one (BWR) in permanent shut down, and the remaining six (5 PWR, 1 BWR) scheduled to close by the end of 2021 (Grohnde, Grundremmingen C, Brokdorf) and the end of 2022 (Neckarwestheim II, Isar 2, Emsland) respectively as the use of nuclear power for electricity generation is phased out. With the exception of Obrigheim, each NPP has its own on-site dry storage facility utilizing dual purpose casks (DPCs).

There are two centralized storage facilities in Ahaus and Gorleben used for storing spent fuel and high-level waste from reprocessing. There is also the Storage Facility North (ZLN) in Rubenow that is mainly used for the storage of WWER fuel and radioactive waste from the decommissioned former East German NPPs Greifswald (WWER-440) and Rheinsberg (WWER-70).

Since 1 July 2005, reprocessing of fissile material in spent fuel has been prohibited in accordance with an amendment of the German Atomic Energy Act. Therefore, only direct disposal of spent fuel as radioactive waste is permissible today in Germany [11]. As there is no repository available for spent fuel at present, it has to be stored.

On 16 June 2017, the Act on the Reorganisation of Responsibility in Nuclear Waste Management entered into force [12]. The Act has reorganised the responsibility for nuclear waste management. The operators of the NPPs will continue to be responsible for the entire management and financing of decommissioning, dismantling and proper packaging of the radioactive waste. However, the responsibility for action in the fields of storage and disposal lies with the German State. The operators have transferred financial means into a public-law fund in the legal form of a foundation, which provides funds for the waste management. In return, the management of spent fuel and radioactive waste storage facilities[2] has been transferred to a publicly owned storage company (Gesellschaft für Zwischenlagerung mbH (BGZ)) [11], with the exception of ZLN, which is managed by Entsorgungswerk für Nuklearanlagen (EWN).

According to the Site Selection Act, a disposal site will be selected by 2031, with disposal of spent fuel and high-level waste expected to have started by 2050.

3.3.1. Wet storage experience

Since the beginning of the 1970s, spent nuclear fuel (SNF) was stored in the NPP pools. Due to changes in fuel cycle policy, fuel was no longer shipped for reprocessing so there was a need

[2] BGZ took over the management of spent fuel and high level waste (HLW) storage facilities as of 1 January 2019, and low and intermediate level waste facilities as of 1 January 2020.

for increased storage capabilities at the NPPs; this was initially achieved by the introduction of higher density racks in the storage pools in most NPPs around end of the 1980s. A centralized wet storage facility was considered as a further measure, but not implemented.

Wet storage experience in Germany is good, with some fuel assemblies stored wet for up to 40 years. As of December 2018, 9086 FAs (2755 tHM) were stored at NPP pools. Except for one site, all intact fuel of the eight reactors shut down after 2011 has been transitioned into dry storage.

3.3.2. Dry storage experience

The introduction of dry storage in metallic casks in Germany occurred in the 1990s. Spent fuel and vitrified HLW from reprocessing of fuel assemblies are kept in dry storage using DPCs. The technical concept and safety considerations for dry storage are addressed in the recommendations of the Entsorgungskommission (ESK) [13]. These recommendations are considered by the German licensing authority and are implemented by site-specific licenses, which are currently limited to 40 years, starting from the first emplacement of a DPC.

The German storage concept envisages that on-site dry storage is preferred to avoid transportation of spent fuel until it can be conditioned to meet the requirements for disposal.

The spent fuel is stored at 12 on-site dry storage facilities near the NPPs and at central storage facilities in Ahaus, Gorleben, and Rubenow. DPCs loaded with spent fuel are emplaced in these facilities.

The Gorleben storage facility and the on-site facility at Biblis are also licensed for the storage of HLW canisters in addition to spent LWR fuel. In total, 108 casks with vitrified HLW waste, transferred from France, are already stored at the Gorleben facility. Mainly CASTOR HAW 20/28 CG, CASTOR HAW 28M, and TN 85 cask types are in use.

According to its licence, the Ahaus facility may store spent fuel from various German NPPs. In addition, the Ahaus facility is also licensed as a central storage facility for the storage of the CASTOR THTR/AVR (Thorium High-Temperature Reactor, Hamm-Uentrop) and CASTOR MTR 2 (Material Testing Reactor) cask types.

Spent fuel from the WWER reactors in Rheinsberg and Greifswald is stored in CASTOR 440/84 and CASTOR KRB-MOX casks at the ZLN. Fuel rods from the compact sodium-cooled NPP (KNK II) in Karlsruhe and the research vessel ‘Otto Hahn’ are also stored in CASTOR KNK casks at this facility. Additionally, HLW glass canisters with high level waste from the Karlsruhe reprocessing plant (WAK) are stored in CASTOR HAW 20/28 CG casks at the ZLN site.

As more than 1000 casks have been loaded and stored, an extensive experience in loading, processing, and dry storage of DPCs, especially of the CASTOR V cask types loaded with spent fuel from German NPPs, has been gained. The leak tightness of each loaded cask during the storage period is verified by continuous pressure monitoring of the space between the primary and secondary lids. During the operating time from 1995 up to now, no out-of-allowable-limit pressure drops in the inter-lid space due to increased leakage rates of the lid sealing system have been detected; the only alarm signals detected have been false alarms to indicate a faulty switch.

In Germany, a periodic safety review (PSR) of storage facilities is required every ten years after the start of operations to evaluate and continuously improve the safety of the facility. In March

2014, recommendations for the PSR were published by the ESK as Guidelines for Performance of Periodic Safety Review and on Technical Ageing Management for Storage Facilities for Spent Fuel and Heat-Generating Radioactive Waste [14]. These recommendations consider the experience from a prior multi-year testing phase review for two selected storage facilities (Gorleben and Lingen).

In the meantime, there is consensus that extended storage beyond 40 years will have to be considered in the mid-term future because a repository will not be operable when current interim storage licenses expire in the early 2030s. According to a discussion paper on the extended storage of spent fuel and other heat-generating radioactive waste, the ESK likewise expects temporary dry storage for periods up to 100 years [15]. The ESK advised that storage duration should be limited to the absolutely necessary period and, as stipulated in § 6(5) of the German Atomic Energy Act, a license may only be renewed on imperative grounds and after this issue has been discussed in the German parliament (Bundestag).

From the technical point of view, extended storage leads to the need of additional safety demonstrations over the significantly longer storage periods that are under consideration. R&D programmes on ageing effects of containers, materials and components (e.g. metal seals and fuel assemblies) have already been launched to address relevant knowledge and data gaps. Inspections and PSRs will provide additional valuable data.

3.4. HUNGARY

The Parliament adopted the new National Policy (hereinafter referred to as 'Policy') by a resolution in 2015, formulating the policies for the back-end of the fuel cycle, the management of radioactive waste and the decommissioning of nuclear facilities.

Regarding the back-end of the fuel cycle, a final decision has not yet been made; rather the principle of 'do and see' is being applied that allows for the possibility of following domestic and international developments, with technological advancements to be integrated into the Policy as necessary. For the calculations, a reference scenario of an open fuel cycle has been selected, which includes the direct, domestic disposal of spent fuel from the NPP.

The current situation in Hungary shows very little change since the publication of Ref. [6]. About 50% of the country's electricity production is provided by the 4 units of Paks NPP, which has been running with a 15-month cycle since 2015. Preparations for the expansion of Paks with two further units, each of 1200 MW(e) capacity, are in progress.

3.4.1. Wet storage experience

Each unit at Paks NPP has an AR pool, with the first becoming operational in 1982. A three-year storage period for SFAs was envisaged during the original design of the NPP, after which they would have been transported to the Soviet Union for reprocessing. Consequently, spent fuel racks were designed with a capacity of 349 SFAs, achieved by using a subcritical lattice structure without built-in absorbers.

Once it became known that the spent fuel needed a longer cooling period (at least 5 years), the storage pools were reconfigured to provide increased capacity by the installation of compact storage racks. At each of the four units, the new compact storage racks provide 706 cells for fuel assemblies, of which 650 cells are normal compact storage cells and 56 cells are for hermetic casings. The SFAs are placed into a 3050 mm long, hexagonal stainless-steel absorber tube with a 3 mm wall thickness, containing 1.05–1.25% natural boron. The rack structure holding the absorber tubes is made of stainless steel.

In the case of an emergency, spent fuel can be unloaded from the reactor and placed into a second so-called 'emergency rack'. This reserve rack, which is erected on top of the normal rack, is normally kept in the Reactor Hall.

3.4.2. Dry storage experience

A modular vault dry storage (MVDS) system operates at the Paks NPP site. Its construction started in March 1995. The facility, which had an original design lifetime of 50 years, was commissioned in 1997 and the first 450 assemblies, filling one vault, were loaded in the same year. Successive vaults were constructed during the subsequent years.

A total of 9550 assemblies (approx. 1150 tHM) were in storage at the end of 2019. The MVDS has 24 vaults constructed; construction of modules 25–28 began in 2020. The storage capacity of the newer vaults has been increased by reducing the spacing, benefitting from the reduced heat load of the old assemblies and improved calculations.

3.5. REPUBLIC OF KOREA

The Republic of Korea has a total of 26 NPPs across four sites. Of these, 24 NPPs (21 PWR, 3 PHWR) are in operation, and 2 NPPs (1 PWR, 1 PHWR) have been permanently shut down. Four new PWR type NPPs are currently under construction[3].

The Public Engagement Commission on Spent nuclear fuel management (PECOS) started in 2014 to identify a strategy for managing spent fuel and published a recommendation to the government in 2016. The recommendation consisted of three parts:

- AR dry storage by the utility until a decision is taken on a disposal site;
- A centralized dry storage developed and operated by a governmental organization from 2035 at the identified disposal site;
- Final geological disposal at the centralized dry storage site after 2053.

A committee for the review of the spent nuclear fuel management policy was launched in May 2019 in order to revaluate the PECOS recommendation against the changed energy resource plan and resulting changes to waste predictions and to collect public opinions. The agenda for the review process was completed in August 2019, with opinion gathering from experts ongoing until February 2020.

The first stage of the review included a civic participation group of 549 people deliberating on:

- The principles of high-level waste management;
- Scenarios and options for spent fuel management;
- A decision-making process for the national policy;
- A siting process for spent fuel management facilities;
- Principles and methods of regional support.

The second stage will be focused on the construction of AR facilities at each NPP site, before current ones become saturated.

Regardless of the outcome, dry storage will be required to manage spent fuel arisings in the interim due to the exhaustion of current storage capacity.

[3] Data taken from IAEA PRIS database, December 2020.

3.5.1. Wet storage experience

Wet storage of PWR spent fuel in AR pools is the only current option available, while for PHWR spent fuel it can be transitioned from the AR pools to dry storage. As has been the case in other countries, re-racking has been undertaken to increase wet storage capacity, but limits are being reached and capacity is reaching saturation. Table 2 shows the capacity status of AR storage for all NPP sites as of August 2019.

TABLE 2: SATURATION OF AR WET STORAGE (AS OF AUGUST 2019)

NPP Site	Type	Number of Units	Pool Capacity used, (%)
Kori & Shin Kori	PWR	8	77
Hanbit	PWR	6	71
Hanul	PWR	6	80
Shin Wolsong	PWR	2	37
Wolsong	PHWR	4	82

3.5.2. Dry storage experience

Only PHWR spent fuel is currently stored dry.

Presently, there are 300 concrete silo units (162 000 bundles) and seven MACSTOR/KN-400 units (168 000 bundles) at Wolsong. Each concrete silo can accommodate nine baskets with 60 CANDU spent fuel bundles in each basket, giving a total of 540 bundles per silo. Each MACSTOR/KN-400 can accommodate 40 canisters, each storing 10 baskets.

Due to the high accumulation rate of spent PHWR fuel, the dry storage capacity requires expansion. An additional seven MACSTOR modules were given regulatory approval for construction starting in January 2020 [16].

Dry storage of PWR spent fuel may become necessary as SFP capacities are reaching exhaustion.

3.6. SLOVAKIA

Slovakia has two sites with four operational WWER-440 type units, three units are undergoing decommissioning and two new units are under construction. At the Jaslovské Bohunice site there are two operational units (EBO-3,4) and three decommissioned units (A-1, EBO-1,2). All the SFAs from the decommissioned units were removed; A-1 fuel was transported to the Russian Federation, while EBO-1,2 fuel is stored in the interim spent fuel storage facility (ISFS) at Jaslovské Bohunice. At the Mochovce site there are two operational units (EMO-1,2) and two units under construction (EMO-3,4, operation expected in 2021 and 2022 respectively).

The basic policy for spent fuel and radioactive waste management is derived from the Slovak Government resolutions 328/2008, 26/2014 and 387/2015; they detail the strategy for the back-end of the fuel cycle. Spent fuel from all units is stored short term in an AR pool for at least three years before transfer to the ISFS at the Jaslovské Bohunice site for long term storage. Currently there is no ISFS at Mochovce and spent fuel from units 1 and 2 is transported to Jaslovské Bohunice.

The longer term goal is to construct a deep geological repository for spent fuel and highly active waste. This aside, the Slovak policy does not exclude an international or regional solution and follows developments in spent fuel management.

3.6.1. Wet storage experience

Away from reactor (AFR) storage for the WWER units has been available in the ISFS since 1987. After removal from the reactor core, spent fuel is stored the AR pool for at least three years. After this period, it is transported from the AR pool to the ISFS at Jaslovské Bohunice for long term storage. This interim storage facility is of Russian Federation design and utilizes the wet storage principle, with four pools — three operational and one reserve.

In the period 1997–1999, the ISFS was refurbished and seismically upgraded. The introduction of new compact racks within the storage baskets increased the storage capacity by 2.8 times, resulting in a maximum capacity of 14 112 fuel assemblies. As of October 2019, the ISFS has sufficient free storage capacity until around 2022.

The spent fuel is stored in compact racks each containing 48 WWER fuel assemblies, while the old baskets had a capacity of 30 fuel assemblies. The compact racks' structural materials are 08Ch18N10T type stainless steel and AISI 304 stainless steel with a minimum 1.1% boron content (ATABOR).

The pools are filled with demineralized water.

The safety records covering more than 30 years of operations are very good, with no degradation or rupture of spent fuel in pool storage observed, as well as no storage equipment issues being encountered.

3.6.2. Dry storage experience

Currently there is no dry storage of SNF in Slovakia. Commissioning of a dry ISFSF at the Jaslovské Bohunice is planned in 2022.

3.7. SPAIN

There are seven operating NPPs at five sites in Spain:

- Five Westinghouse-PWRs: Almaraz I and II, Asco I and II, Vandellos II;
- One GE-BWR NPP: Cofrentes;
- One KWU-PWR NPP: Trillo.

Two other NPPs are currently undergoing decommissioning and dismantling; a small one-loop Westinghouse-PWR (Jose Cabrera) in the final stages of dismantling, and a GE-BWR (Santa María de Garoña), which is preparing for pool emptying in order to commence dismantling operations. Another NPP, a Gas Cooled Reactor (GCR), is in a latency period pending the final dismantling to be performed by 2030 (Vandellós I).

The spent fuel managed in Spain comes from the operation of these reactors, with the exception of Vandellos I where all fuel was reprocessed. As of December 2019, more than 16 300 SFAs have been generated.

The strategy for SNF management in Spain is established in the General Radioactive Waste Plan (GRWP), of which the 6th Revision (dated 2006) is in force [17]. This considers the development of a Centralized Temporary Storage (CTS) facility to gather all the SNF generated at a site to be selected by the Spanish Government. In July 2018, the Government put the licensing process on hold for the facility, which was expected to be built in Villar de Cañas, in

order to review the GRWP. The review forms the basis of the 7th Revision of the GRWP, which is awaiting governmental approval. Within this update, an NPP shutdown schedule was agreed between Enresa and the Spanish utilities, which will be reflected in the radioactive waste inventories (including SNF) to be considered. The CTS capacity will be ~7 500 tU, covering an average of 46 years of NPP operations. The design life for the CTS facility is 100 years and will bridge the gap between shutdown of the NPPs and implementation of deep geological disposal.

Due to the delay in commissioning of the centralized storage facility, pool saturation and a lack of further re-racking possibilities, most NPPs have established specific away from reactor on-site (AFR-OS) dry storage facilities.

3.7.1. Wet storage experience

Spent fuel has been wet stored in Spain since the 1970s. In view of the forthcoming saturation of the capacity, pools were progressively re-racked during the 1990s and 2000s. The last NPP to be re-racked will be Vandellos II in 2020–21. All wet fuel storage is AR, and storage experience has been good.

There were minor issues with top nozzle degradation in early manufactured PWR fuel and, in one BWR, one fuel element fell off into the pool rack in 2009 while being inspected (INES-1 event). Moreover, there were some issues concerning rack neutron absorber degradation. All fuel assemblies in storage have been moved at least once. As of December 2019, around 14 400 SFAs were stored at NPP pools.

3.7.2. Dry storage experience

The status of dry storage facilities, as of December 2019:

- 32 DPT and 2 ENUN 32P dual purpose casks (736 PWR fuel assemblies) are housed in the dry storage facility at Trillo NPP site, commissioned in 2002.
- 12 HI-STORM 100Z concrete storage systems (377 PWR fuel assemblies) are placed in the dry storage facility at Jose Cabrera NPP site, commissioned in 2009.
- 21 HI-STORM 100 concrete storage systems (672 PWR fuel assemblies) are placed in the dry storage facility at Ascó NPP site, commissioned in 2013.
- 2 ENUN 32P dual purpose cask (64 PWR fuel assemblies) are emplaced in the dry storage facility at Almaraz NPP site, commissioned in 2018.

Dry storage facilities have also been built at Santa María de Garoña NPP site (awaiting commissioning), and at Cofrentes NPP site (awaiting licensing).

The dual-purpose (storage and transport) ENSA-DPT metal casks at the Trillo NPP can store 21 PWR fuel assemblies with a maximum burnup of 49 GWd/tHM, 4% initial enrichment and a minimum of 9 years of cooling, in a helium environment. The initial cask license is for 20 years (storage mode) and 5 years (for transport). The first loading was in 2002, meaning that renewal of the storage license needs to be completed by 2022. The facility has a total capacity of 80 casks. Currently, the facility has been re-licensed to include a different dual-purpose cask, the ENSA ENUN 32P that can store and transport 32 fuel assemblies with a burnup up to 58 GWd/tHM, 4.75% initial enrichment and minimum 7.6 years of cooling. Two casks of this type are stored at the facility as of December 2019.

At the Jose Cabrera NPP, welded canister and steel-lined concrete overpack storage systems (HI–STORM) have been designed, licensed, and manufactured to store 32 fuel assemblies. The total spent fuel inventory has been loaded into 12 HI-STORM systems to allow for fully

dismantling of the NPP. A total of 377 fuel assemblies including 26 classified as damaged, are stored at the site. The system allows for storage and transport of fuel with burnup <45 GWd/tHM and low initial enrichment. After three years of cooling, fuel from the final cores was placed into dry storage in 2009.

For the Asco I and II NPPs, the HI-STORM storage system has also been used. As of December 2019, 21 HI–STORM modules holding 32 fuel assemblies each have been loaded. The storage license allows for fuel with burnup up to 55 GWd/tHM, 5% initial enrichment. However, in order to comply with the transport license of the associated HI-STAR transport system, the storage containers have been loading fuel with burnup <45 GWd/tHM. The transport license is now being reviewed to include higher burnup fuel (up to 55 GWd/tHM) in order to enable storage and subsequent transportation of high burnup fuel assemblies.

At the Santa María de Garoña site, a metal dual-purpose cask, the ENSA-ENUN 52B, was licensed to store up to 52 BWR fuel assemblies of relatively low burnup and high cooling times. Five casks were manufactured to allow for the continuation of NPP operation and a dry storage facility was constructed. Because the NPP was shut down in 2017, the dry storage facility, including the potential for a new type of cask, needs to be reassessed in order to accommodate the full spent fuel inventory in the pool. This will also allow for full dismantling of the NPP.

At the Almaraz NPP, a dry storage facility was commissioned in 2018 utilizing ENSA-ENUN 32P casks that can store 32 PWR fuel assemblies; two casks have been loaded as of December 2019. This cask is similar to the one for the Trillo NPP, with a different basket to hold Westinghouse-like 17×17 fuel assemblies. The current burnup limit for storage is 65 GWd/tHM, but only 45 GWd/tHM for transport. As it is mandatory in Spain to comply with the contents of both licenses, fuel with burnup <45 GWd/tHM will be stored initially, with the cask being relicensed in the future to transport higher burnup fuel.

At the Cofrentes NPP, a dry storage facility is being licensed. The cask expected for this facility is the HI-STAR 150 that can store up to 52 BWR fuel assemblies. The cask is currently in the licensing process for storage and transportation.

The design of the presently on-hold centralized temporary storage facility (CTS) is based on a modular vault storage system. It includes a dry storage facility that is expected to be available in 2026, while full commissioning is expected in 2028 [17].

3.8. SWITZERLAND

In Switzerland, spent fuel arising from the operation of the five NPPs (on four sites: Beznau 1 and 2, Gösgen, Leibstadt and Mühleberg) has to be stored for several decades. Before 2006, spent fuel generated in Switzerland (1139 tHM) was transported abroad for reprocessing. However, the Swiss government foreclosed (from 2003 provisionally, from 2017 definitively) the reprocessing of spent fuel [18], so spent fuel will go to geological disposal, following a period of storage and a conditioning process. After the Fukushima accident in 2011, Switzerland decided to phase out nuclear energy using a stepwise strategy. All utilities plan to operate for a minimum of 50 years, upon the fulfilment of safety requirements, with the exception of Mühleberg BWR that ceased operation at the end of 2019 (after 47 years of operation).

The SFAs are currently stored in pools at the NPP sites and, after a period of decay cooling, are transferred to DPCs[4] for transport to centralised dry AFR facilities. Gösgen NPP also has an AFR pool. These fuels come from a wide range of LWR fuel types (UO_2 and MOX) produced

[4] In Switzerland, the term used for DPCs is Transport/Storage Casks, or TSCs.

by several fuel vendors, and so factors such as cladding materials, initial enrichment and operational histories vary. Much of the spent fuel is characterized by a very high burnup at discharge (60–70 GWd/tHM).

The Nationale Genossenschaft für die Lagerung radioaktiver Abfälle (Nagra), founded in 1972 by all Swiss producers of radioactive waste, has proposed a deep geological repository as a solution for the management of radioactive waste [19]. Strict requirements relating to long term safety aspects are to be ensured after the disposal of the waste, to cover a temporal spectrum of 1 million years, which implies the development of a process of qualification using appropriate research programmes to reasonably reduce the level of uncertainties in the characterisation of the spent fuel. Other relevant requirements also apply to predisposal activities, such as extended storage and subsequent transport of spent fuel, and in particular for the spent fuel encapsulation facility and related unloading/loading and handling operations from the DPCs into final disposal canisters (FDCs).

3.8.1. Wet storage experience

In Switzerland, five AR pools are currently in operation at the four NPP sites. Moreover, an AFR pool that was commissioned in 2008 operates at the Gösgen NPP. The Gösgen pool has a storage capacity of 1056 SFAs and has a 1.25 MW heat removal capability. It was the first AFR wet storage facility to be designed with a passive cooling capability in normal operation and in the case of accidents. It was also designed with considerations of scenarios including an accidental airplane crash, and seismic events, and to be standalone once the NPP permanently shuts down. To minimize induced vibrations as a result of an airplane crash and earthquake, damping units have been installed below the fuel pool.

The spent fuel inventory in the storage pools of the NPPs as of the end of 2016 is as follows: [20]:

- Beznau NPP: 712 SFAs;
- Mühleberg NPP: 376 SFAs;
- Gösgen NPP: 589 SFAs;
- Leibstadt NPP: 1768 SFAs.

3.8.2. Dry storage experience

There are two operational dry storage facilities in Switzerland.

A centralized storage facility, ZWILAG located at Würenlingen, has been in operation since 2001 and was designed to accommodate 200 DPCs for vitrified HLW and spent fuel (TN97, TN52, TN24BH, TN81 and CASTOR). At the end of 2016, ZWILAG contained 29 fully loaded DPCs with a total of 2236 spent fuel assemblies of the BWR type and four fully loaded DPCs with a total of 148 spent fuel assemblies of the PWR type. An additional DPC contains 349 fuel assemblies from the DIORIT research reactor operating at the Paul Scherrer Institute (PSI). The facility has also access to an airplane crash resistant ‘Hot Cell’ to inspect or re-work casks if needed. Due to weight limitations, the Mühleberg NPP uses a small capacity transportation cask TN12 to transfer used fuel assemblies to ZWILAG. These assemblies are reloaded into a higher capacity storage cask within the ’Hot Cell’. Given the permanent shutdown of the Mühleberg NPP in 2019, less transport intensive solutions are being evaluated.

ZWIBEZ, located at Beznau NPP, started operations in 2008. The storage hall for dry storage of spent fuel and vitrified HLW can accommodate up to 48 DPCs. At the end of 2016, ZWIBEZ contained 8 DPCs with a total of 296 spent fuel assemblies.

3.9. UKRAINE

There are 15 operational NPPs in Ukraine (2 WWER-440 and 13 WWER-1000) at four sites, supplying around 60% of Ukraine's electricity. In addition, there are three RBMK-1000 reactors under decommissioning at Chernobyl NPP (excluding Unit 4, which was destroyed by the accident in 1986 and is now in new safe confinement).

Ukraine is currently adopting a deferred decision on the fate of spent fuel, with all fuel to be transitioned to dry storage in the long term. Previously, fuel from Rivne, Khmelnitsky and South Ukrainian NPPs has been returned to the Russian Federation for reprocessing.

Interim spent fuel storage (ISFS) facilities are located in Zaporizhye NPP and at Chernobyl. A centralised spent fuel storage facility (CSFSF) is under construction in the Chernobyl Exclusion zone and is designed for fuel from both the WWER-440 and WWER-1000 reactors (excluding Zaporizhye). The permit to enable commissioning is expected by the end of 2020. The storage facility was designed by Holtec International for 100 years of operation and will use welded canisters and ventilated concrete overpacks located on open-air platforms. The project capacity of the CSFSF is 458 HI-STORM storage containers, which can contain 16 529 SFAs.

3.9.1. Wet storage experience

There is one AFR wet spent nuclear fuel storage facility operated in Ukraine located at the Chernobyl NPP; the Spent Nuclear Fuel Storage Facility No. 1 (ISF-1) was commissioned in 1986 to store fuel from the RBMK reactors and has a capacity of over 21 000 SFAs, including 56 damaged. Its original operation period is until 2025. ISF-1 consists of five storage pools, one of which is a reserve with capacity for 4300 SFAs. Currently more than 17 000 spent RBMK-1000 fuel assemblies are stored in ISF-1.

3.9.2. Dry storage experience

Dry spent fuel storage was implemented in Ukraine in 2001, with the dry spent fuel storage facility (DSFSF) commencing operation at the Zaporizhye NPP. DSFSF is an on-site open-air storage facility using vertical concrete storage containers based on the Duke Engineering & Services (DE&S) and Sierra Nuclear Corporation (SNC) VSC-24 design. DSFSF is designed for 380 containers, each with a capacity of 24, five-year cooled WWER-1000 SFAs. Each container utilizes passive cooling based on natural air circulation. The design operation period is 50 years, which is sufficient for the operational lifetime of the Zaporizhye NPP.

The interim spent nuclear fuel dry storage facility (ISF-2) is a dry store designed for RBMK-1000 that will replace ISF-1, with the permit to commence commissioning received from the regulator in September 2020. ISF-2 consists of two parts: a spent fuel processing facility and a spent fuel storage facility. The processing facility is designed for the preparation and packaging of spent fuel assemblies, spent absorbers and extension rods from ChNPP Units 1, 2, 3 and from the wet storage facility ISF-1. The storage facility has a modular structure where fuel is stored in sealed canisters filled with inert gas. The canisters can hold 93 spent fuel assemblies and are horizontally placed in concrete modules. The canisters are cooled by natural circulation of air. The storage facility is designed for an operational lifetime of 100 years.

3.10. UNITED KINGDOM

The UK is transitioning from a closed to an open fuel cycle, with the cessation of both oxide (2018) and Magnox (2021) fuel reprocessing. While the amount of Magnox fuel planned for long term management will be restricted to a small amount of non-conforming material, all

future arisings of Advanced Gas-cooled Reactor (AGR) fuel will be wet stored pending disposal within a deep geological repository. Along with the AGR fuel, there is also a quantity of legacy fuels and fuel bearing materials from prototype reactors and legacy operations that require management until a disposal route becomes available.

Fuel from the Sizewell B NPP and the new generation of NPPs under construction will be stored pending disposal.

The UK has 15 operational NPPs; 14 AGR and one PWR, with another EPR type under construction. The Magnox NPP fleet have all been shut down and are at varying stages of decommissioning and safe-store.

3.10.1. Wet storage experience

Spent fuel has been wet stored in the UK since the 1950s. The first GCR was built without an AR pool and the fuel was cask transferred to the existing AFR wet pool that had originally been built to service the Windscale Pile Reactors.

Subsequently, aluminium and Magnox clad uranium metal fuels, AGR fuels (Stainless-steel clad uranium oxide pellets) and standard LWR fuels have all been stored in pools prior to reprocessing. These pools were initially demineralized water (neutral pH) cooled outdoor storage facilities, with subsequent pools being indoor facilities, dosed with sodium hydroxide to pH 11.4.

Metal fuels are stored in ~1 m cuboid open skips, stacked two high. AGR fuel is stored in skips with compartments; 15 compartments prior to dismantling and 20 compartments post dismantling[5]. Skips are currently stored within containers that can be segregated from the bulk pool water should activity leaks be detected.

LWR fuels are stored in compartmentalised multi-element bottles (MEBs), which are segregated from bulk pool water using a bubbler system.

The latest development has been the transition of Thorp receipt and storage (TR&S) from a buffer storage facility supporting Thorp reprocessing activities to a long-term wet AFR store in 2018. For planning purposes it is assumed that the fuel will be stored there until the geological disposal facility (GDF) becomes available (planning date is 2075), although a formal decision on long term storage and final disposition has yet to be made. In order to have sufficient capacity to store all of the AGR fuel, a higher storage density container is required. Fuel will therefore be transitioned from storage in the 20 compartment skips currently used to 63-can racks in the early 2020s. These racks will also have the ability to be sealed from the bulk pool water if leaks are detected, in order to allow for ion exchange of any contaminated water.

3.10.2. Dry storage experience

Dry storage has not been commonly deployed within the UK. The Windscale Advanced Gas-Cooled Reactor, a demonstration reactor for fuel and reactor testing to support development of the AGR fleet, operated with a CO_2 cooled AR facility, although this was not intended to be used for long term storage. The Magnox station at Wylfa had an all dry fuel route comprised of two types of dry vault store for magnesium-clad, uranium metal fuel. The first vaults, for initial cooling, operated with a pressurized CO_2 coolant, whilst the second naturally convective air-cooled vault stores were provided later on in station life as a storage buffer. The CO_2 cooled

[5] Dismantled AGR fuel elements are consolidated into stainless steel slotted cans. Each can is of similar dimension to an AGR fuel element and holds 108 pins (equivalent to three fuel elements).

stores operated throughout the station life and for a number of years thereafter to store fuel pending its transfer to Sellafield for its reprocessing, which was completed in 2019.

The UK's only operating PWR NPP at Sizewell employs canister-based dry storage systems to increase its on-site fuel storage capacity and allow continued power generation. The canister design is an evolution of a US Holtec design, modified to meet UK regulatory requirements. The fuel store was commissioned in 2016 and it is anticipated that off-loading of fuel to dry storage will continue until the end of operations, and that fuel will be dry stored until it is ready for disposal. The storage canisters are not compatible with UK surface transport infrastructure nor the UK disposal facility design, therefore it is expected that the fuel will have to be repackaged before disposal.

3.11. UNITED STATES OF AMERICA

The USA has 95 operating commercial NPPs, 33 shutdown NPPs, and 2 NPPs currently under construction[6]. Most NPPs have their own Independent Spent Fuel Storage Installations (ISFSIs) and there is one wet storage ISFSI. There are two applications for consolidated interim storage currently under review. The total spent fuel inventory is ~85 500 tHM (as of the end of 2017).

The USA is continuing a robust research and development (R&D) programme to support spent fuel management. This was reflected in the US Department of Energy (USDOE) 6th National Report [21], in which it is stated:

> *"Objectives of the U.S. R&D program are to develop and initiate activities to improve the overall integration of storage as a planned part of the waste management system, and develop information, resources, and capabilities to assist future disposal implementation decisions and actions. DOE is performing R&D regarding the long-term management of spent fuel to ensure any potential concerns are identified and addressed before safety is compromised.*
>
> *The principal focus of DOE's R&D activities is to develop a suite of options that will enable future decision makers to make informed choices about how to safely manage the spent fuel from nuclear reactors. An additional objective is to demonstrate technologies to allow commercial deployment of solutions for spent fuel management that are safe, economic, and secure.*
>
> *A sound technical basis for evaluating multiple viable disposal options will increase confidence in the robustness of generic disposal concepts and support development of the science and engineering tools needed to support disposal concept implementation. Significant testing, modelling, and demonstration activities will be conducted to enhance and confirm the technical basis for safe storage and disposal of spent fuel, particularly as spent fuel discharge burn-up is increased and as storage times extend beyond what was originally intended."* [21]

In addition to the domestic programme, USDOE is also actively involved in a number of international and bilateral R&D activities, with programmes covering different fuel cycle steps from storage through to disposal.

In August 2013, the US Court of Appeals for the District of Columbia Circuit ordered the US Nuclear Regulatory Commission (USNRC) to continue the licensing process for the US Department of Energy (USDOE) Yucca Mountain construction authorization application, with the licensing process to continue until Congress directs otherwise or until there are no

[6] Data taken from the IAEA PRIS database August 2020.

appropriated funds remaining. After the court's decision, USNRC completed the Yucca Mountain Safety Evaluation Report [22]. In addition, USNRC staff developed a supplement to USDOE's Environmental Impact Statement to address groundwater impacts that were previously identified by USNRC staff as requiring additional analysis [23].

In its January 2015 safety evaluation report [22], USNRC staff found that USDOE's license application met the regulatory requirements for the proposed repository with two exceptions: USDOE had not obtained certain land withdrawal and water rights necessary for construction and operation of the repository.

3.11.1. Wet storage experience

Spent fuel has been stored wet in SFPs for more than 60 years in the US. In addition to the pools at reactor sites, there is an AFR facility at the General Electric Morris facility in Illinois. The current storage capacity is around 60 000 tHM. As SFPs reached capacity, most sites have re-racked their pools with higher density storage racks to increase storage capacity. Rod consolidation was explored in the 1980s to increase wet storage capacity by removing all the fuel rods from an assembly, placing them in a single container and compacting the remaining fuel assembly structure for disposal. In this manner, a consolidation ratio of 2:1 could be achieved as rods from two assemblies could be stored in one storage cell. However, difficulties with the compacting process and cutting the empty assembly structure led to this option not being pursued.

The performance of wet storage systems has been very good, with only occasional operational problems or incidents. Top nozzle separations in older PWR Westinghouse assemblies occurred at the North Anna and Prairie Island sites, as was observed at other international NPPs; intergranular stress corrosion cracking (SCC) of sensitized 304 stainless steel led to failure of the load path for handling these assemblies. Design and material changes were implemented in later designs and procedural controls or hardware fixes have been implemented for managing SFAs susceptible to this issue. Limited degradation of neutron absorber materials has also occurred (see Section 6.1.2. for more details).

3.11.2. Dry storage experience

Many NPPs in the USA are approaching or have already fully utilized their capacity for storage of spent fuel in their respective AR pools. Despite the additional storage capacity realised by re-racking, further storage was required to keep the plants operating, given that there was no disposal site or other offsite location(s) where the spent fuel could be transported to. Thus, the NPPs began moving the spent fuel from the pools to AFR-OS dry cask storage facilities. Between 1986 and 2018, over 2800 dry storage systems (DSSs) have been placed into service in the USA, storing nearly 123 000 SFAs. The movement of spent fuel to DSSs has reached an equilibrium at nearly every plant in the country; averaged over every 18–48 month period (depending on the plant type, operating cycle length and frequency of dry storage campaigns), the amount of spent fuel permanently discharged from the reactors to pools equals the amount being moved from the pools to the on-site dry storage facilities.

Currently only three NPP sites in the USA remain without an ISFSI — Shearon Harris, Three Mile Island, and Wolf Creek — all of which are expected to eventually add ISFSIs to their sites.

In addition to the ISFSIs located at NPP sites, two private centralized storage initiatives are planned in New Mexico and Texas. Both facilities are in the USNRC license application review phase.

Several NPPs in the USA are being decommissioned ahead of their license expirations. To support decommissioning efforts, the fuel stored in the spent fuel pools at these sites is being

moved to dry storage on an accelerated basis, with the expectation of moving all of the spent fuel into dry cask storage systems within approximately three years after the plants' respective shutdowns. In 2017, the commercial US nuclear power industry set a new record for DSSs loaded in a single calendar year by loading 235 DSSs containing 10 922 SFAs (3170 tHM). This exceeded the prior record of 214 DSSs loaded in 2014.

4. WET STORAGE

4.1. INTRODUCTION

The essential safety functions of pool water are fuel cooling, radiation protection and maintenance of sub-criticality. Wet storage also facilitates unrestricted access for spent fuel inspection and monitoring.

Concerning radiation protection of people and the environment, the pool water acts as a radiological barrier. Maintaining the water level at a minimum height, under all conditions (normal, incidental, and accidental), ensures the protection of workers against ionizing radiation. Confinement or containment of radioactive substances is normally ensured by a minimum of two independent barriers. The number of barriers is design-specific, but normally credit is taken for the fuel cladding as the primary containment barrier, the water retaining structure (pool walls and base) and pool hall ventilation as the secondary. Where the water retaining structure is made up of several containment barriers, or the fuel is stored in containers which can be sealed[7], credit may be taken for these additional barriers.

In order to ensure safe operations, maintaining pool water quality and visibility is key. A system for cleaning the pool water is used (filtration and/or resin ion exchangers) and the water is purified continuously.

4.2. CREDIBLE DEGRADATION MECHANISMS IN WET STORAGE

4.2.1. Uniform (aqueous) corrosion

4.2.1.1. Zirconium cladding

The generalized corrosion of zirconium alloys is very limited at low temperatures (below 150°C), and thus difficult to measure. Published findings from Ref. [24] are summarized in Table 3.

TABLE 3. ZIRCALOY CORROSION RATES REPORTED IN THE LITERATURE FOR VARIOUS EXTERNAL CONDITIONS

Reference in [24]	Material	Aqueous medium	Temperature	Corrosion rate ($nm \cdot year^{-1}$)
Rothman (1984)	Irradiated Zircaloy		150°C	~1
Johnson (1977)	Irradiated Zircaloy	Hanford River, deaerated	90°	3–5
Videm (1981)	Unirradiated Zircaloy	KBS groundwater, aerated		0.1–1
Mattsson et al. (1984, 1990)	Titanium	Saturated bentonite groundwater		~2

The cladding corrosion rate in pool storage can be estimated by extrapolating values measured in water at high temperatures (> 250°C), assuming generalized corrosion follows an Arrhenius law over the entire temperature range with an experimentally determined activation energy of

[7] As is the case in the United Kingdom, for both AGR and LWR fuel stored at the Sellafield Site.

115 kJ/mol. One day in water at 320°C is thus equivalent to 8×10^5 years in water at 50°C, i.e. the Zircaloy corrosion rate in pool water at 50°C is about 3×10^{-9} times the rate in the reactor.

4.2.1.2. Stainless steel cladding

General corrosion of stainless steel in water is very slow due to the formation of a highly tenacious chromium oxide protective layer. For AGR fuels with stainless steel cladding the concern is focused on localized corrosion at grain boundaries rather than general corrosion, which has been shown to be less than 0.5 μm/y [25]. Confirmatory evidence of the performance of AGR fuel cladding during long term storage was obtained by examination of fuel pins after 25 years storage in caustic dosed pond water, which failed to identify any visible deterioration on cladding condition or thickness using high power microscopy [26].

4.2.2. Localized corrosion (Pitting, galvanic, and microbiologically-influenced corrosion)

Localized corrosion is driven by electrochemical processes, where oxidative and reductive processes are spatially separated. Dissolution of the metal surfaces causes disturbances in the solution, resulting in localized changes in electrochemical potential. This leads to enhanced local corrosion rates. Localized corrosion processes may be transitory or may become established and lead to substantial localized metal loss that results in a loss of material or component performance.

AGR fuel cladding is a stabilized, high-nickel austenitic stainless steel designed for long term operation at high temperatures. In demineralised water storage the irradiated cladding is not generally susceptible to localized corrosion. When exposed to very high chloride levels, thermally sensitized AGR fuel cladding is susceptible to classical pitting corrosion [27], however such conditions are outside credible storage conditions.

Radiation induced segregation (RIS) [28, 29] in a small fraction of AGR fuel pins gives rise to a number of localized corrosion phenomena where the RIS results in grain boundary chromium concentrations falling below ~12% over at least 4 nm [30]. The observed effects in demineralised water with up to 10 ppm Cl^- are:

- Intergranular attack (IGA) near the surface of fuel cladding in affected fuel pins;
- Intergranular SCC (igSCC) in high stress regions of affected fuel pins;
- Crevice corrosion and igSCC in fabricated braces, used to maintain fuel pin geometry within the fuel elements. AGR fuel elements are dismantled for long term storage and therefore braces are not present in long term storage.

These effects have been controlled through the use of sodium hydroxide as a corrosion inhibitor over storage periods in excess of 25 years and, as a result, galvanic and microbiologically-influenced corrosion (MIC) effects have not been seen in AGR fuels [31].

There has been some evidence of degradation of Zircaloy-2 materials when stored in mild steel containers in sub-optimal water chemistry for extended periods. Whether this is due to MIC or galvanic effects is currently under investigation.

4.2.3. Chemical interaction

Use of sodium hydroxide as a corrosion inhibitor has been successfully deployed in UK SFPs. Magnox cladding corrosion has been shown to be effectively inhibited by pH 13 water, whilst pH 11.4 has been used to reduce corrosion rates of uranium metal. Both pH 13 and pH 11.4 have also been used as an inhibitor for sensitized AGR steel cladding.

4.3. RESEARCH ACTIVITIES, INVESTIGATIONS & MONITORING RELATED TO WET STORAGE

Wet storage is a mature technology in common use, with over 60 years of operational experience and ongoing technological improvement. Current research relating to wet stored spent fuel amongst the SPAR-IV participants is focused on ongoing operations, the implications of extended storage periods and safety performance in severe accident conditions.

4.3.1. France

Research activities on wet storage are related to the maintenance of safety functions during storage.

One of the main safety considerations of wet storage is the high radiological inventory in the pool and, in the event of loss of water and uncovering stored spent fuel, the risk of release of radioactive material (due in particular to the phenomena of the intense oxidation of zircaloy cladding at high temperature) and the emergence of a very high dose rate around the pool, preventing direct human intervention; it would be necessary to provide countermeasures using remote capabilities and with remote access. From the point of view of safety, as the potential consequences of pool dewatering or uncovering fuels are severe, the possibility of conditions arising that could lead to an early radioactive release or a large radioactive release has to be 'practically eliminated', i.e. made physically impossible for the conditions to arise or with a high level of confidence to be extremely unlikely to arise [32]. This point was notably the subject of work within the framework of lessons learned and feedback of experience from the Fukushima accident, based on the consideration of extreme hazards (exceeding those considered in the design), on the deterministic review of a significant leak scenario for a storage pool and the increase in means of water recharge for pool.

For these reasons, since 2012 IRSN has been conducting the research programme 'Accidental DENOyage (de-watering) of Nuclear Fuel Storage', or DENOPI, as part of the post-Fukushima projects [33]. The project involves conducting experiments, modelling work and validation of calculation software that aims to improve knowledge of the physical phenomena occurring during accidents in the storage pool, in addition to prevention or mitigation measures that could be implemented; presently, this research work is still underway.

4.3.2. Hungary

The following parameters of the storage pools are monitored:

- Temperature (°C) (t <60°C during refuelling operations, <50°C during storage);
- Optical transparency (>90%);
- Chemical composition (H_3BO_3, Cl^-);
- Isotope specific activity (Bq/dm^3).

Chemical conditions are measured, and corrected if necessary, as a minimum daily, during refuelling operations, and weekly during storage periods.

Pool water activity of the pools has two limit values:

- A lower intervention level, at which cleaning of the pool water starts;
- A higher accident level, taken into account in emergency calculations. Actions at this stage are the same as above.

Only longer half-life corrosion or fission products can be used to trigger action; the fission products ^{137}Cs and ^{134} Cs were selected for this purpose (as iodine activity decreases quickly after refuelling). The intervention level for the sum of the two isotopes is 10^4 Bq/dm^3. For the corrosion product, there are five isotopes monitored (^{51}Cr, ^{59}Fe, ^{54}Mn, ^{58}Co and ^{60}Co). The intervention level for the sum of the five isotopes is 4×10^3 Bq/dm^3.

The emergency level is 200 times the intervention level.

4.3.3. Slovakia

Activities related to ISFS can be divided to two main areas:

- Corrosion monitoring programme of ISFS structural materials;
- Activities oriented to microbial contamination in the pools.

These activities are reported in Section 6.1.1.

4.3.4. Switzerland

A specific feature of the Gösgen (KKG) wet storage facility is the capability to do more than routine inspection and repair of fuel rods; this includes the ability to modify original fuel assemblies by removal and insertion of fuel rods, reshuffling and guide tube cutting. The experience gained by the KKG personnel for on-site fuel service operations have enabled the possibility to irradiate individual lead rods and samples, in the frame of numerous R&D programmes.

The SFP at the reactor is equipped with a box sipping facility and a multi-inspection facility (MIF) for fuel assembly inspections (Fig. 1). The SFP is connected to the loading pool via a horizontal transfer channel. Within the loading pool is the automatic fuel repair facility (so-called ABERE), as shown in Fig. 2, which allows for more specific capabilities, such as fuel rod reshuffling and fuel assembly reconfiguration. The ABERE allows the reinsertion of multiple fuel rods in a fuel assembly and makes it possible for the utility to operate fuel rods to very high burnup (e.g. a fuel rod was irradiated up to ten reactor cycles) without detrimental effects on the core safety.

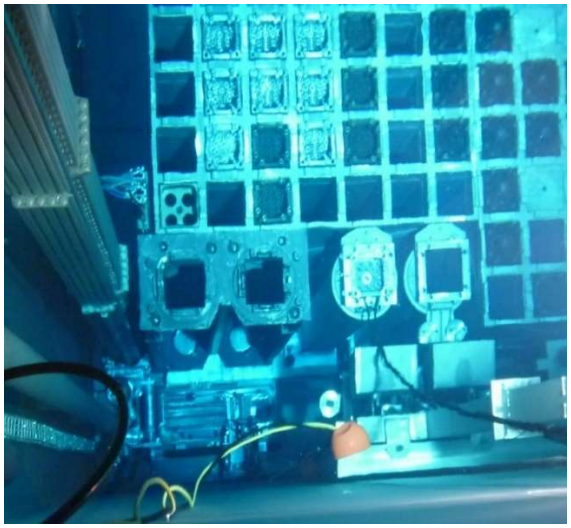

FIG. 1. Spent fuel pool with MIF (left) and Sipping-Boxes (right) (image courtesy of Gösgen-Däniken AG).

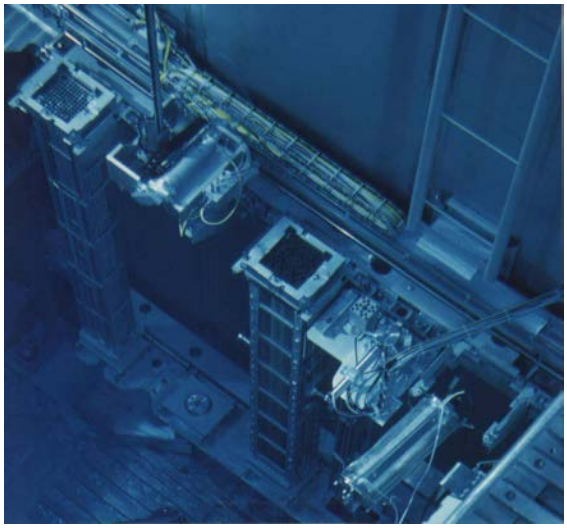

FIG. 2. Loading pool with the automatic fuel repair facility 'ABERE' (image courtesy of Gösgen-Däniken AG).

Some of the irradiated materials are unique and innovative, and, as they have been made available to the scientific community for post irradiation examination, have led to the generation of data for use by the nuclear community for several licensing and validation & verification programmes (e.g. ARIANE, MALIBU and PROTEUS Phase II). Further extension of inspection capabilities at the Gösgen SFPs are currently under investigation.

4.3.5. United Kingdom

4.3.5.1. Underpinning of sodium hydroxide as a corrosion inhibitor for higher burnup AGR fuel

The storage regime for stainless-steel clad gas cooled reactor fuel from AGRs was developed in the 1980s when the typical fuel stringer burnup was in the region of 18–21 GWd/tU. Currently, stringer mean irradiation is substantially higher, with 33–35 GWd/tU being the typical range and a peak element burnup around 43 GWd/tU. With the transition of AGR fuel management from reprocessing to long term storage in 2018, a series of examinations have been undertaken to understand whether there have been any significant changes in cladding microstructure as a result of the higher burnup and associated longer in-reactor dwell time (presently, typically 6–7 years), that could affect fuel performance during storage.

AGR fuel differs from LWR assemblies, in that each fuel channel in the reactor is fuelled with a stringer consisting of eight, axially stacked, fuel elements containing 36 fuel pins of 1 metre length. Thus, the irradiation conditions experienced by the individual fuel pins varies considerably, as shown in Fig. 3. In subsequent paragraphs reference to an element number (e.g. element 4) refers to the position in the stringer, with position 1 being the lowest located at the coolant inlet to the core.

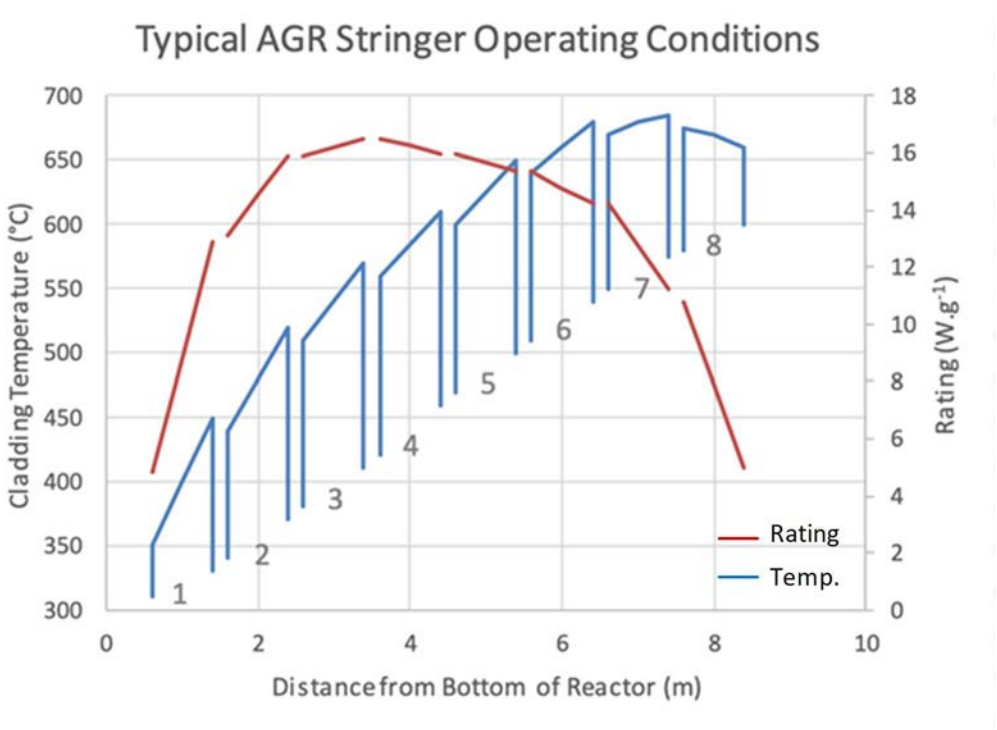

FIG. 3. Typical AGR fuel cladding operating conditions (based on Ref. [6]) (courtesy of NNL).

It is well known that neutron irradiation of stainless steels can lead to changes in grain boundary composition under certain combinations of neutron flux and temperature, leading to RIS [28, 34]. Therefore, the objective of the examination work was to characterise the microstructure and grain-boundary composition profiles in recently discharged fuel. Samples from element positions 2 to 8 have been examined as part of recent studies.

Historically, significant levels of chromium segregation at grain boundaries of AGR fuel cladding have been observed for cladding operating between 350°C and 520°C, with peak segregation being determined to be around 420°C [28, 29]. This is consistent with observations of localised cladding corrosion predominantly in pins from elements 1 and 2.

Measurements on modern cladding samples extracted from locations with operating temperatures between around ~500°C and ~750°C concluded that the pattern of Cr depletion followed the same trends as had been displayed by samples examined at much lower burnups. There was some evidence that the maximum degree of sensitization may have been marginally greater at higher burnup, as shown in Fig. 4, however the extent of the difference was small and unlikely to have a significant implication for fuel performance in storage.

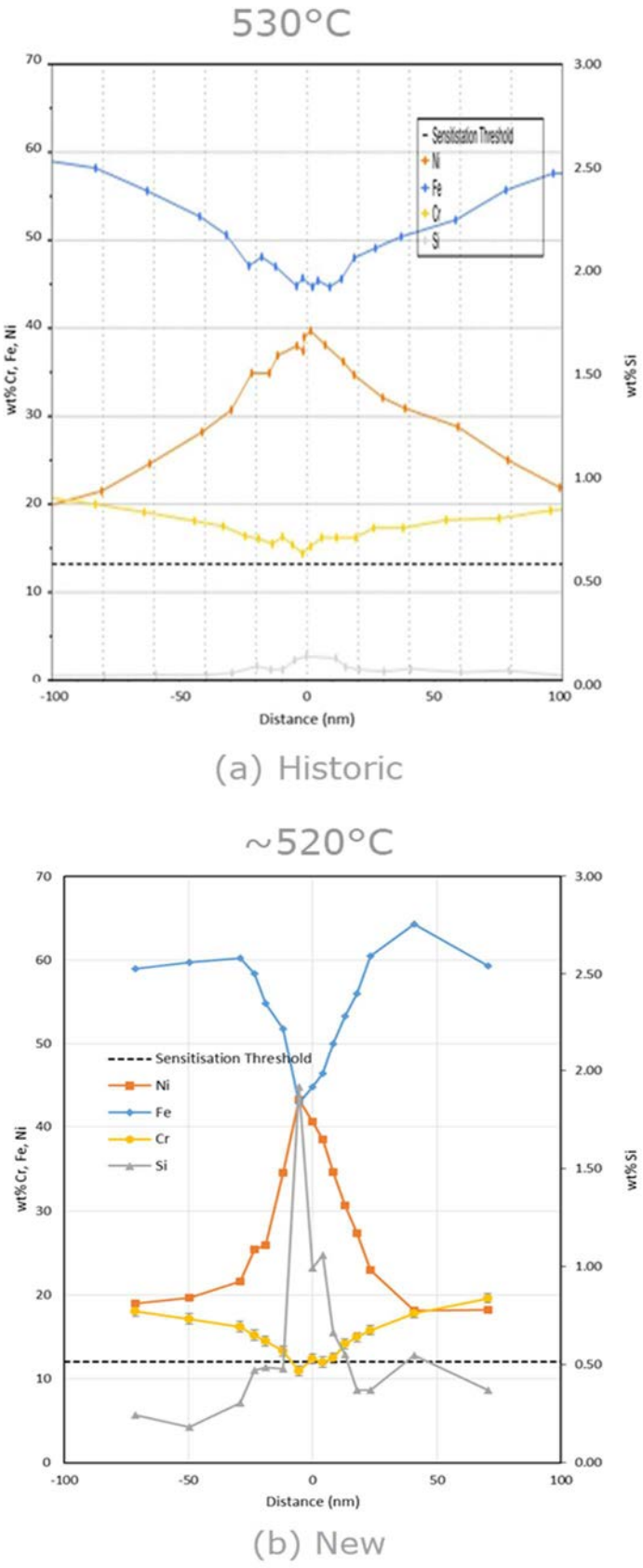

FIG. 4. Measured grain boundary compositions of (a) historic cladding samples and (b) modern cladding samples (courtesy of NNL).

Examination of cladding microstructure confirmed that cladding oxide layers remained essentially similar to those observed historically, with no indication of changes in thickness or integrity as a result of longer in-reactor operations. Historic observations of a 'dark etching' effect in cladding that has a significant degree of grain boundary segregation were repeated in the current work (Fig. 5(a)). Detailed transmission electron microscope (TEM) examinations identified within-grain segregation that is likely to be the source of this effect (Fig. 5(b)).

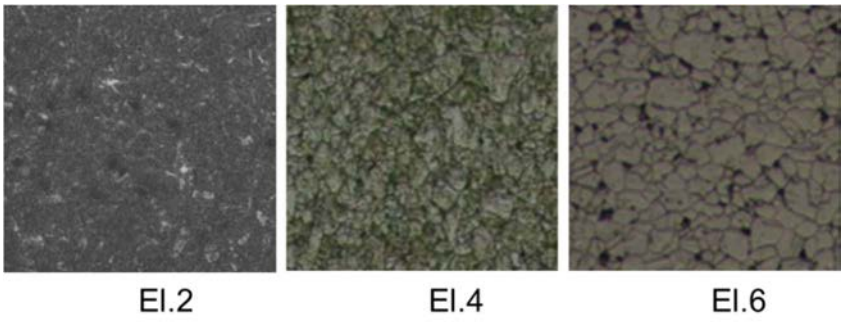

(a) Variation in dark etching response with element position

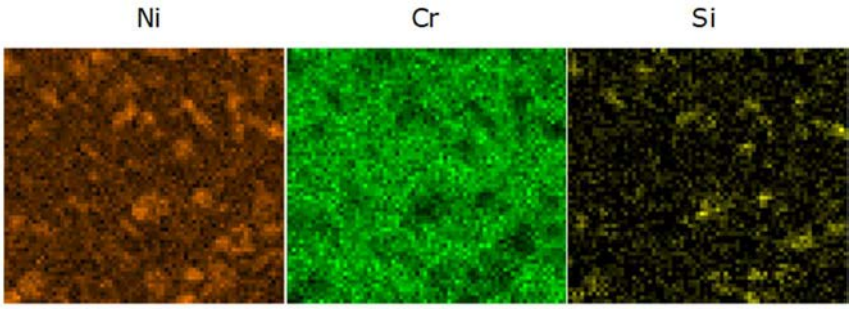

(b) TEM images of intra-grain segregation

FIG. 5. Dark etching effect and associated within-grain segregation (courtesy of NNL).

Precipitates within the cladding displayed the previously observed variations with temperature and lack of significant levels of within-grain precipitation. Intergranular G phase precipitates were observed in all locations, except element 2, whilst $M_{23}C_6$ precipitates increased in size with temperature. Overall the changes in observed precipitates, compared to lower burnup cladding, were small and not considered significant in relation to fuel performance in storage.

Nanometre-scale cavities were found in samples taken from cladding near the peak sensitization temperature. Cavities were identified on grain boundaries, in lines along prior grain boundaries, on NbC precipitates and on the interfaces of intragranular G phase and Ni_xSi precipitates. In addition, cavities were also found within grains. The size of cavities increased with temperature and were generally in the range ~6–25 nm. The implied strain caused by the cavities was assessed to be low and well below those known to cause concern in fast reactor fuel pins.

Available results confirm the findings of work on lower dose material, namely that there is:

- A strong axial variation in segregation, being most significant in the lower two elements;
- Significant variability in the grain boundary segregation in different stringers;
- Appropriately fitted semi-empirical models provide good predictions for segregation in AGR cladding.

Current work does not provide evidence that would indicate any increase in corrosion susceptibility associated with higher burnup AGR fuel cladding.

4.3.5.2. Support to interim storage of AGR fuel within Thorp Receipt & Storage (TR&S)

Pool Chemistry

Transitioning to long term storage within TR&S required the pool chemistry to be changed from demineralized water to pH 11.4 sodium hydroxide dosed. The process involved an initial transition to pH 9 in 2016, with pH 11.4 being achieved after cessation of reprocessing operations at the end of 2018.

Due to some potential material compatibility issues at higher pH storage conditions, a series of container trials were undertaken to begin to understand how these materials would behave at these pH levels at different chloride concentrations. The results of the early stages of the container trial programme were reported in SPAR-III [6], and this section aims to provide an update to those results that have been obtained since 2014, primarily reporting the results of the higher chloride levels.

The objectives of the work were to further underpin and implement temporary pool water chemistry for AGR storage and to further develop and deliver a programme of work to support the transition and safety case delivery for long term storage of AGR fuel.

The temporary pH 9 pool water chemistry for AGR storage was underpinned by lead container studies evaluating the impact of increasing chloride concentrations on the ability of pH 9 sodium hydroxide to inhibit IGA corrosion. In the study, samples of container water were taken on a monthly basis and evaluated for evidence of fuel cladding failure. Figure 6 illustrates the trial set-up of vertically stacked containers, with the higher chloride containers highlighted in blue.

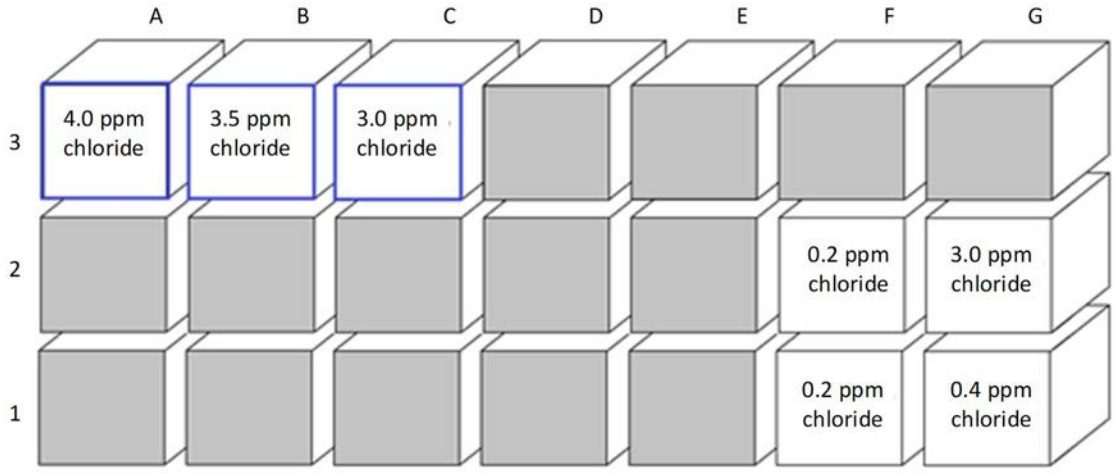

FIG. 6. Schematic of lead container trial set-up (courtesy of Sellafield Limited).

Figure 7. shows a schematic of the rig used to control the study; (a) shows the liquor sampling and dosing equipment, whilst (b) shows the nitrogen equipment used to generate and maintain a gas barrier between the pool and the containers contents.

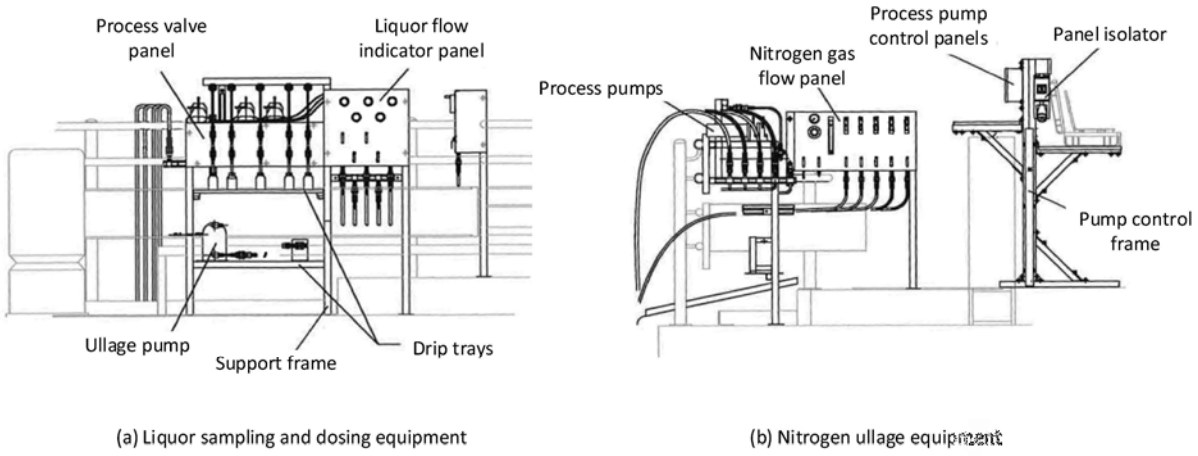

FIG. 7. Schematic of rig used in dosing trials (courtesy of Sellafield Limited).

The principle result from the lead container studies is that sensitized AGR fuel stored in <pH 9 sodium hydroxide with 2.5 ppm chloride showed no evidence of systemic cladding failure over a period of greater than 1400 days. Sample results indicate a potentially limited number of pins (<2%) could have failed during periods of relatively low pH for sodium hydroxide systems (<8.3). In addition, sensitized AGR fuel has been stored in pH 9 sodium hydroxide with 1 ppm chloride without evidence of cladding failure for more than 2000 days.

Thermal Modelling

To support long term storage of AGR fuel, a number of predictive thermal models have been developed. The purpose of the models was to predict:

- The maximum temperature reached by the pin cladding structure during storage;
- The pool water temperature using transient analysis.

As the UK strategy transitions towards long term storage of AGR fuel following the cessation of reprocessing and with the introduction of a compact storage system, it is essential to understand the temperature that the fuel could reach in storage. Corrosion trials have been undertaken on AGR fuel cladding materials at the relevant pHs that it will be exposed to during storage; the temperature ranges were selected to provide what should have been a bounding case (i.e. maximum temperatures higher than those expected in reality). Modelling of the fuel cladding temperatures is therefore a requirement to prove that the theoretical temperatures that the fuel will reach over the duration of pond storage are less than those bound by the corrosion trials.

An additional challenge to thermal modelling is that two types of storage containers will be in use:

- The traditional arrangement of a 20-compartment skip within a container;
- The new 63-can rack that provides higher storage density.

Therefore, models have to take into account both designs. Modelling results from the traditional arrangement were compared to results from on-plant trials for validation.

To predict the maximum fuel pin cladding temperature within the 63-can rack, it was essential to understand the relationship between the storage container, fuel can and fuel pin. The complex storage geometry meant that a single thermal model would not be able to accurately represent the heat transfer mechanisms. The geometric challenges to be resolved covered length scales ranging from a few millimetres to metres. This led to the development of a multi-phase model, with interaction between all phases of the model to capture the effects of heat flow.

The temperature profile of the channel with the maximum predicted temperature calculated using the full rack model was used as the starting boundary condition for the next phase of the calculation, the individual channel. The maximum predicted temperature at the centre of a fuel can, taken from the channel model, was then used to predict the likely peak cladding temperature within the central fuel pin and its 18 nearest neighbours within this fuel storage can (with pin spacing modelled so as to provide a conservative estimate of cladding temperature). This process is illustrated in Fig. 8.

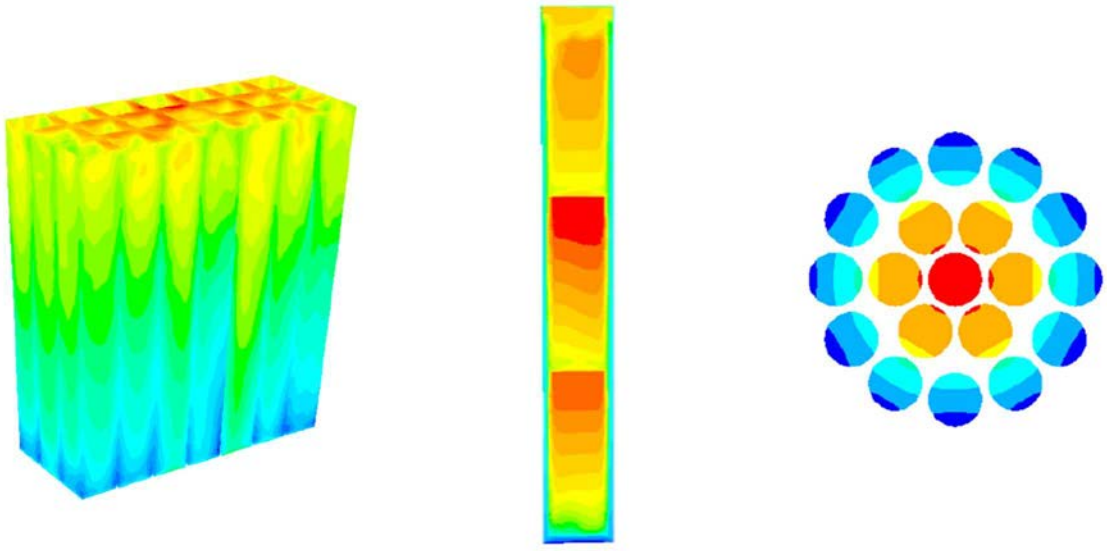

FIG. 8. Illustrative images of the three phases of the model (from left to right); (a) full rack, (b) channel containing three storage cans, (c) individual fuel pins within the central region of a can (courtesy of Sellafield Limited.).

One of the key variables in the 63-can rack modelling is the temperature of the fuel storage pool. The temperature of the pool is a function of the heat load from the fuel within the pond, as well as the cooling mechanisms that are available to the pool.

To understand the transient thermal performance of the fuel storage pool, a large scale model was developed. The model used a porous mesh to account for the fuel storage racks. Modelling was undertaken on the heat loss from the water surface primarily through evaporation over the large surface area. The large scale pool model used time step (transient) analysis in its predictions of pool water temperature. A three-dimensional computational fluid dynamic (CFD) model was created for the large-scale cooling pool including the water zone. A user interface model was constructed that allowed multiple cooling mechanisms in the model to be turned on/off, enabling the user to vary these cooling mechanisms to understand the cooling mechanism which provides the best capability to maintain the pond water temperature within its operating envelope. It is also possible to model the cooling mechanism capability required should there be a temperature excursion in the pond to enable a return to the normal pond water temperature operating range.

Although the macro scale thermal pool model and the micro scale container models are built in different modelling codes, they interact through the results and starting parameters maintained by the model. The micro model uses the pool water temperature predictions that arise from the macro model as its starting boundary conditions.

4.3.6. United States of America

Long term management of neutron absorber materials used in SFPs is necessary to detect any degradation and allow timely mitigation actions in order to offset any potential loss of neutron absorbing capability. In the USA, BORAL is a widely used neutron absorber material. The Electric Power Research Institute (EPRI) developed a long-term strategy for managing the use of BORAL. Research findings are detailed in Section 6.1.2.

4.4. SYSTEM ACCIDENT CONDITIONS

Various assessments of pool accidents studies have been performed by IRSN with different severe accident codes for different pool geometries. In these studies, both loss of cooling and loss of water transients have been analysed. In the case of a loss of coolant accident, fuel behaviour at high temperature and dry conditions (de-watering) has been studied to validate the emergency response plan. Focus was given to microstructural changes in the cladding, stress-strain curves, oxidation phenomena kinetics in the studies.

Synthesis of SFP accident assessments using severe accident codes is presented in Ref. [35], which deals with degradation mechanisms. The vulnerability of SFPs highlighted by the Fukushima accident is due to the potential loss of sufficient fuel cooling in the case of extreme external events, such as flooding or earthquake, or in the case of internal events.

5. DRY STORAGE

5.1. INTRODUCTION

As capacities are reached in wet storage facilities worldwide, provision for additional capacity using dry technologies is becoming increasingly common. There is a wide variety of technologies available from various vendors, but they can be grouped into three main categories: casks, vaults, and dry storage units. DSSs can be designed for storage only (single purpose) or designed for storage and transportation (dual purpose). In some systems, the fuel storage canisters may be utilized for transport and/or final disposal (multipurpose). Dual and multi-purpose systems were introduced and designed to reduce handling of fuel assemblies in back-end activities. Due to the modular nature of DSSs, capacities can be extended incrementally.

Casks can be made of metal or concrete and can be used for spent fuel storage and/or transport. They may be stored externally on a pad or enclosed in a building. The spent fuel is either placed directly into a basket that fits inside the cask or is sealed within a canister. The system is backfilled with inert gas. There are variations in features, such as structural materials, transportability, and orientation of fuel elements, depending on the specific cask system.

Dry cask storage facilities in the participating countries have been constructed in Germany, Japan, Spain, Switzerland, and the USA.

Vaults consist of above- or below-ground reinforced concrete buildings containing arrays of storage cavities suitable for containment of one or more SFAs.

Spent fuel is stored within storage cavities. Depending on the design, this may be within a metal storage tube or sealed within a storage cylinder. The storage tubes or cylinders are sealed, and depending on fuel type, may be backfilled with inert cover gas.

Vault facilities for power reactor fuel in the participating countries have been constructed in Hungary, the UK and the USA using a variety of vault dry storage technologies.

Dry storage units (commonly referred to as silos) are immovable monolithic or modular concrete reinforced structures, for vertical or horizontal storage of spent fuel.

The vertical modular structure is generally an array of cylinders, which can either be individual cylinders, or can be assembled together in a single monolithic structure. Spent fuel may be loaded vertically into metal canisters before being inserted in the structure.

Spent fuel is placed in the cavity of the silos, which may be backfilled with an inert gas to improve heat transfer from the fuel and prevent oxidation of spent fuel while in storage.

With horizontal concrete silo systems (also known as horizontal storage modules), fuel is loaded vertically into metal canisters that are stored in a horizontal orientation inside the concrete storage module.

In both cases, vertical or horizontal storage, the sealed metal canisters may be licensed for transportation as part of a transportation package.

Silos or concrete modules facilities in the countries participating in SPAR-IV have been constructed in Argentina, Republic of Korea, Spain, Ukraine, the UK, and the USA.

Average burnups of spent fuel presently in dry storage range from 4.5 to 33.5 GWd/tHM, while the maximum burnups range from 7.5 to 55 GWd/tHM. The majority of dry storage systems are limited to a maximum fuel burnup between 45 and 65 GWd/tHM for LWR fuel. However, there is an almost universal tendency towards increasing the discharge burnup of the fuel assemblies. In Germany, for instance, average discharge burnups for PWR fuel assemblies have

increased from 35 GWd/tHM in 1983 to 50 GWd/tHM in 1998, and a value of 65 GWd/tHM is currently achieved. In the USA and most other participating SPAR countries, most of the SFAs are being discharged with burnups in excess of 45 GWd/tHM.

5.2. CREDIBLE DEGRADATION MECHANISMS IN DRY STORAGE

5.2.1. Air oxidation

Spent fuel is generally stored dry under inert atmosphere conditions, which are obtained by appropriate drying and inerting operations that rule out oxidation of the stored spent fuel elements by significant amounts of air. Oxidation is not an active degradation mechanism under normal, inert storage conditions.

Off normal or accident conditions could result in a failure of the storage system seals, leading to air ingress. Another potential exposure could be from handling operations performed in air. In the event of a fault during handling operations (dry cask loading, transfer to a transport cask or a disposal canister), cooling of the facility may be interrupted and decay heat generation would give rise to an increase in temperature. If during this postulated scenario damaged fuel is present, oxidation from UO_2 to U_3O_8 could occur. If the oxidation event were severe, the resulting volume expansion could result in gross cladding failure with the potential to release fuel debris into the transfer facility.

Many studies in this area have been undertaken and the progression of UO_2 oxidation is reasonably well known [36–39]. Some areas for future study have been identified in relation to their effect of the kinetics of UO_2 oxidation, such as UO_2 grain size, fuel burnup, high burnup structure, and reactor type (in relation to cladding type and pellet size), but no specific contributions were provided over the course of the SPAR-IV programme.

5.2.2. Thermal creep

Thermal creep is a slow deformation of a metal at high temperature under stress and was thought to be one of the limiting mechanisms of PWR spent fuel cladding, owing to concerns regarding high temperature and rod internal pressure. Review of the many studies completed on this phenomenon has led regulatory authorities in many Member States to the conclusion that creep rupture is unlikely to occur under normal dry storage conditions, especially if temperatures remain below the 400°C limit due to creep's self-limiting properties. The results from a Korean contribution are reported in Section 5.3.3

5.2.3. Delayed hydride cracking

Delayed hydride cracking (DHC) is a time-dependent mechanism of crack propagation in zirconium alloys. It involves the diffusion of hydrogen, but also the microscopic fracture of zirconium hydride, leading to the initiation and propagation of a macroscopic crack. A threshold mechanical loading for crack initiation is required. If no flaw is present, the process can only start with very large tensile stresses. If a sharp flaw is present in the component, a threshold stress intensity factor, K_{IH}, has to be exceeded. Based on available data, a reference stress intensity factor (K_{IH}) value of 5.0 MPa$\sqrt{m}$ can be used. Minimum (critical) crack sizes to sustain DHC in PWR fuel rod 17 x 17 design are typically greater than the cladding wall thickness for K_{IH} = 5.0 MPa$\sqrt{m}$. For a flaw equal to 25% through the cladding wall (~140 μm for 17×17 PWR fuel design) to propagate, K_{IH} would have to be very low (~1.3 for a semi-

elliptical flaw or 1.6 MPa$\sqrt{m}$ for a sharp flaw). There is no experimental evidence for K_{IH} values this low.

5.2.4. Hydride-related issues

Fuel cladding is the first containment barrier for radioactive material. Its continued integrity under core conditions or during transport and wet storage is therefore an important radiological safety consideration.

Cladding hydriding during irradiation results in degradation of its mechanical properties. This phenomenon is becoming increasingly important with prolonged fuel operation and increasing fuel burnups, although this trend is counter-balanced by the deployment of claddings having much better corrosion resistance and lower hydrogen pickup. During storage, the presence of hydrides in the fuel cladding may result in embrittlement. In France, IRSN is performing research to better characterize this phenomenon and to develop tools for simulating fuel behaviour.

Following the publication of studies by CEA, [40, 41], IRSN recently performed additional work on the degradation mechanisms of spent fuel cladding under dry storage conditions to predict potential ruptures [42, 43].

At the macroscopic scale, two main aspects are studied; the hydrogen precipitation conditions, in particular those that favour the formation of radially oriented hydrides across the thickness of the cladding; and the mobility of hydrogen throughout the cladding.

One of the important parameters is the orientation of precipitated hydrides; the radial zirconium hydrides (perpendicular to the wall of the cladding) promote the formation of radial cracks in the cladding, especially during handling operations (in transport or storage). Tests were carried out to identify the conditions under which radial hydrides precipitated. Cladding samples containing hydrogen at different concentrations were brought to two temperatures (350°C and 450°C) by subjecting them to mechanical stresses representing the pressure of gases in the cladding; the pressure is a function of temperature, as per the Ideal Gas law. These tests made it possible to identify and describe the precipitation of the hydrides (in the radial or axial direction) as a function of stress, temperature, and hydrogen content. These tests also measured the embrittlement induced by radial hydrides.

Based on these results and on simulations using mechanical calculation software, models have been developed to predict the concentration of radial hydrides in cladding after transport or at the end of storage. These new models need to be validated by means of more representative irradiated material samples.

5.3. RESEARCH ACTIVITIES RELATED TO FUEL DRY STORAGE

Research activities relevant to dry storage have been carried out since the early 1960s and have been reported in earlier BEFAST/SPAR projects [2–6] and elsewhere. Research conducted during this phase of SPAR is reported here.

5.3.1. Argentina

5.3.1.1. Hydride reorientation around blisters during long interim dry storage

Blisters can be formed in the fuel assembly cladding during in-service life, for example, by thermal gradients produced by oxide spalling, stress gradient, or by secondary hydriding [44]. Some hydrides in the blister–matrix interface produce a hydride distribution similar to a

‘sunburst’. During cooling, many hydride platelets are precipitated radially to the blister, even in the absence of external stresses. This means that the stress necessary to produce radial orientation has been reached in the blister region. These stresses arise from the larger volume of the hydride phase compared to the zirconium matrix, and they are tensile around the blister in the circumferential direction.

Remaining consistent with a process controlled by hydrogen diffusion, hydride precipitation in a radial direction to the blister is favoured by a slow cooling rate. The length of these radial hydrides around the blister is limited by the previous existence of circumferential hydrides, but favours their precipitation in a larger zone around the blister.

When external stresses are applied on the circumferential direction, the blister acts as a stress concentrator and the radial hydrides may grow in both length and thickness. Hydrides crack when a critical size is attained; the crack originated by this process may join to the cracks inside the blister. Under this condition, the critical stress intensity factor for DHC (K_{IH}) can be reached [45, 46].

A complete description of the work performed related to this topic is provided in Appendix I.

The possibility of radial hydride precipitation, affected by residual stresses around a blister, has been analysed under conditions similar to those existing during dry storage of CNA-1 spent fuel assemblies (maximum temperature: 200°C, maximum inner pressure: 75 bar, hydrogen concentration: 100 wt. ppm). Sections (50 to 120 mm length) were cut from an Atucha Zry-4 non-irradiated cladding and subjected to the following tests:

- Gaseous hydrogen charging with gaseous pure hydrogen in a Sieverts device;
- Heat treatment for hydrogen homogenization at 370°C during 24 h;
- Blister formation by heating the tube and applying a cold spot on its external surface.
- Hydride reorientation test (HRT): The tube section was pressurized with argon at temperature for a period of time; the pressure was calculated considering the extreme value at the end of operation life (100 bar at 350°C). Three different conditions were applied during HRT:
  1. Heating up to 200°C, pressurization of the tube at 75 bar, holding at this temperature/pressure for 30 days, removing the pressure and cooling to room temperature;
  2. Heating up to 90°C, pressurization of the tube at 59 bar, holding at this temperature/pressure for 30 days, removing the pressure and cooling to room temperature;
  3. Heating up to 190–200°C, pressurization of the tube at 75 bar, holding at this temperature/pressure for 4 hours, and cooling to room temperature at a rate of 0.24°C/h under inner gas pressure.
- Finally, the tubes were metallographically analysed for the presence of reoriented radial hydrides around the blisters (Fig. 9). Some blisters were sectioned without HRT in order to compare with the reorientation of hydrides in samples subjected to HRT.

Figure 10 is a scheme of the metallographic section (radial-circumferential plane) of a blister showing its depth (*a*), diameter (*d*) and protrusion (*p*) produced by the increase in volume associated to the lower density of zirconium hydride in comparison to the zirconium matrix. The distribution of the reoriented hydride particles grown in the radial direction of the blister was characterized by the reach (*R*) which is the distance from the blister–matrix interface to the farthest radial hydride.

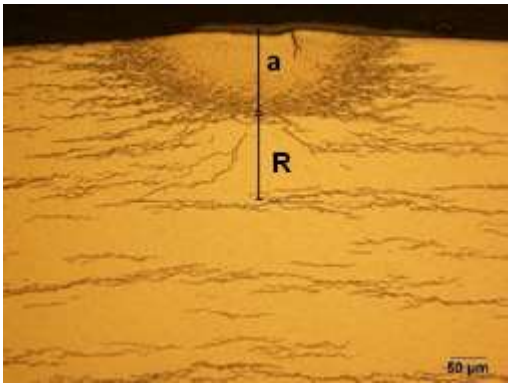

FIG. 9. Optical micrograph of a blister (20-2) showing depth (a) and reach (R) (courtesy of CNEA)

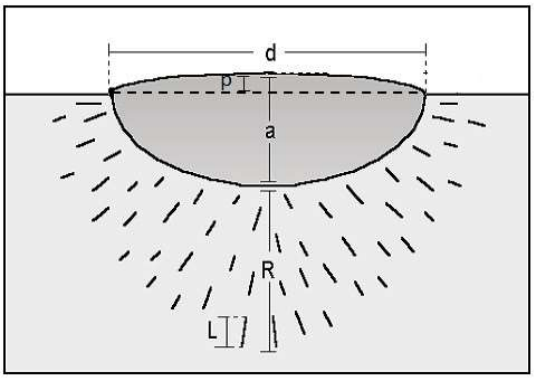

FIG. 10. Description of the parameters used to characterize the blister and radial reoriented hydrides (courtesy of CNEA).

In Fig. 11, the reach of radial hydrides added to the blister depth is presented as a function of blister depth, the protrusion *p* has been subtracted. The figure also shows that, (considering the error bars) there is no evident increase of the radial hydride reach after the reorientation tests. It is clear that the effect of the stresses surrounding the blister increases with the depth of the blister. For blisters deeper than 230 µm, the radial hydrides reach the inner surface of the cladding. Cracking of the hydrides was not observed in any of the samples.

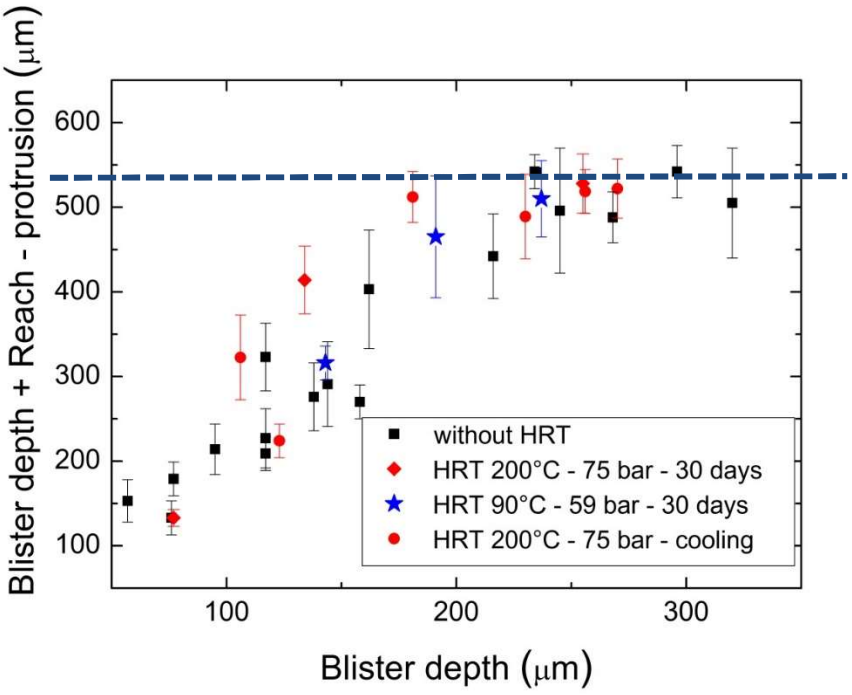

FIG. 11 Reach of radial hydrides added to the blister depth vs. blister depth. The dashed line represents the cladding thickness (courtesy of CNEA).

Conclusions:

- No difference was observed in samples treated with the HRT at 200°C for one month - cooled without pressure, and HRT at 200°C - 4 hours and cooled with pressure;
- After the HRT at 90°C and 200°C, for 30 days, no evidence of increase in radial hydride reach was detected;
- Without HRT, cracks inside blisters that nearly cross the cladding thickness remain inside the blister. After HRT at 200°C -75 bar and at 90°C - 59 bar, cracks have been observed to grow and reach the blister–matrix interface;
- When blisters are dissolved by increasing the sample temperature, the remaining cracks act as stress concentrator and promote hydrogen diffusion to, and hydride precipitation at the crack tip (first and second stages of delayed hydride cracking)

5.3.1.2. Characterization of hydrides and the α-Zr matrix in zirconium alloys: effects of stresses, microstructure and neutron irradiation on hydride texture, terminal solid solubility and dislocation structure

Synchrotron X ray diffraction, TEM and high resolution TEM experiments were performed on samples from Zr-2.5Nb pressure tubes and Zircaloy-4 tubing in order to define hydride precipitation temperatures, hydride texture, matrix hydride orientation relationship and dislocation densities. For Zr-2.5Nb, studies included in-situ constant stress tests performed on dog bone specimens cycled between room temperature and 400°C, during which hydrides were completely dissolved and re-precipitated. For Zircaloy-4, analysis included ex-service Zircaloy-4 irradiated to ~1022 neutrons/cm^2.

A complete list of publications detailing this work can be found in Annex A-2. The main findings were:

- Zr-2.5Nb pressure tubes
    - The terminal solid solubility for hydride dissolution (TSSD) and precipitation (TSSP) temperatures depend on the orientation of the parent α-Zr grain. Hydrides both precipitate and dissolve at slightly lower temperatures (~5°C and ~15°C, respectively), in grains having their c-axis parallel to the tube hoop direction, than those with their c-axis ~20° off from the hoop direction;
    - Application of a stress along the tube hoop direction during precipitation increases TSSP temperatures and favours hydride precipitation on grains with c-axes stretched by the load. For grains with c-axes parallel to the applied load, TSSP temperatures increases at a rate of 0.08 (± 0.02) °C/MPa, nearly two orders of magnitude higher than previous estimates, as can be observed in Fig. 12.
- Zircaloy-4
    - Precipitates of δ-hydride are heavily dislocated, contribute to increasing the dislocation structure of the α-Zr matrix, yet display large variations (dislocation density 1.6–10 × 10^{14} m^{-2}) depending on the microstructure and hydrogen content of the parent material (Fig. 13).

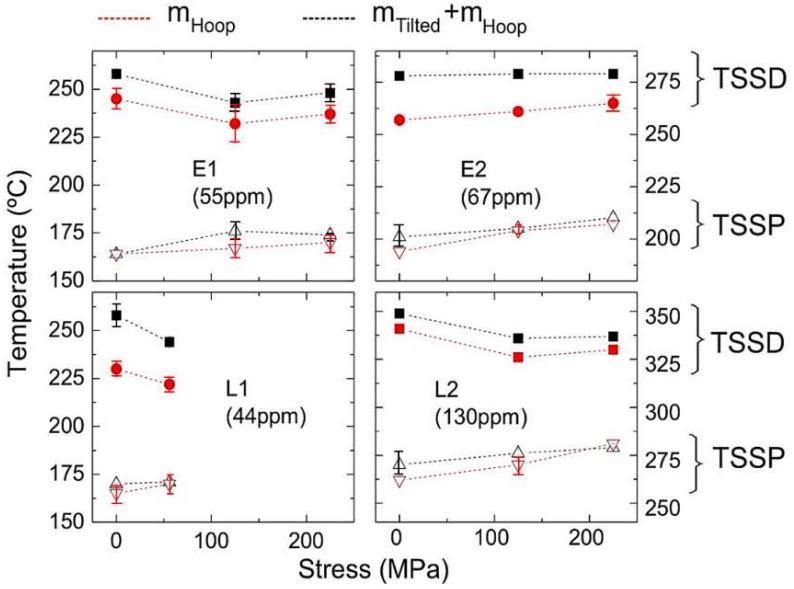

FIG. 12. Dependence of TSSD and TSSP temperatures on applied stress for all Zr2.5Nb specimens investigated. Load was applied along the pressure tube hoop direction. Values are discriminated for hydrides precipitated in α-Zr grains of the orientations represented in Fig. 13(a) (courtesy of CNEA).

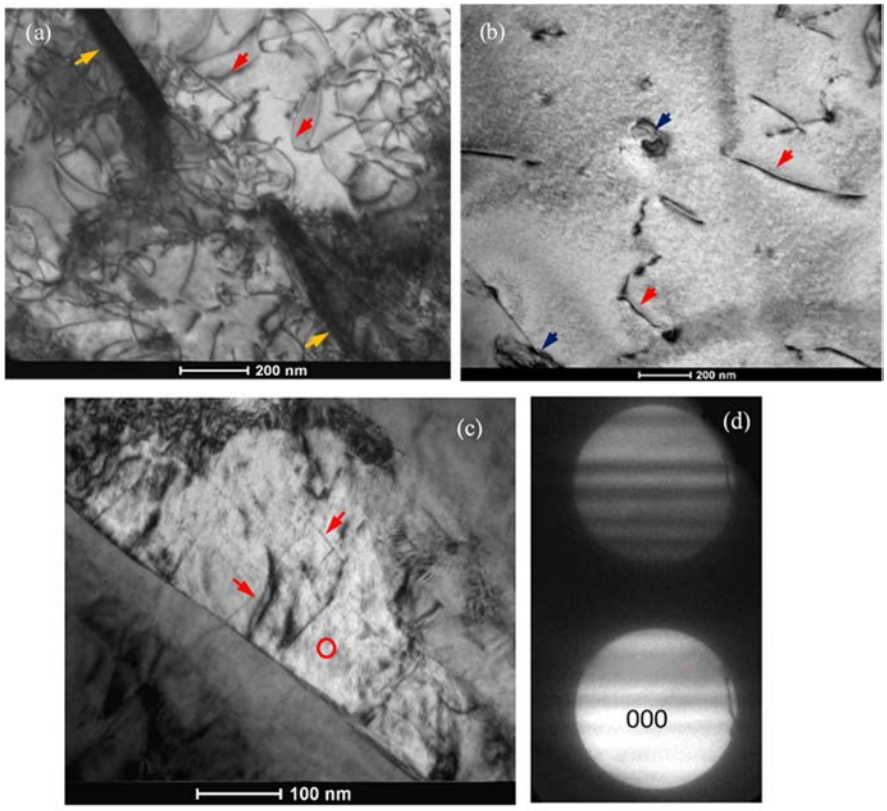

FIG. 13. (a) Bright field images for unirradiated Zircaloy-4 containing 3560 wt ppm H, with reflection 1210 in the two-beam condition. <a> type dislocations in the matrix are indicated by red arrows. Hydrides are indicated by yellow arrows. Measured thickness is 110 nm and dislocation density ~2×10^{14} m^{-2}. (b) Non-hydrided Zircaloy-4 displaying second phase particles (Zr(Fe,Cr)2 type, black arrows) and dislocations (red arrows). The measured thickness is 210 nm; the dislocation density is ~$8\times10^{12}\cdot m^{-2}$. (c) Weak beam bright field of a hydride of the highly hydrided sample (a) with reflection 002 showing dislocations within a hydride (red arrows). (d) Convergent beam electron diffraction (CBED) 220 pattern corresponding to the region indicated with a red circle in (c). The measured thickness is 120 nm (courtesy of CNEA).

5.3.2. France

Activities for understanding fuel behaviour in various conditions are performed in France by IRSN, CEA, and for the impact conditions by Orano TN. Concerning the situation of spent nuclear fuel in dry storage and subsequent transportation, only a few recent results have been released since SPAR-III [6].

CEA previously presented the results of their activities for understanding fuel rod cladding behaviour, such as creep, oxidation, hydride precipitation, hydrogen effects, delayed hydride cracking, and embrittlement. In addition, some other studies covered the behaviour of fuel pellets inside the rods (pellet swelling, fission gas release) [40].

A new model on radial hydride precipitation in Zircaloy-4 claddings under decay stress and temperature transient was presented at the 2015 IAEA International Conference "Management of Spent Fuel from Nuclear Power Reactors" [47, 48]. In summary, radial hydride precipitation is considered as an important issue for Zircaloy-4 claddings in spent fuel transportation and storage. The fuel residual thermal power induces a temperature increase within the shipping cask cavity. As a consequence, the zirconium-hydrides contained within irradiated fuel claddings dissolve as solid-solution hydrogen. After transportation and during unloading in the spent fuel storage pool, the fuel rods are cooled down under internal gas pressure, inducing mainly hoop stress within the cladding. At low hoop stress levels, the precipitated hydrides are platelets oriented in the hoop and axial direction. When the hoop stress exceeds a threshold value, the precipitated hydrides preferably develop along the radial-axial direction. These radial hydrides strongly embrittle the cladding.

Laboratory experimental studies were performed to characterize the degree of radial hydride precipitation at room temperature under constant applied stress after a slow cool-down. The model is successfully compared to reference experimental data.

However, considering fuel assembly transportation, the cladding stress induced by internal pressurization decreases during the fuel cool down. There is a need for differential models providing a step by step prediction of the radial hydride precipitation during the fuel cool down. A new model, describing the influence of an applied stress along with a temperature transient, has consequently been developed and compared to experimental data.

Concerning spent fuel transportation after long term storage, Orano TN has developed a methodology [49, 50] to assess used fuel behaviour in impact and transport accident conditions; the Fuel Integrity Project. A technical guide for the safety assessment has been issued by the competent authority. To support criticality safety evaluation, the amount of dispersed fuel material is evaluated when rod rupture is predicted.

5.3.3. Republic of Korea

5.3.3.1. Thermal creep testing

Given that the changes in cladding mechanical properties resulting from creep deformation are not well understood, they were investigated using ring compression testing (RCT) [51, 52]. The test material used in the study was commercial grade cold-worked and stress-relieved Zry-4 cladding. The cladding thickness (t) and outer diameter (OD) were 0.57 mm and 9.5 mm, respectively. In addition, specimens of irradiated Zry-4 samples were cut from a fuel rod characterized by a burnup of 51.8 GWd/tU. Creep tests were performed on 150 mm long specimens in air using an internal pressurization method to ensure uniform stress distribution. The creep tests were carried out at 330–400°C for up to 8500 hours, with applied stresses of 70–150 MPa. Specimens contained 10–600+ ppm of hydrogen. The outer diameter was

measured using a micrometer (ten measurements per specimen) or laser extensometer following depressurization and cooling to room temperature.

Figure. 14 shows the summary of creep strain of unirradiated Zry-4 cladding with associated measurement uncertainty. As reported previously, the results indicate that an increase occurs in the creep strain with increasing temperature and/or applied stress and with decreasing hydrogen content. The results also indicate that the temperature effect is dominant, rather than the effects of stress or hydrogen content within the range of these conditions. The secondary creep rate at 330°C and 360°C was lower than one tenth of the creep rate at 400°C. Meanwhile, creep rates of the irradiated specimens show similar trends to those of the unirradiated specimen having 600 ppm of hydrogen, although for the bottom side of the irradiated sample, laser measurement data shows a large scatter (Fig. 15). Irradiation hardening and recovery by annealing contributed to the results for irradiated samples.

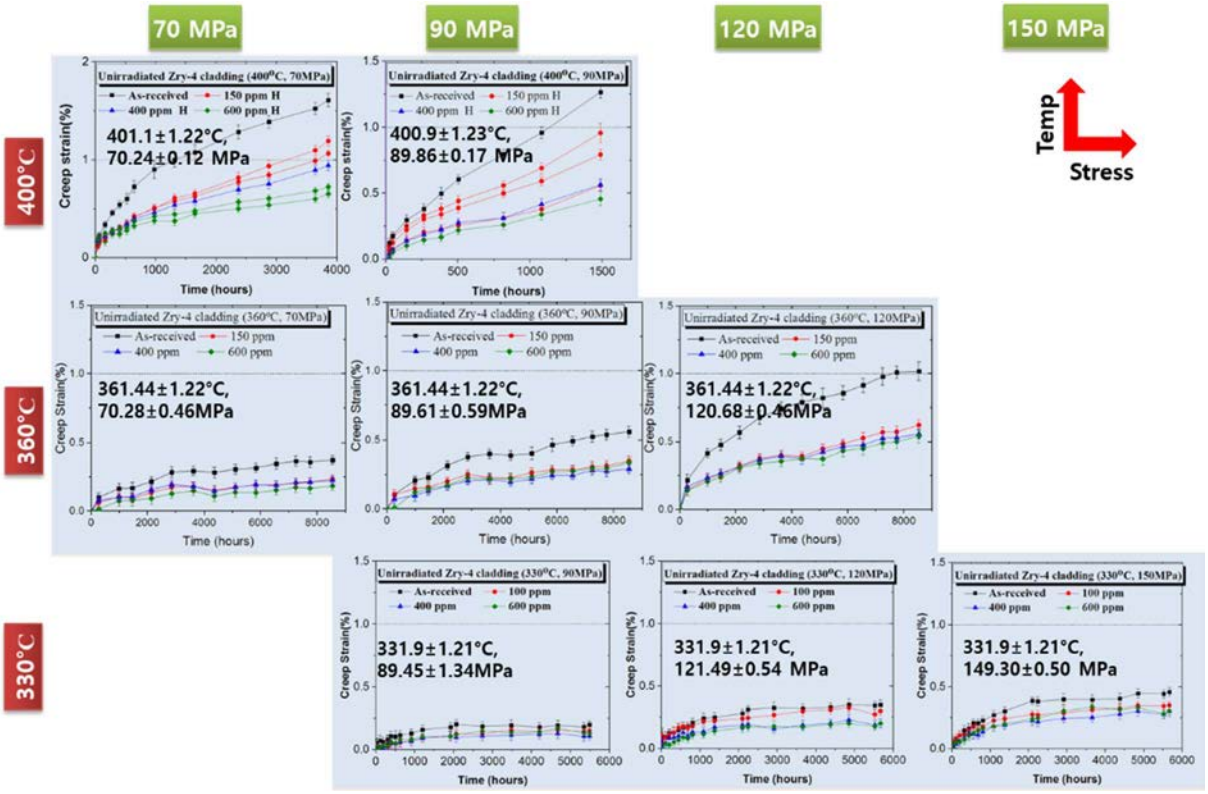

FIG. 14. Summary of creep strain of unirradiated Zircaloy-4 cladding under simulated dry storage conditions (reproduced with permission from ANS).

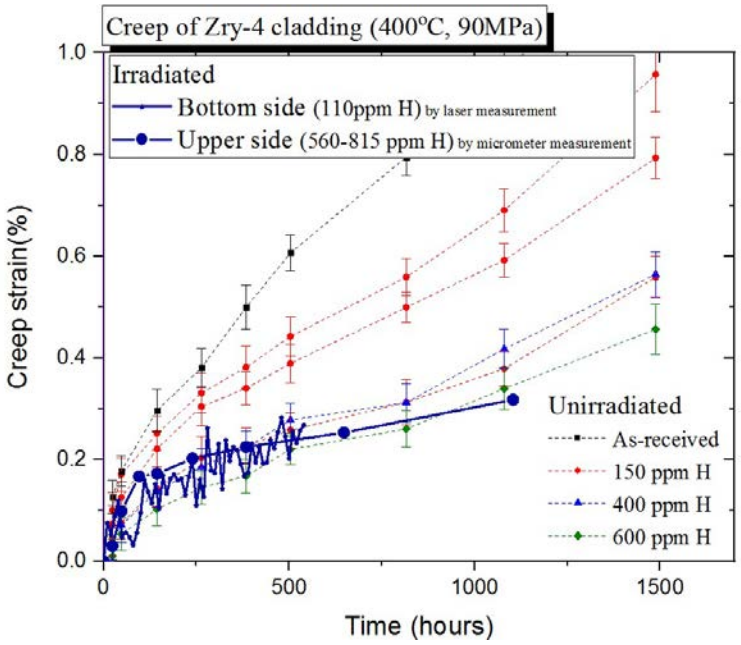

Fig. 15. Creep strain of Zircaloy-4 cladding at 400 °C and 90 MPa (Unirradiated, Irradiated) (reproduced with permission from ANS).

Figure 16 describes the offset strain of unirradiated Zry-4 cladding measured by RCT before and after creep deformation. The ductility decreases with an increase in hydrogen content in all conditions due to the formation of a brittle hydride phase and hydrogen-enhanced plasticity. Also, the changes in ductility were negligible and ductility was maintained after creep deformation. However, reoriented hydrides in the radial direction were observed in some of the creep test specimens when the applied stress was not present during the cooling process, a result that was not expected based on previous experience. The authors of this study indicate that the combined effect of the creep-residual strain and the number of thermal cycles experienced appeared to have promoted hydride reorientation. However, it is well established that hoop stress is the driving force for precipitation in the radial direction during cooling; when no stress is applied during cooling, the driving force for hydride reorientation is not present. Therefore, confirmation of these results would be highly desirable since they are contrary to the present understanding of reorientation phenomena.

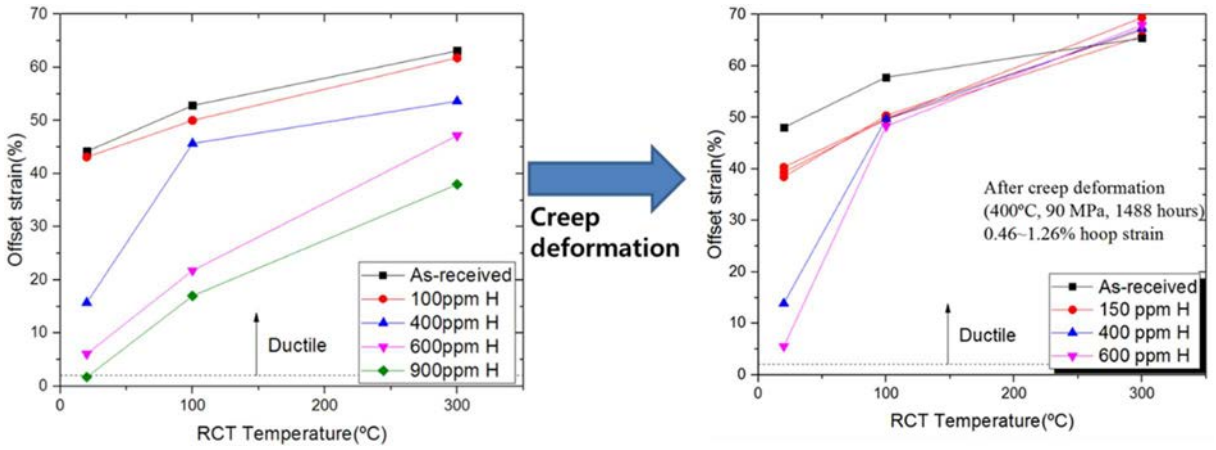

Fig. 16. Changes of offset strain after creep deformation for unirradiated Zircaloy-4 cladding (reproduced with permission from ANS).

5.3.3.2. KAERI's R&D on spent fuel integrity

KAERI's spent fuel integrity R&D work between 2015 and 2019 included both non-destructive and destructive examination of spent fuel with burnups < 45 GWd/tU.

Non-destructive examination of Westinghouse improved Zry-4 14×14 and 17×17 SFAs was undertaken in KAERI's Post Irradiation Examination Facility. The fuel assemblies selected for testing were representative examples from Kori-1 NPP, which will be the first Korean power reactor to be decommissioned and have its spent fuel moved into dry storage. Visual inspection, defect scanning of the cladding surface, gamma scanning for burnup and check for missed pellet, dimension measurement of cladding tubes growth, fuel assembly distortion/buckling, and oxide thickness measurement were all undertaken.

Hydrogen pickup fraction results showed that the fraction increased along the axial rod position and in proportion to the oxide layer thickness, as would be expected, with the fraction value not exceeding the 20% fraction band. For Zry-4, a bounding hydrogen pickup fraction of 20% is acceptable.

The most important data gathered in the SNF destructive tests from a dry storage perspective was the fuel rod internal pressure; this has implications for cladding creep deformation and hydride reorientation during several decades of storage. Rod puncturing data at room temperature shows results under 5 MPa. For rod temperature considerations up to 400°C, calculations of the hoop stress on the cladding inner surface resulted in values below 90 MPa.

Other destructive tests were used to assess creep, hydride reorientation, and delayed hydride cracking.

During the initial period in dry storage, thermal creep was one of the phenomena identified that could affect SNF integrity. Two 30 cm specimens were prepared from two different axial locations of the same rod to identify if there was any dependency on burnup. The method for measuring creep deformation of the first specimen was found to be unreliable due to factors such as the high sensitivity of the laser beam, the detour mirror setting reliance, and imperceptible vibrations around the testing equipment. The second specimen was measured manually. In this case, the heating furnace had to be shutdown to measure the outer diameter of cladding using a micrometer. The initial internal pressure was set to 90 MPa hoop stress level and the test running time was limited to 1100 hours. Data points collected on the secondary creep rate from both specimens demonstrated that the diametral strain was well below the 1% creep deformation limit criterion, so thermal creep was determined to be of no concern under dry storage conditions.

RCT offset strain measurement was used to measure the extent of radial hydride formation. Using a limit of 2% under pinch loading conditions enables cladding to be classified as either brittle (less than 2%) or ductile (more than 2%). For as-irradiated cladding, the hydrogen content's detrimental effect on ductility for samples not subjected to HRT is relatively clear at room temperature, but is not significantly dominant as RCT temperature increases. For selected cases (450 ppm) at temperatures higher than 200°C, as-irradiated cladding is sufficiently ductile. When the hydrogen content is in excess of 450 ppm, room temperature RCT shows more ductile behaviour, which could be explained by the dense hydride distribution layers.

The effect of cooling rate on hydride-related phenomena was also investigated; details of the testing history are planned to be published. This is an interesting R&D topic to determine if there is any relationship between SNF storage duration and cooling rate effect. Laboratory testing has used a cooling rate equal to 5°C/h, whereas in storage the cooling rate is in the region of 3°C/y, which is lower by about four orders of magnitude. Several experiments have been

performed with unirradiated Zry-4 cladding to identify whether the cooling rate has implications for observed hydride behaviours. The tests were performed over 3, 6 and 12 month durations using cooling rates of 0.109, 0.054 and 0.027°C/h respectively. The peak cladding temperature was set at 400°C and the target temperature for the end of testing was set as 100°C. The experimental set up involved canisters, each containing eight 300 mm rods; hydrogen charging for four rods was set as 200 ppm, and 400 ppm for the remaining four rods. The hoop stresses were controlled at 70, 80, 90 and 110 MPa.

RCT results for a three-month cooled HRT specimen under room temperature conditions displayed obvious drop tendency from 30% (one-month cooling case) to 10% (three-month cooling case). It is necessary to recall that room temperature is not the real situation in dry storage and transportation, and this is not irradiated cladding; however, this long term experiment gives unique data to revise cooling rate effect considerations. If hydrogen or hydride has a stronger kinetic effect than known so far, the cooling rate effect should not be underestimated for several decades of dry storage. RCT had been completed at room temperature, 75°C, 100°C, 150°C, and 200°C for the same specimen and showed very ductile behaviour as the RCT temperature increased. An effect of the hydrogen content was observed; for a 200 ppm loading, an decreasing offset tendency was observed, whereas for a 400 ppm loading it was an increasing offset tendency. As the ranges were far outside of those reflective of anticipated storage conditions, further investigation was not undertaken.

The data for the six-month cooled specimens show almost similar values to the one-month cooled data, leading to an investigation to find the cause, which it is not still clearly understood. For the 12-month cooled specimens, the data shows wide variation from 2.85–25%. Even though the lowest value from 12-month data (2.86%), is higher than the 2% offset strain limit, the cooling rate effect test results showed a clear decreasing tendency of offset strain values, based on the limited test cases investigated.

5.3.3.3. Fuel Assembly Hardware Testing

Impact loading on cask/canister down to SNF cladding can be divided into five steps as follows:

(1) Cask/canister;

(2) Basket;

(3) Fuel assembly;

(4) Spacer/grid;

(5) Cladding.

The first and second steps are the responsibilities of the commercial cask vendors, while the fifth step has been dealt with when assessing the effect of cladding degradation mechanisms such as thermal creep and hydriding effects.

R&D covering the remaining third and fourth areas could be conceptually considered together. Points of contact between the spacer grid and fuel rods have high priority in researching SFA hardware. A pendulum-type hammer initiates an impact force on one side of spacer grid and the impact can be spread through each grid cells to the cladding surface.

Because SNF spacer grid testing within a hot cell is extremely limited, using unirradiated spacer grid specimens requires additional SNF simulation conditions (Fig. 17). First, a data set for a

fresh (unirradiated) spacer grid is created; then, cell setting spacer grid data is tested. The meaning of cell setting is to reflect deformation of springs and dimples to mimic the real SNF situation. This technology was supported by KEPCO NF, the nuclear fuel vendor in Korea, under a commercial grade quality control.

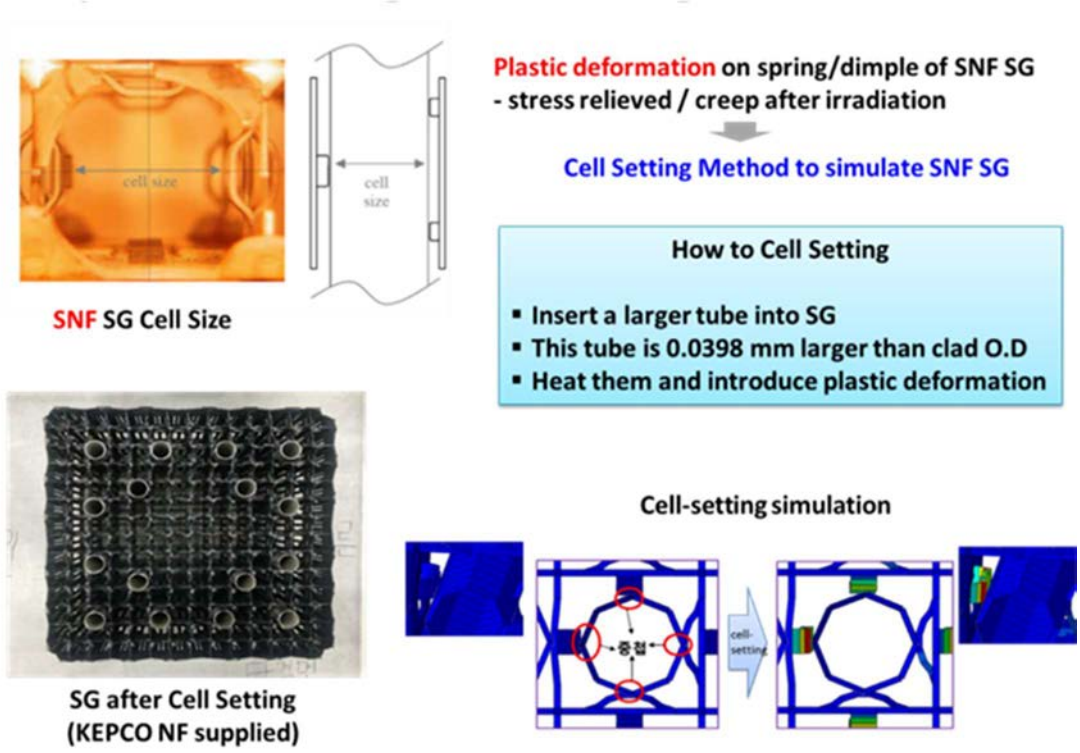

Fig 17. Cell setting for simulating spent fuel spacer grid (courtesy of KAERI).

The final stage was to charge hydrogen into the spacer grid in order to simulate irradiation-induced brittle SNF spacer grid conditions. Hydrogen charging experiments showed failure at the start. Gaseous hydrogen charging of Zircaloy spacer grid plate was challenging; dozens of test results showed a wide range concentration from 19–1701 ppm. Additional experiments were performed for improving homogeneity in hydrogen content. Finally test results showed more even concentration behaviour from 114~181 ppm in the inner side of the spacer grid, and from 85~535 ppm in the outer side of the spacer grid.

5.3.4. Spain

The Spanish spent fuel management strategy considers a centralized temporary storage (CTS) facility to store the entire Spanish inventory. In order to achieve this, spent fuel is first loaded at the reactor sites into systems designed and licensed to comply with regulations covering initially at-reactor storage and subsequent transportation to the CTS. These requirements presently impose specific restrictions on the selection of fuel assemblies that can be loaded at the reactor sites. Therefore, R&D has been focused on spent fuel behaviour in storage and during transport, with the goals of increasing the number of fuel assemblies suitable for loading and gathering more and better-quality data for systems licensing.

The R&D projects reported during SPAR-IV investigated two main topics:

- The phenomenon of spalling that affects a number of SFAs using Zry-4 cladding; spalling may challenge cladding behaviour under spent fuel transport accident conditions;
- The effect of normal conditions of transport on spent fuel as part of an international project.

Another area of increasing interest is ageing management. An R&D project was launched to test methods for monitoring the temperature around a canister based system located at a Spanish facility; a summary is given in Section 5.3.4.3. with the full results of this work reported as part of the IAEA CRP T21028 Ageing management programmes for dry storage systems.

5.3.4.1. Spalling

In some spent nuclear fuel discharged from Spanish PWRs, the cladding was fabricated from cold-worked stress-relieved annealed Zry-4. As a result of the corrosion process during reactor operations, the Zry-4 cladding is oxidized to form a zirconium oxide layer while hydrogen is simultaneously partially absorbed into the cladding alloy matrix. During in-reactor service, hydrogen is in solid solution until the solubility limit is reached; when this happens, the excess hydrogen precipitates in the form of zirconium hydrides. The mechanical properties of this composite system of hydrides in a zirconium based metal matrix are well known.

However, if the zirconium oxide spalls off during operation, a cold spot is formed (because the oxide layer behaves as a thermal insulation barrier) to which hydrogen may migrate and precipitate. At high hydrogen levels, the zirconium hydride can form a hydride blister. Since hydrides are relatively brittle compared to the metallic cladding alloy, the presence of hydride blisters in the Zry-4 spent fuel cladding has been identified as a degradation mechanism, which could potentially compromise its structural integrity during the further processes of dry storage and transportation.

In order to investigate blister characterization as a defect in Zry-4 and its effect on the mechanical behaviour of the cladding, a Spanish programme involving Enresa, Enusa and CSN was developed. The programme had two parallel components; one using irradiated material and the other using non-irradiated cladding.

First, spalled oxide fuel rods from Spanish reactors were metallographically and mechanically examined. It was observed that most of the spalled oxide areas did not present any blisters beneath. The few blisters found were fully characterized and the hydrogen concentration and distribution through the cladding thickness determined. Figure 18 shows one of the blisters found after a mechanical test [53].

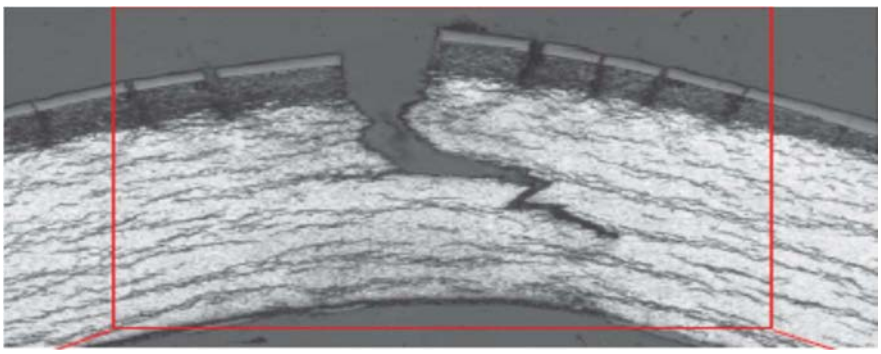

FIG. 18. View of a hydride blister in an irradiated spalled rod after mechanical testing (courtesy of CSN).

In addition, several mechanical tests were carried out — burst, ring compression and 4-point bending tests — covering the stress state of the fuel rod during dry storage and transport accidents. The results of these tests quantified the impact of the hydride blister on the mechanical performance of the fuel rod. In particular, the 4-point bending test was remarkable because it was performed on a fuel rod segment with pellets inside, showing the margin that the fuel column provides to the fuel rod under bending, even with a blister present in the cladding (Fig. 19).

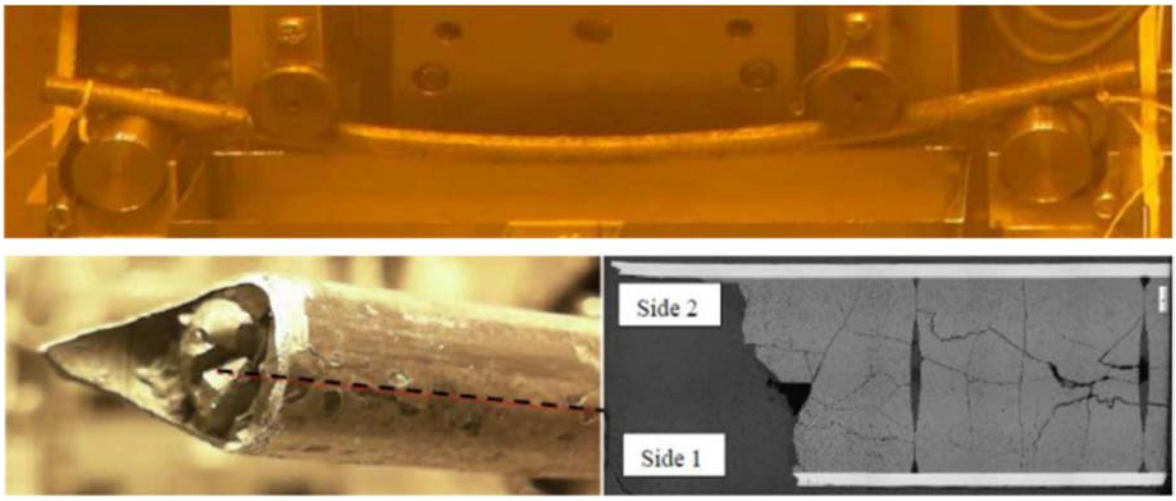

FIG. 19. Bending testing on irradiated spalled fuel rod segment (courtesy of CSN).

Non-irradiated clad tests were performed at the Polytechnic University of Madrid (UPM) on samples with artificial blisters. The blister generation technique developed during this programme resulted in samples with blisters of differing characteristics (dimensions, morphology, and hydrogen concentration); two of them are depicted in Fig. 20 [54].

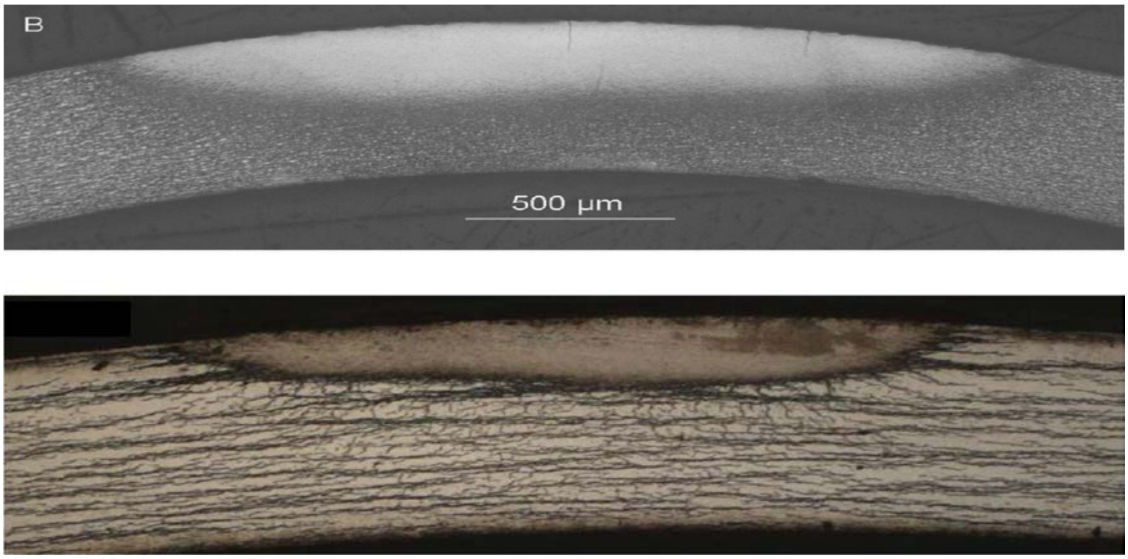

FIG. 20. Artificial blisters with different characteristics (courtesy of UPM).

Both the irradiated and non-irradiated tests collected a complete set of metallographic and mechanical test results that correlated the blister characteristics with their impact on the mechanical properties of the cladding.

In addition, mechanical properties and the constitutive stress-strain curve of the hydride blister were obtained from nanoindentation measurements combined with numerical modelling by finite element analysis as is shown in Fig. 21 [55].

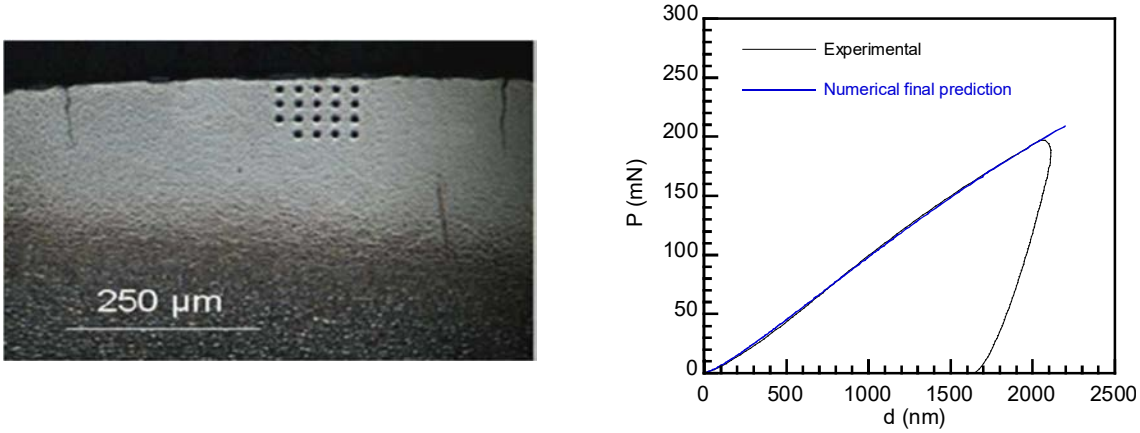

FIG. 21. Measurement of Young Modulus on hydride blister (courtesy of UPM).

Results gathered from this work were used for justification of classifying part of the SFA population with spalled fuel as 'undamaged' for dry storage and transportation conditions. This justification was accepted by the regulatory authority (CSN) in February 2018, and some spalled assemblies were successfully loaded thereafter. Additional work is scheduled to enlarge the population considered undamaged by performing similar and more specific analysis.

5.3.4.2. Normal conditions of transport

Paragraph 613 of the IAEA Transport Regulations, SSR-6 (Rev. 1) [56] states that a "package shall be capable of withstanding the effects of any acceleration, vibration or vibration resonance that may arise under routine conditions of transport without any deterioration in the effectiveness of the closing devices on the various receptacles or in the integrity of the package as a whole". A joint project between USA, Korean and Spanish entities was conceived and designed to quantify the shocks and vibrations SNF experiences during normal conditions of transport[8] [57]. This work is discussed in Section 7.2.1.

5.3.4.3. Cask Temperature Monitoring

From June 2014 until September 2015, an optical 'fibre Bragg grating' (FBG) type system monitored in real time the vertical profile of the annulus between the canister and overpack for a HI-STORM 100Z system loaded with spent nuclear fuel at the Jose Cabrera NPP ISFSI [58]. The HI-STORM 100Z is a variant of the HI-STORM 100 system, adapted for the Jose Cabrera NPP specific fuel assemblies.

The aim of the project was twofold: firstly, to show the feasibility of FBG monitoring technology under real temperature and radiation exposure conditions, in view of further developing an ageing management monitoring system, and secondly, obtaining a thermal profile of the annulus for comparison with thermal models.

[8] Routine conditions of transport are incident free, whereas normal conditions of transport include minor mishaps.

The project allowed for the development of a monitoring system, with its associated commissioning and decommissioning procedures, for a canister-based spent nuclear fuel system (in this case, the HI-STORM 100Z). Four sensing fibres (two with Type I FBG and two with Type II FBG sensors) were installed, one at each overpack outlet (See Fig. 22).

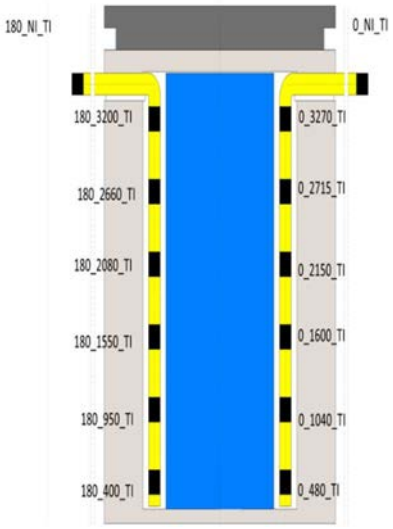

FIG. 22. Type I monitoring sensors on two opposing outlets (0° and 180°). Type II FBG sensors were installed at 90° and 270°, not shown (courtesy of IFCA (CSIC-UC)).

After commissioning, the system operated for 15 months without incident, with no data interruption issues; more than 2 million data sets were recorded from the system. The analysis showed that less than 1% of the readings were anomalous, with anomalies due mainly to quick and spurious fluctuations of the measurements, defined as >3σ compared with the trend.

Type II sensors showed an instable behaviour due to interference from the excessive number of sensors per fibre. The data analysis was considered to be not reliable enough, so Type I fibres were used for the thermal profile analysis.

A clear correlation was shown between the internal FBG sensors and the external FBG sensors, as well as with the ambient temperature registered by the meteorological station at the NPP site. Seasonal and day-night cycles were correctly observed.

The wave signal characteristics (Bragg peaks) were analysed. The changes observed on the signal over time did not impose a relevant signal degradation from the point of view of Bragg peak detection and reconstruction. However, a displacement was observed, resulting in an increasing bias over time on the temperature measured due to radiation. The bias observed can presumably be avoided during a future test by using pre-irradiated and saturated fibres.

Thermal models were developed and a benchmark was performed with publicly available data from the licensed system. Then, selected data sets were chosen for comparison with the benchmarked model. However, models were not conclusive for detailed comparison between measured and calculated data. This is due to the relatively important temperature change in the annulus between the canister and the overpack, the lack of certainty on the position of the sensor when installed, and the influence of the source term determination on the model. Even though the source term was calculated at the moment of commissioning of the monitoring system, using the licensed model for SFAs vs. a best-estimate model showed differences in the range of 8–13% for every fuel assembly among the 32 assemblies loaded, mainly due to conservatisms introduced into the licensing calculations.

A future project is being envisaged in support of AMPs in Spain, refining the monitoring system and the models used to analyse them.

5.3.5. Switzerland

5.3.5.1. Mechanical testing of spent nuclear fuel

In Switzerland, spent fuel is planned to be transported in DPCs from interim storage to the planned repository surface facility, for encapsulation in FDCs and subsequent disposal in the deep geological repository [19]. Therefore, the performance of SNF during dry storage, transport and handling operations has to be properly considered with respect to aspects relevant to SNF and cladding degradation [59], in particular focusing to the unloading/loading of the SFAs in the hot cells at the Nagra encapsulation facility. Several docking stations dedicated to DPCs and to FDCs are planned to operate simultaneously. A simplified illustration of the SFA handling and canister encapsulation operations is shown in Fig. 23. Each DPC will be transferred from the interim storage facility to the Nagra encapsulation facility. The DPC will eventually be loaded into a hot cell where the SFAs will be transferred into the FDCs using a crane.

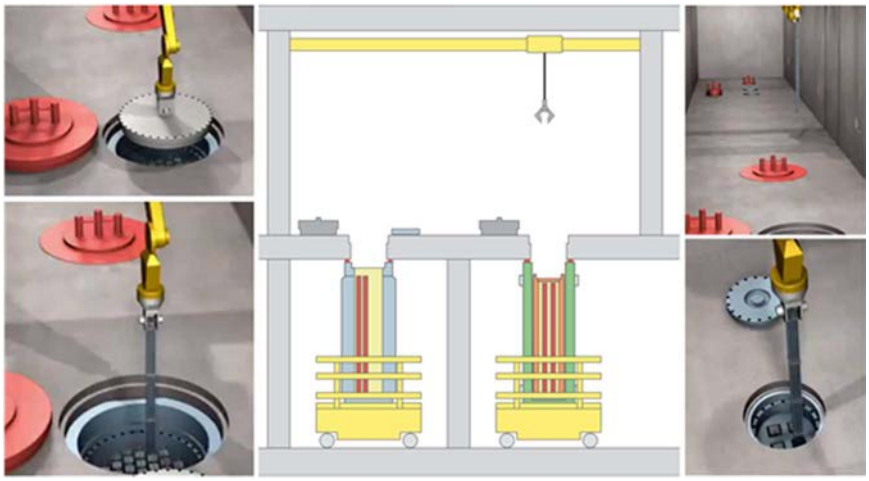

Fig. 23. Simplified illustration of SNF unloading/loading in the Nagra encapsulation facility. DPC docking station (left), canister docking station (right) (courtesy of Nagra).

In line with the decision by the Swiss Federal Council and ENSI Guideline [60], Nagra together with JRC Karlsruhe, and with the support of the fuel owner (Gösgen NPP) and the fuel vendor (Framatome AG), initiated several studies and research, development and demonstration activities aimed at not only assessing the mechanical performance of spent fuel with respect to pre-disposal activities, but also at developing concepts for handling scenarios resulting in fuel rod breakage.

The main experimental campaign is being conducted in JRC Karlsruhe taking advantage of their hot cell facilities and their past experience in mechanical testing of SNF [61]. The focus of the experimental studies is to verify the response of spent fuel rods to mechanical stresses and to investigate any possible effects of hydrogen content, hydride distribution and fuel–cladding interaction on cladding integrity. The campaign is carried out using mainly PWR UO_2 spent fuel rod segments with different burnup levels, varying from low burnup (18 GWd/tHM) to ultra-high burnup (100 GWd/tHM). Fuel rods were cut in segments, pressurized to the original fuel rod pressure after discharge, and then subjected to bending and impact tests.

The main emphasis was to test commercial SNF rods in their original composite fuel–cladding configuration, in order to be more representative of real post-irradiation conditions. Furthermore, the results could be directly correlated to the hydrogen content in cladding, such as soluble hydrogen concentration and hydride formation, orientation, and distribution. This investigation could provide evidence of any changes of SNF mechanical properties with respect to irradiation conditions.

The first main achievement consisted in observing and analysing the behaviour of the fuel–cladding system when stressed with external loads, both in quasi-static and dynamic regime. Three-point bending tests were carried out to study the mechanical response of the sample by derivation of load-deflection curves. All samples experienced plastic deformations, but at different extents and under different applied loads. The higher the burnup was, the stiffer the material was. The rupturing load for the high burnup sample was higher with respect to the lower (ca. 20% for samples reported in Appendix II).

Another major achievement resulted from the analysis of the consequences of a fuel rod break, i.e. assessment of the fuel mass released from bending and impact tests. The observed equivalent masses of fuel dispersed during both type of experiments was significantly less than a single fuel pellet. Only fuel fragments from the immediate vicinity of the rod fracture locations were released. For decontamination studies, the characterization of fuel fragments and particles released is of great interest.

Furthermore, an image analysis methodology was developed to elaborate the behaviour of the samples under dynamic loads. Optical and electron microscopy were used to observe the morphology, orientation, and population of the cladding hydrides, whereas the overall hydrogen concentration in the cladding was measured by a hot extraction technique. Size distribution analysis on the released fuel particles was also performed. The study is customized by modelling to evaluate the individual phenomena and parameters affecting the SNF properties.

A description of the Nagra/JRC experimental campaign, including recent results, is given in Appendix II.

5.3.5.2. Cladding Integrity Studies

Other research activities in Switzerland have focused on demonstrating fuel cladding integrity and have been performed by PSI mostly on behalf of the Swiss nuclear industry and, more recently, also by Nagra. Cladding properties, i.e. understanding thermal creep properties, fatigue behaviour of cladding [62], hydride distribution and reorientation, impact of liner on hydride distribution, cladding oxidation, and study on failure mechanism by DHC, have been investigated using surrogate materials as well as commercial fuel samples from BWRs and PWRs with different burnups.

The direction of formation of hydride in fuel cladding tube is a major issue for the assessment of the cladding's remaining ductility after service. In Ref. [63], the reorientation behaviour of a Zircaloy-4 DX-D4[9] cladding sample with ~72 GWd/tHM burnup was investigated. This involved determining how repeated thermo-mechanical loading resulted in an increase of the fraction of reoriented hydrides; the use of pure thermal loading cycles to determine how a state of minimized reoriented hydrides could be recovered was undertaken in addition. A qualitative assessment of the hydrogen density in the duplex layer was carried out, showing a dependence of the hydride density on the hoop stress state.

[9] DX-DX is also known as Duplex D4.

During dry storage and transportation of spent fuel, there is a concern for the cladding ductility linked to the potential for the reorientation of circumferential zirconium hydrides subjected to hoop stress to the radial orientation; it should be noted that this concern is only applicable to those hydrides that are dissolved during the start of dry storage, when temperatures are at the maximum. Cladding liners can prevent this reorientation; examinations of irradiated cladding materials have shown a significant hydrogen migration into the liner post cool down. The migration of dissolved hydrogen in samples of cladding materials was investigated at slow cooling rate for fuel employed in Swiss LWRs. Analysis results show no significant evidence of hydride reorientation, in agreement with the examinations noted previously; material undergoing slow cool down showed little evidence of hydrides, and where hydrogen concentrations were higher, insufficient hydrogen in solution to initiate reorientation [64].

Hydrogen uptake in zirconium claddings is one of the most limiting factors of fuel rod lifetime in LWRs, including subsequent spent fuel handling, storage, and transportation. Hydrogen diffusion under stress is the physical process underlying delayed hydride cracking. A quantitative hydrogen concentration was measured by high-resolution neutron imaging, allowing analysis on stress-induced hydrogen concentration fields in a sub-10 μm scale by referring to the stress field calculated by finite element modelling. A notched Zircaloy-4 sheet was pre-charged with ~600 wppm of hydrogen followed by annealing for homogeneity. Then the sample underwent a thermo-mechanical test. Before and after the test, neutron imaging was consecutively performed to determine the variation of the hydrogen concentration field due to the stress. The results revealed an area of hydrogen concentration at the notch, with a concentration gradient detectable over 700 μm. A maximum elevation of 160 wppm hydrogen was found at ~200 μm off the notch, where the largest tensile stress is located (according to finite element analysis) [65].

In order to quantify hydrogen diffusion occurring under stress conditions, high resolution neutron radiography (~10 μm) was used to measure the diffusion of solid solution hydrogen under a stress raiser. A thermo-mechanical test was completed using a Zry-4 notched plate with ~600 wppm hydrogen. An elevated concentration of hydrogen was observed at the notch; a hydrogen gradient with a maximum elevation of 130 wppm was detected over 700 μm. Using hydrogen-induced anisotropic transformation trains as the hydrogen diffusion driving force and utilizing the Cauchy stress tensor, finite element computation was then performed [66].

Concerning the DHC behaviour, current work aims to investigate the fracture mechanics of unirradiated Zircaloy-2 cladding tubes based on the various cases of crack propagation [67]. The experiments focused on induction of directionally specific oriented DHC. Specimens varied in geometry and hydrogen loading, while experiment conditions varied in test temperatures and loading setups. Induction of axial cracks occurred through tensile loading of complete ring sections, while radial cracks occurred through compression of C-shaped ring samples. Post DHC examinations were also carried out using light optical microscopy, focused ion beam, scanning electron microscopy, fractography, and neutron radiography, having the scope to observe the hydrogen precipitation around the crack tip and relative to the cladding grain structure. While the axial crack displays hydrides aligned parallel to the crack flanks, the radial crack also displays hydrides that are perpendicular to the crack flanks, probably due to the loading conditions. The crack directions appear to play a role in the re-orientation of the hydrides, however more tests are to be done to confirm these observations. Fractographic results provided initial estimations of the crack velocity of the two different crack orientations which are well in line with what is expected in literature. The shape of the crack front was also observed allowing for post-test modelling of the stress intensity factor. Additionally, the crack front gave insight into how the forces acted on the sample. Through neutron imaging,

radiographs illustrate a qualitative view of the hydrogen concentration around the crack edge. Finite element modelling supports estimated stress fields as well as stress intensity factors expected at various stages of crack propagation. Further work is to be done to confirm tendencies in hydride re-orientation with respect to crack direction and give a larger statistical base for crack velocity estimation.

5.3.6. Ukraine

The design of the SNF containers can make direct simulation of their thermal state difficult. Large differences between characteristic sizes (for example, height of fuel rod and its diameter) require high quality meshing, increasing computational time and requiring high speed computer clusters. One approach is to divide the calculation into separate parts and combine the results. For calculating the temperature of WWER fuel in VSC-24 type containers, an iterative methodology based on this approach was developed, as illustrated in Fig. 24 (partially described in Ref. [68]).

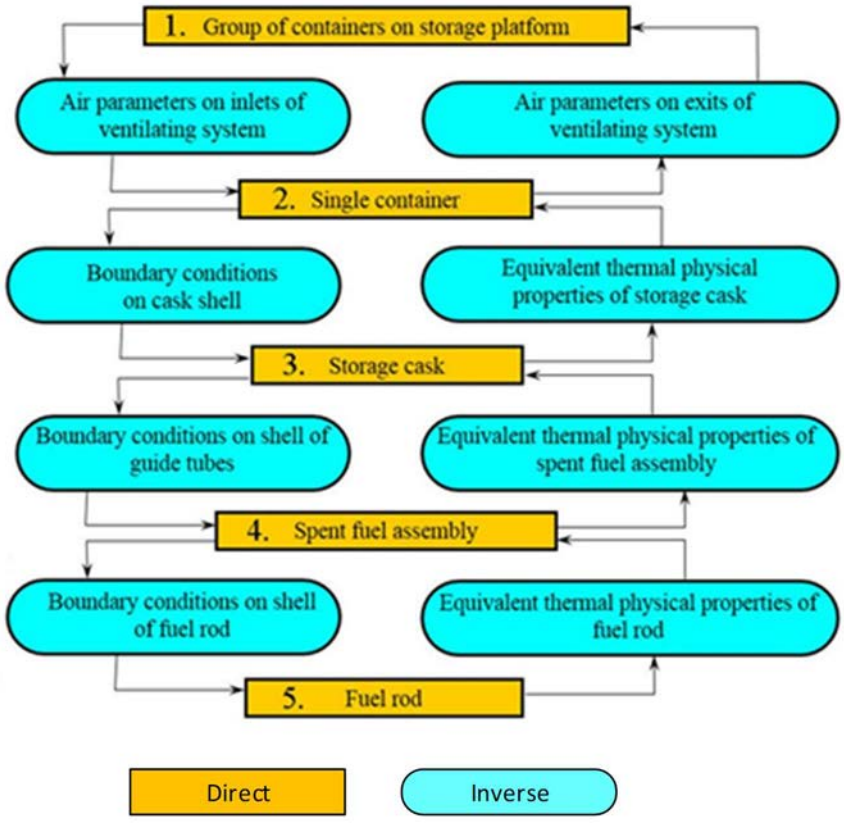

FIG. 24. Iterative methodology of the SNF thermal state definition (courtesy of S. Alyokhina).

The methodology involves the combination of direct and inverse heat transfer problems. The calculations are then processed iteratively, with initial simplifications later replaced by calculated boundary conditions from corresponding calculations. Typical results are illustrated in Fig. 25.

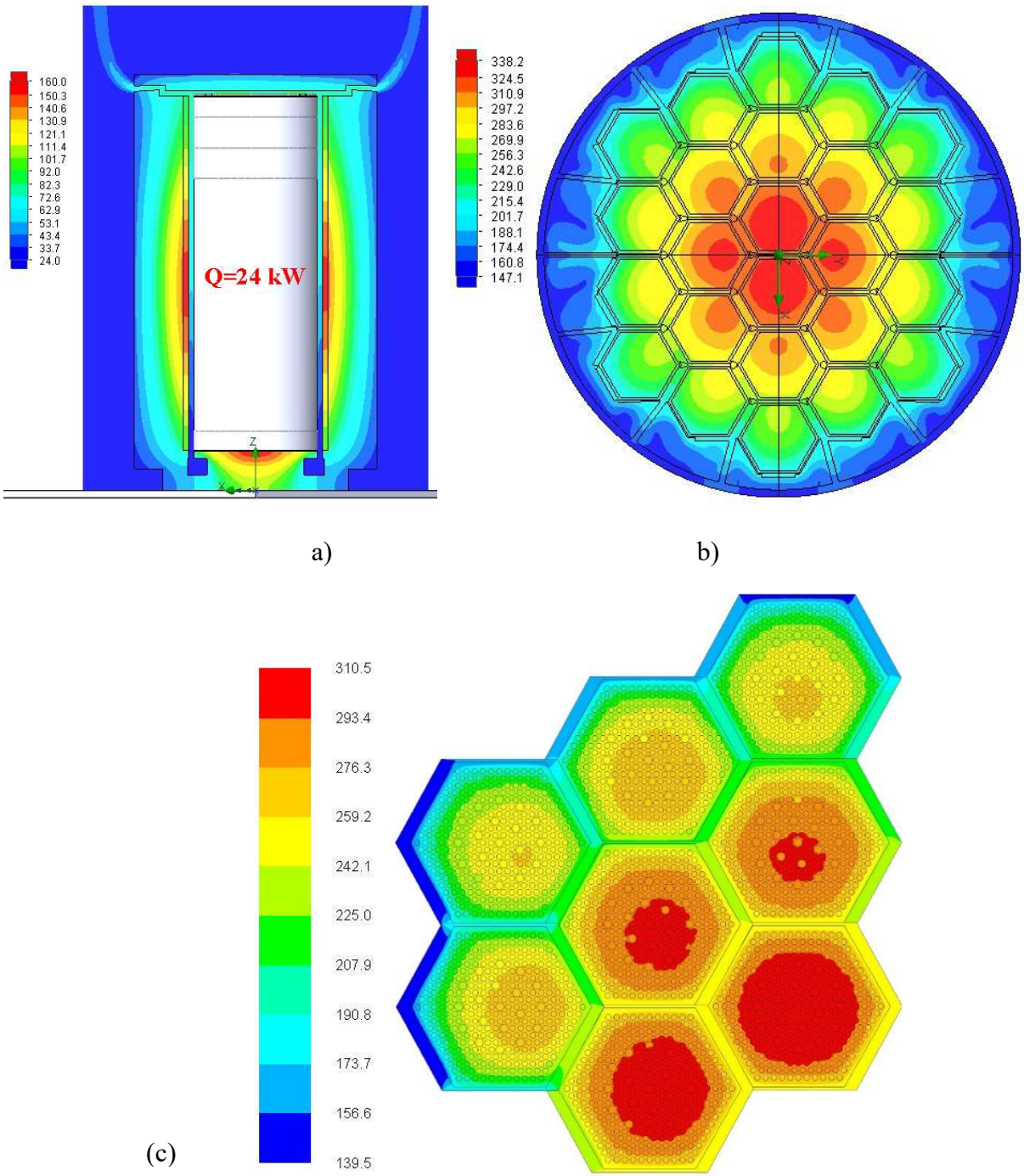

FIG. 25. Temperature profile of the spent nuclear fuel under dry storage in the ventilated container (courtesy of S. Alyokhina).

These simulations were completed for the VSC-24 type containers at Zaporizhye NPP, which are stored in the open air and are therefore exposed to external influencing factors on their temperature. These factors, which may occur under normal or accident conditions, are illustrated in Fig. 26.

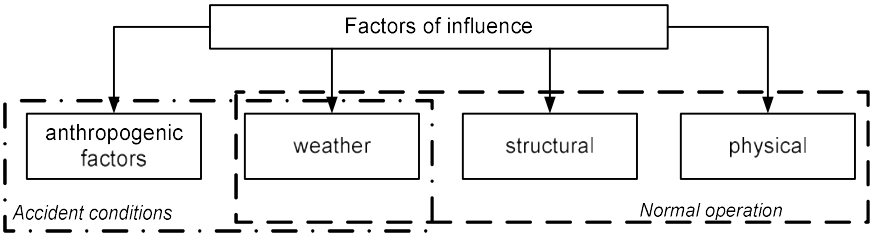

FIG. 26. Classification of the factors which have influence on the thermals state of SNF (courtesy of S. Alyokhina).

The physical factor of influence (decay heat) and weather factor (temperature of atmospheric air) have to be taken into account to calculate (predict) the maximum temperature inside a storage container. Based on results achieved by numerical simulation, the dependence of the maximum temperature (T_{max}) in storage container from decay heat (Q) and temperature of atmospheric air (T_a) is determined by Eq. (1):

$$T_{\max} = 26.96 + 0.74T_a + 0.014Q - 0.0036T_a^2 - 1.141 \cdot 10^{-7} Q^2 + 1.07 \cdot 10^{-5} T_a Q, \quad (1)$$

and the temperature of the ventilated air (T_{exit}) could be calculated from Eq. (2):

$$T_{exit} = 8.13 + 0.8694T_a + 0.002Q - 0.00085T_a^2 - 1.432 \cdot 10^{-8} Q^2 + 6.116 \cdot 10^{-6} T_a Q. \quad (2)$$

The dependence of the maximum temperature from the wind direction and velocity is presented in Fig. 27.

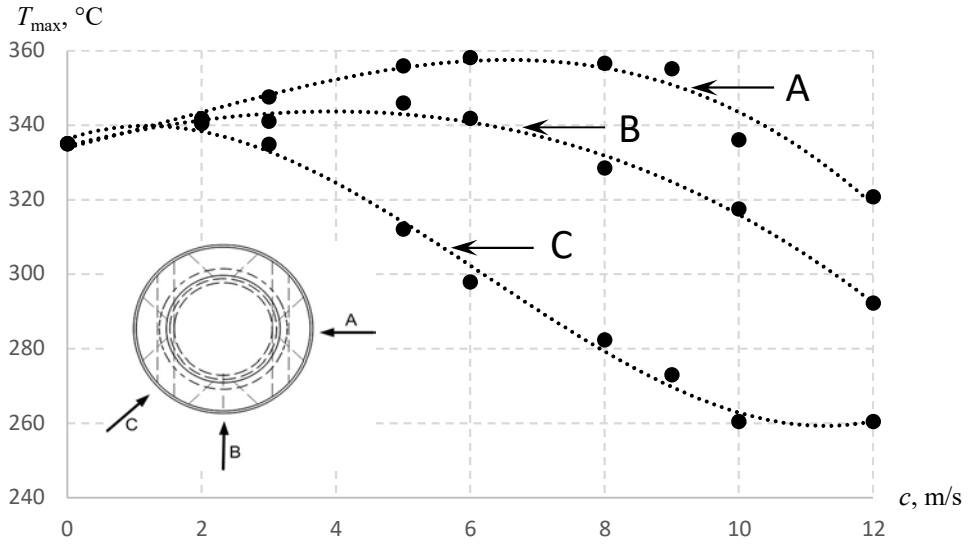

FIG. 27. Maximum temperature in storage container depending of wind direction and velocity (courtesy of S. Alyokhina).

Other factors of influence onto the thermal state of SNF, including the daily temperature fluctuations [69] and solar irradiation [70] were investigated. Both were found not to have a large influence on the temperature of spent fuel stored inside the VSCs.

Modern CFD techniques were used to analyse a whole range of accident scenarios. The loss of cooling for the dry storage containers would be the most significant accident from a thermal perspective [71]. Such a situation could arise due to a ventilation duct blockage or reduction in duct capacity. The highest temperatures were obtained for a VSC falling onto its side and blocking the outlet vents (Fig. 28), which is as expected given that cooling is via natural circulation through the VSC.

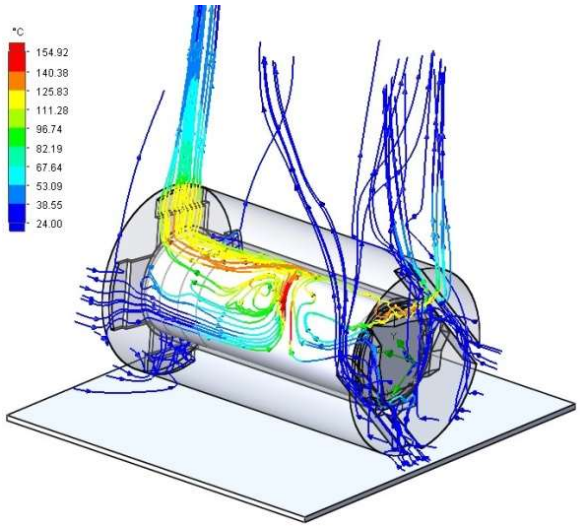

FIG. 28. Flow structure at container falling down (courtesy of S. Alyokhina).

5.3.7. United Kingdom

AGR fuel cladding is manufactured from a ductile, corrosion-resistant stainless steel. However, the effects of long-term exposure to high temperature and neutron fluxes during irradiation lead to changes to the fuel pin that reduce the resilience of the cladding. A wide range of potential cladding failure mechanisms have been examined, leading to the identification of two mechanisms that are of greatest concern during drying and dry storage: stress corrosion cracking in fuel that has been sensitized during irradiation and creep failure of fuel [70]. The remainder of this section presents recent work addressing aspects of these two uncertainties.

5.3.7.1. Cladding creep in AGR fuel

The dominant concern in relation to creep failure during storage arises from exposure to elevated temperatures, during either drying or storage. Work has previously been done to identify a likely upper acceptable limit for AGR fuel storage using NNL's fuel performance code ENIGMA. As it was exploratory, a highly conservative fuel irradiation was used to give an indication of the likely lowest level for a maximum temperature limit. The results provided a clear indication that the bounding fuel could experience temperatures of up to around 600°C during drying/dry storage without significant risk of creep failure and that storage of AGR fuel at temperatures up to at least this level should be acceptable with respect to creep failure [72].

The assessment did not address the effects of long-term fuel swelling that occurs due to the build-up of interstitial helium produced by alpha decay in the fuel matrix and its interaction

with defects in the lattice structure. At expected storage temperatures, defect annealing is not expected and hence there is a potential for fuel to swell to a level that could affect the conditions experienced by the cladding. Information from accelerated testing indicates that the swelling eventually reaches a maximum of around 2% [73]. Since there is a loss of ductility in AGR fuel cladding during irradiation, NNL recently undertook an initial assessment of this 'gap'.

Changes to ENIGMA 5.2a were made to simulate helium lattice swelling due to alpha decay damage, using a simple lattice swelling model, based on Ref. [73]. This model has previously been incorporated by USNRC into their fuel performance code FRAPCON.

Four cases were assessed using existing literature surveys to determine best estimate and upper bound values for the fitting parameters in the swelling equations from Refs [73, 74]. The fuel swelling during irradiation and initial storage are identical as they are conducted for the same, bounding, irradiation conditions and the additional swelling due to post-discharge effects is in the range 1–2% (Fig. 29). It is also clear that only under the most pessimistic conditions will the swelling be likely to result in lattice swelling saturation during interim storage of AGR fuel, which is expected to be less than 100 years.

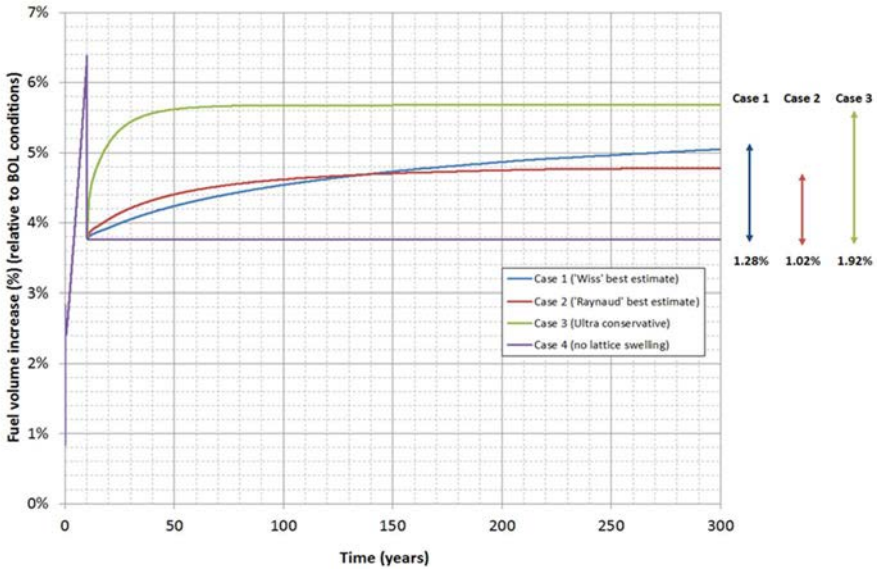

FIG. 29. Failure probabilities for AGR fuel (courtesy of NNL).

The impact of volume swelling on the cladding strain and failure probability of the fuel during storage was assessed using ENIGMA, in the same manner as the higher temperature creep failure assessment referred to above. For the best estimate case, the effects of fuel volume swelling after around 700 years are estimated to be below the 5% failure probability typically used as the basis for reactor safety assessments; more specifically the impact is predicted to be:

- An increase in plastic clad strain from 1.5%[10] to 2.0%;
- An increase in cladding failure probability from 4.6%[10] to 4.9%.

[10] Values at the end of a highly conservative irradiation.

Therefore, it can be concluded that the majority of the risk from creep failure is related to damage occurring during in-reactor rather than post-irradiation helium lattice swelling and that the additional failure probability due to helium lattice swelling over 250 years is not significant compared with the effects of irradiation.

The predictions generated by ENIGMA at long cooling times show some unexpected variations in concentrated cladding stress at the later stages of the cooling period modelled. This is thought to be related to either:

- Modifications introduced to accommodate post irradiation conditions, or
- Localized strain followed by relaxation at the fuel–cladding interface.

The observation does not affect predictions in timescales relevant to storage and is in alignment with observations made by EC-JRC, but warrants further investigation to provide greater confidence in the conclusions.

5.3.7.2. Drying of AGR fuel deposits

Since a small proportion of the fuel discharged from AGR reactors is sensitized to localized corrosion, it is important to understand whether the environment within a storage system will support localized corrosion. The quantity of water that can be carried over into drying and dry storage and the difficulty of removing water from the fuel are therefore important.

In CO_2 gas cooled reactors, radiolysis of the coolant results in the formation of carbonyl radicals which cause the deposition of a dense carbon layer on the cladding surface. The morphology and thickness of the layer can vary considerably in response to changes in coolant chemistry and operating temperatures; examples are shown in Fig. 30. Some of the deposits have complex structures which suggested that it could be difficult to remove adsorbed water from the deposits and therefore work was undertaken to measure the drying behaviour of such deposits.

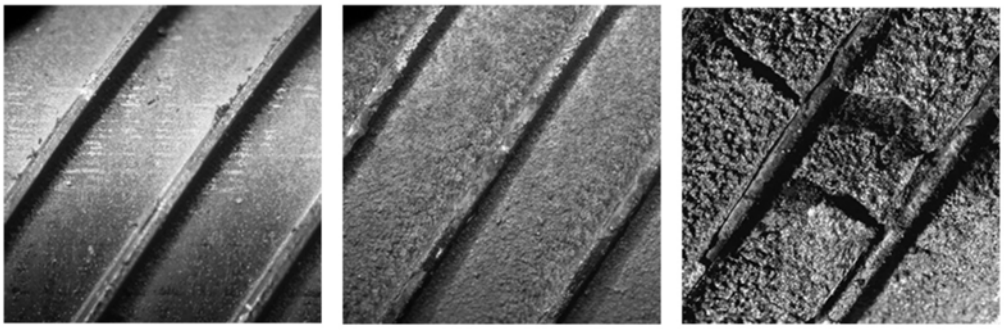

FIG. 30. Examples of carbonaceous deposits (presented by D.I. Hambley at EPRI Extended Storage Collaboration Programme Winter Meeting November 13–16 2017, Charlotte, NC, USA and reproduced with permission).

The literature on water adsorption onto carbon surfaces is not extensive and observed behaviours are greatly affected by microcrystal sizes, the densities and species of surface groups, the topological nature of the pore structures and pore size distribution [75].

A total of 12 samples of fuel pin deposits (each a few mm in size) were selected for subsequent testing to determine whether the extent to which the irradiated deposits resembled the simulants. The deposits selected were all representative of the thickest deposits as these could be reliably removed and were relatively large enough to facilitate drying measurements. Testing was conducted with demineralized water to understand the fundamental behaviour of water–deposit interactions and in a solution containing NaOH dosed to the normal pH used in the storage pools. In order to maximize water loading into the complex deposit morphologies, the samples were loaded into the solution and a vacuum was applied to draw out gasses in accessible pores.

A nominally dry deposit sample, that had not been immersed in water, showed no significant mass loss below 100°C and a small reduction in mass (2%) at 200°C. However, the recorded range is not much greater than the measurement error and hence may not be significant and the deposit experienced no mass change upon completion of the experiment compared to before the experiment within the measurable range.

All the wetted samples showed a similar pattern of mass loss when using thermogravimetric analysis, as seen in Fig. 31. These results show that almost the entire mass loss occurs very rapidly after the experiment begins and that there is no evidence of significant water release at elevated temperatures for deposits immersed in demineralised water and very little for deposits immersed in sodium hydroxide dosed solutions. There was no indication of any higher temperature secondary release of water, as was observed on the deposit simulants.

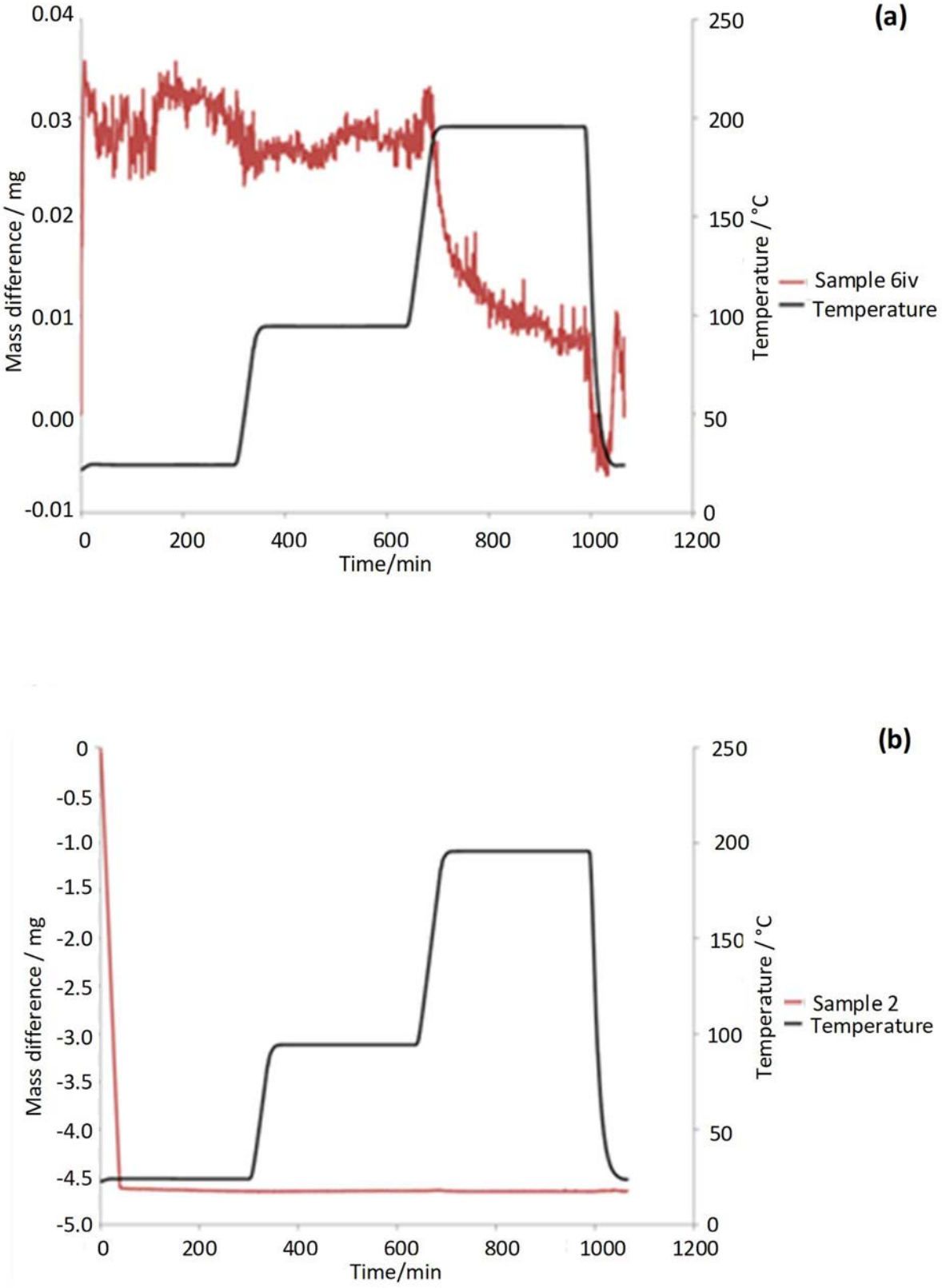

FIG. 31. Example of thermogravimetric analysis results for a wetted deposit (presented by D.I. Hambley at EPRI Extended Storage Collaboration Programme Winter Meeting November 13–16 2017, Charlotte, NC, USA and reproduced with permission).

The results of the drying trials indicated that less than 10% of the initial water in the deposits after immersion was retained after exposure to warm air for a few minutes. Mass loss from wetted deposits occurred predominantly at ≤25°C, from which it can be concluded that the majority of water in AGR deposit is physiosorbed. Only two deposits showed a mass loss above 25°C and the maximum mass gain after wetting and drying was 290 μg or 10% of the carbon mass, equivalent to 0.5 g/pin.

The residual mass difference was shown to vary broadly in line with the ^{60}Co inventory in the deposits obtained by gamma scanning, which is likely to be associated with oxide particulate from the surface of the fuel pin cladding. Given that there was little evidence of water being retained on the deposits after the initial release, it was provisionally concluded that the residual mass is likely to be associated with water retention on the metallic oxide particulates rather than the deposits themselves, although further work may be required to support this conclusion.

These scoping tests therefore indicate that the majority of deposits should dry readily in any industrial drying process with minimal heating.

5.3.8. United States of America

5.3.8.1. High Burnup Demonstration Project

In 2013, the USDOE initiated the High Burnup Demonstration project (HBU Demo) to design and implement a high burnup, large scale, long term, dry storage cask research and development project for spent nuclear fuel. Data from the project can be used to support license renewals and transportation licensing for HBU fuel, as well as for model validation and improvement to future cask designs. The objective of this project is to validate the technical basis for extended dry storage of HBU fuel by providing data on HBU fuel under actual dry storage conditions. This included, or will include, determining the properties of the cladding before and after dry storage to quantify any changes to the fuel cladding during the dry storage period. The project is led by EPRI. Participants in the project include the host utility Dominion Energy Virginia; technology vendors Orano (formerly AREVA), Framatome, Westinghouse, and NAC International; and six USDOE national laboratories. A draft test plan for the project was developed and made available for comment. The comments were reviewed, the test plan revised and a final test plan was published in February 2014 [76].

The HBU Demo Cask, a TN-32B type, was designed, licensed, and modified for storage of high burnup fuel with four different cladding types at Dominion Virginia Power's North Anna Power Station. Thirty-two high burnup assemblies were carefully selected to provide the most research value from this one demonstration; details for the assemblies are given in Table 4. A number of considerations, predominantly driven by the desired temperature ranges for each cladding type, led to selecting the fuel to include in the project based on the ability to provide data on filling research gaps.

TABLE 4. FUEL SELECTION SUMMARY

Cladding type	Quantity	Enrichment range (w/o U-235)	Burnup range (GWd/tU)
Zry-4	1	3.59	50.6
Low tin Zr-4	1	4.00	50.0
ZIRLO	12	4.20–4.45	51.9–55.5
M5	18	4.40–4.55	50.5–53.5

The cask lid was modified to allow insertion of temperature probes inside the cask at various axial and radial locations (Fig. 32). Seven thermocouple lances were inserted into a specific guide tube within the selected fuel assemblies in the cask (Fig. 33). Each thermocouple lance contained nine axially spaced thermocouples, giving a total of 63 thermocouples to gather data.

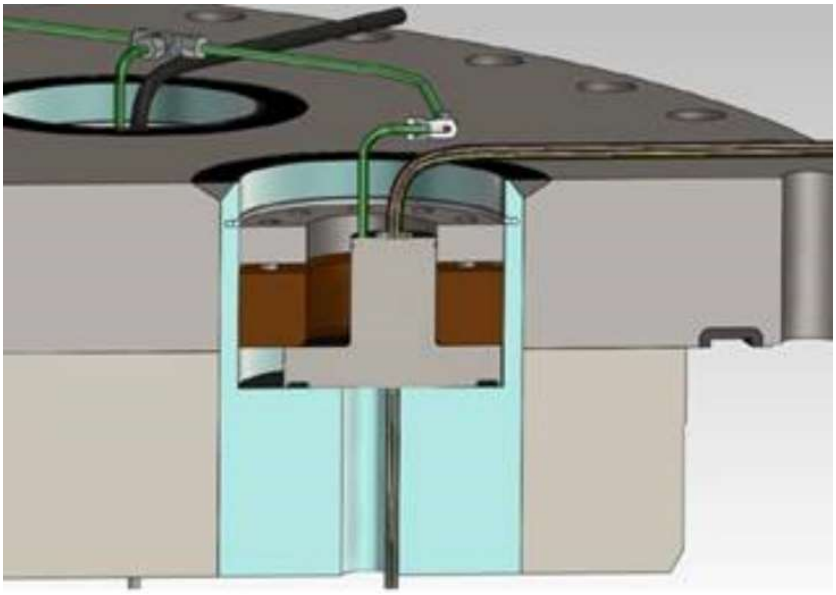

FIG. 32. Lid, penetration sleeve and thermocouple (courtesy of Orano TN).

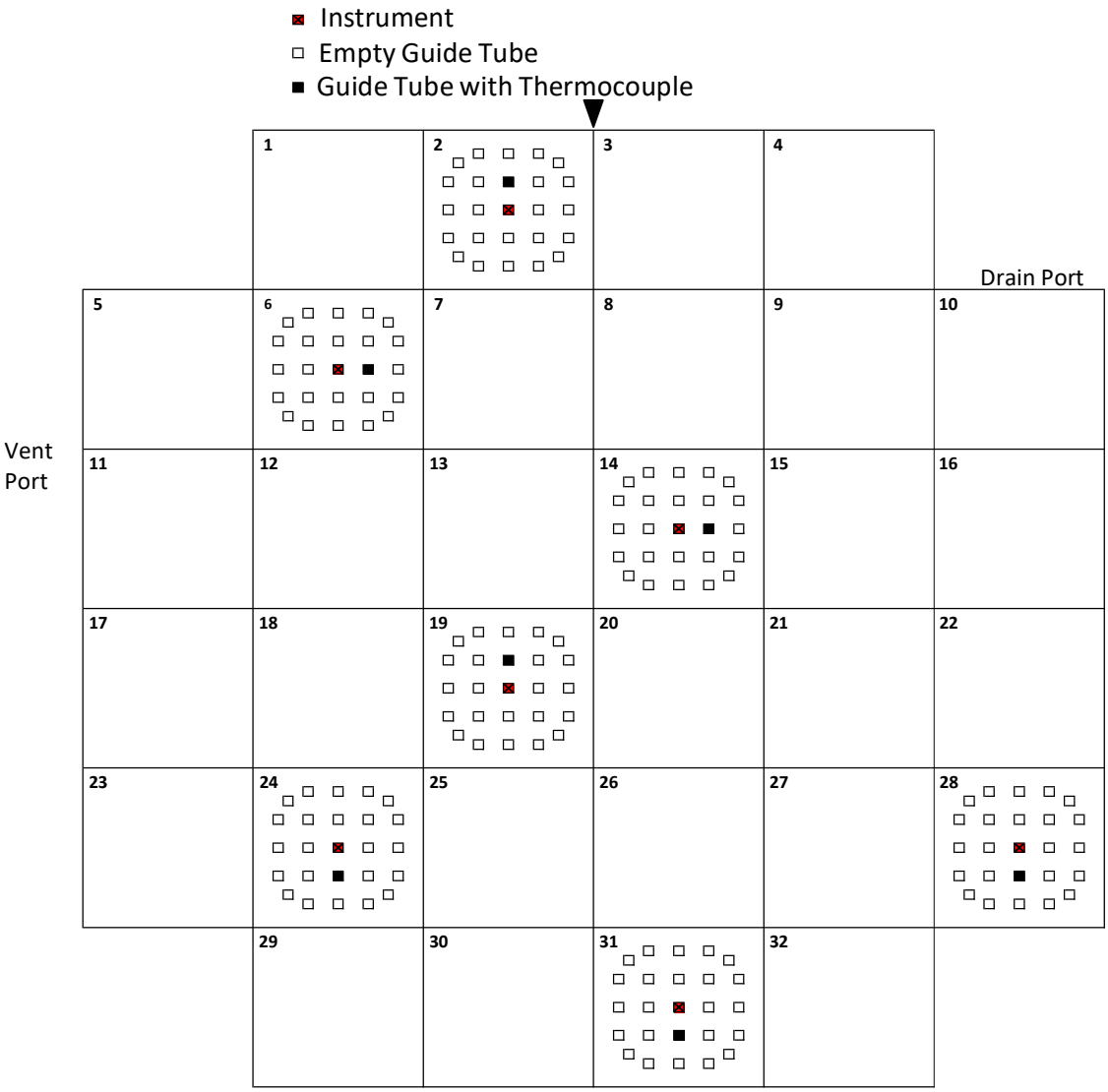

FIG. 33. Thermocouple radial locations (courtesy of EPRI).

Twenty-five fuel rods were selected and extracted from several fuel assemblies before the cask was loaded in order to obtain baseline cladding properties before dry storage. These 'sister rods' are representative of rods that are stored in the cask; details are given in Table 5.

TABLE 5. SISTER ROD SUMMARY

Cladding type	Quantity	Enrichment range (w/o U-235)	Burnup range (GWd/tU)
Zr-4	2	3.59	57.9
Low tin Zr-4	2	4.00	50.0
ZIRLO	12	4.20–4.45	52.3–55.0
M5	9	4.55	52.0–53.0

The cask was loaded at North Anna in November 2017. Temperature data were collected through the loading process and storage period. Gas samples were collected from the cask cavity to provide data on the conditions inside the cask from the moment it was loaded.

The peak measured thermocouple temperature was 237°C (459°F), which corresponds to a peak cladding temperature (PCT) of about 240°C (465°F). This is far below the USNRC guidance PCT of 400°C and below the temperature at which any appreciable hydride reorientation would be expected. To address this apparent gap between actual cladding temperatures and the USNRC recommended PCT, testing of the sister rods will be performed at 400°C. While this will be laboratory testing and not conditions in an actual cask, the testing will use realistic rod internal pressures obtained from measurements on the sister rods. Several rods will even be in their original, un-punctured configuration.

The measured temperature data from the HBU Demo Cask provided a unique opportunity to perform a blind thermal benchmark to gain insights into developing more accurate best-estimate thermal models. The benchmark exercise provided significant value by identifying some key insights for thermal modelling that can be expanded on in future planned work with the goal of developing more accurate best-estimate models to enable risk-informed dry storage and aging management analysis. This work is described in Section 5.3.8.2.

The cask met the requirements of the dryness verification (pressure rebound test), remaining well below 400 Pa (4 mbar) for 30 minutes; however, the pressure continued to rise at a constant rate during the 30 minute hold indicating the existence of some residual water, which is expected. Following drying and helium backfill, the cask pressure rose about 0.0137 MPa (137 mbar) over the first four days. Most of this pressure increase can be attributed to the increase in temperature over this period; however, about a third of the pressure increase is likely from residual water. Once thermal equilibrium was reached, the cask pressure remained fairly constant.

No fission gas was detected from the gas sample analysis, indicating no fuel failures occurred during the loading process. Small amounts of hydrogen and oxygen were detected. One set of tests using high sensitivity equipment measured as high as 498 ppmv hydrogen and 680 ppmv oxygen [77], although due to suspected contamination of the sample, the high value for oxygen is in question and it is reasoned that the amount of oxygen was very low (<200 ppmv) based on the other samples. Analysis performed at North Anna did not detect any oxygen; and hydrogen was detected but was below the sensitivity of the equipment used. The very low levels of hydrogen and oxygen are not of concern. The maximum amount of water calculated from the gas analysis in the High Burnup Research Project Cask was about 5.6 moles which is about an order of magnitude greater than the 0.43 moles recommended in the example High Burnup Aging Management Program [78]; this amount is still an order of magnitude less than the amount evaluated where degradation is not expected [79], and over three times less than the amount that could lead to hydrogen flammability.

5.3.8.2. HBU Demo thermal modelling

The temperature data gathered from the HBU Demo Cask provided a unique opportunity to perform a blind thermal benchmark by performing best-estimate thermal calculations and comparing to the actual measured temperatures recorded to gain insights into developing more accurate best estimate thermal models [80].

Thermal analyses of dry storage systems for spent nuclear fuel are conducted using subchannel analysis or CFD using design basis assumptions and inputs to ensure the peak cladding temperature does not exceed an established limit. Consequently, a best estimate understanding of the thermal behaviour of the system including quantified uncertainties is not available from those models. Using the temperature data gathered for the High Burnup Research Project, a double blind benchmark was performed to assess the accuracy of dry storage thermal models and gain insight on the main causes of modelling uncertainty. A total of four submissions are compared with the measured data acquired.

In addition to the 63 thermocouples located within the cask, external temperature measurements were taken on the external surface using an infrared gun at predetermined locations marked on the cask outer surface.

Modellers were asked to use the proprietary geometry of the TN-32B cask system and were provided information about the surrounding environment and loaded fuel, including the external temperature. Modellers were asked to all use the same inputs, although model assumptions and methods could vary. Using the same inputs allows for separation of model uncertainty from input sensitivity, as model results are strongly sensitive to decay heat, external temperature, and internal gaps. Decay heat and external temperature were provided to modellers; however, internal gap sizes could not be measured in the loaded condition and were taken from the design basis model that tended to predict higher temperatures (open gaps rather than closed).

Following the submissions from the modellers, the results were compared to the measured temperatures. The modelling submissions replicated the measured external temperatures accurately, with the exception of one submission that used conservative assumptions in their evaluation of heat transfer with the environment. The calculated temperature axial profiles from the modelling submissions were in fairly good agreement with the measurement, but all have a bias toward higher temperatures (typically 20–50°C and a range from about -10°C to as high as 95°C of the actual temperature). Figure 34 compares the measured internal temperatures with the four submissions for the hottest cell near the centre of the cask and also shows the difference between the measurement and each submission. The measured data indicate that models used for system design and licensing for the TN-32B storage system have calculated cladding temperature values approximately 90°C higher than those measured in the HBU demonstration cask. The modeller submissions tended to have very good agreement with the external measured temperatures. Figure 35 compares the measured external temperatures with the four submissions for one column on the cask surface as well as the difference between the measurement and each submission. Among all sources of input sensitivity for the system considered, it was believed that the size of internal gaps inside the system might be the major source of deviation.

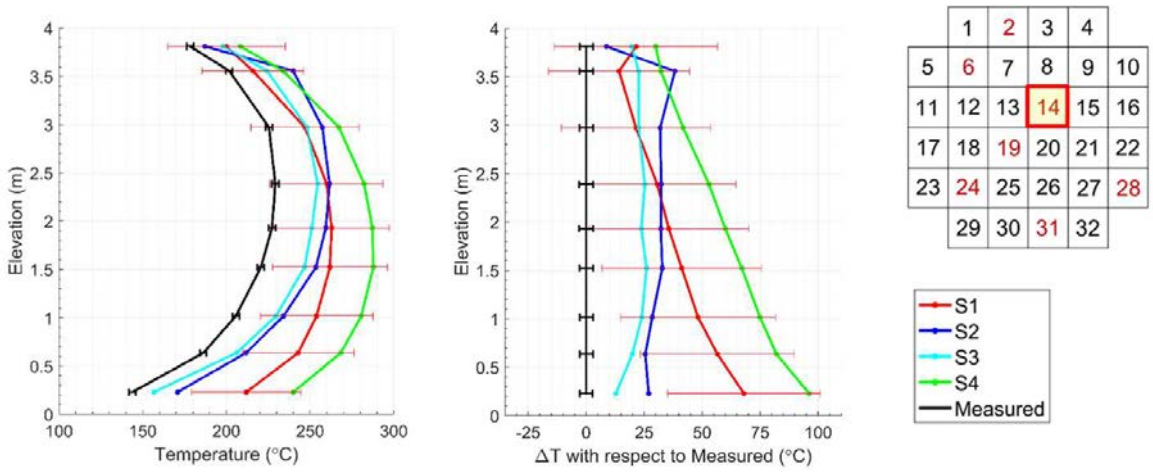

FIG. 34. Benchmark results at internal thermocouple locations, cell 14 (hottest cell) (courtesy of EPRI).

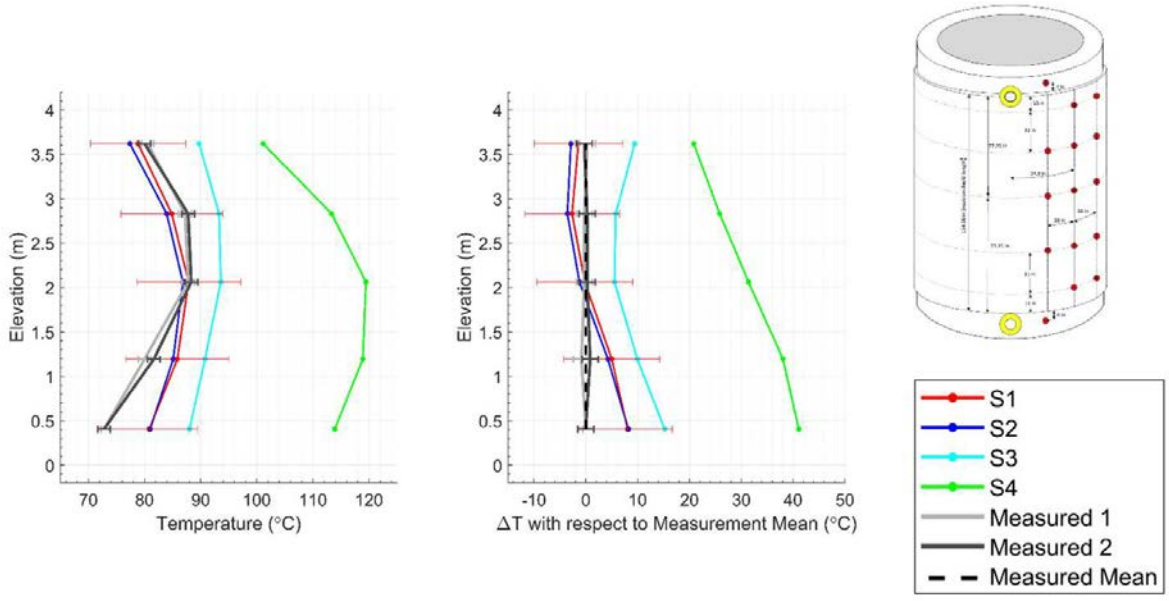

FIG. 35. Benchmark results at external temperature measurement locations, second column (courtesy of EPRI).

Overall, the results of this study highlight the need for research to assess the knowledge levels needed to achieve best estimate thermal models with associated uncertainty quantification methods. Despite the observed bias towards higher temperatures, all models demonstrated the capability to qualitatively capture the measured physical phenomena.

5.3.8.3. Shutdown site research

There are currently 18 sites[11] in the USA where commercial NPPs were operated but have been permanently shut down. The sites are generally referred to as 'shutdown sites' and are in varying stages of decommissioning. Significant efforts have been undertaken to understand the existing conditions as they relate to SNF transportation at each of these sites. This research has been documented in Ref. [81], which describes the SNF inventory, on-site transportation infrastructure conditions, near-site transportation infrastructure, and shipping experiences at each of the shutdown sites. Reference [81] also provides an overview of requirements for off-site transportation by rail, highway, and navigable waterway in the USA, discusses actions necessary to remove SNF from these sites, and provides conclusions and recommendations.

Reference [81] was initially published in 2013 and has been updated several times since. As this report matured, USDOE decided to begin a more in-depth look at individual shutdown sites and the logistics necessary to remove SNF from each of the sites by contracting with an entity with experience conducting similar operations. These initial, site specific de-inventory reports provide pertinent site information, a description of the possible transportation routes that could be used, and a list of the entities that would need to be involved in a de-inventory operation. A key aspect of the reports is the presentation of the results of a multi-attribute utility analysis of the possible transportation routes resulting in the recommendation of a specific route, including transportation modes, from a logistics standpoint. The analyses do not consider input from the sites, their surrounding communities, or rail carriers. Based on this recommended route, the reports provide detailed discussion of the concept of operations, the budget and spending profile, safety and security plans, and the emergency response and preparedness needed to execute the complete de-inventory of the site being examined. These reports have been completed for 6 of the 18 shutdown sites [82–87].

These reports only provide consideration of the purely logistical aspects of inventory removal from these sites rather than representing USDOE's final decision on SNF transport. USDOE is currently interested in identifying the technical and logistical information for SNF removal, but recognizes that further engagement will be required to fully plan SNF removal.

[11] As of September 2020.

6. STORAGE FACILITY AND COMPONENT DEGRADATION IN WET AND DRY STORAGE

Components used in wet and dry storage systems and facilities need to be designed and fabricated from suitable materials to ensure necessary safety functions are maintained for the required duty (design storage duration) and subsequent transportation after storage (in the case of fuel canisters or DPCs). Consequently, consideration needs to be given to potential ageing deterioration of components and materials that may occur during operation of the storage system or facility [88].

Effective AMPs require a technical understanding of the ageing degradation mechanisms, inspection and assessment techniques/requirements, mitigation measures and as needed, guidance on repairs or replacements for each storage component. In recent years there has been particular attention paid to degradation mechanisms and ageing prediction of components used in dry storage and although much has been clarified, nevertheless some knowledge gaps remain. Section 6.2. provides a summary of the investigations and R&D programmes undertaken in SPAR-IV dedicated to closing these knowledge gaps.

6.1. WET STORAGE

SPAR-IV studies related to the long term behaviour of materials used in wet storage include the on-going performance of stainless steel grades used in storage racks (Slovakia) and the neutron absorber material Boral (USA).

6.1.1. Stainless steel/borated stainless steel

Slovakia developed a comprehensive monitoring programme for the Jaslovské Bohunice ISFS in 1999. Two systems for monitoring the corrosion of ISFS structural materials are in use:

- A corrosion monitoring system based on the principle of surveillance samples:
  - All specimens are made from original or archive materials;
  - Specimens are placed into the original environment;
  - Specimens are loaded with stresses similar or higher to the operational ones.

  The following types of samples are exposed in each pool:
  - Corrosion coupons;
  - Crevice bent beam samples;
  - Circular bead weldment samples;
  - U-bend samples;
  - Metallographic samples;
  - ATABOR weld joint samples.
- A monitoring system for the pool liner based on acoustic emission:
  - Six sensors are installed in each pool and measurements are periodically performed by a portable measurement system;
  - Acquired data are archived and evaluated by modern mathematical methods and the obtained results are compared with the previous ones.

The latest analysis relates to corrosion coupons that have been removed from pool 117. The test matrix is shown in Table 6 and the results of coupon analysis in Table 7. The composition of ATABOR steel is provided in Table 8.

TABLE 6. TEST MATRIX OF MATERIALS AND CORROSION COUPONS IMMERSED INTO POOL 117 AT JASLOVSKÉ BOHUNICE

Sample Type	Marking	Material	Pool Position	Total exposure time (years)
Corrosion coupons	6-1, 6-2, 6-3	Steel 1.4541	At the water level	16
	6-4, 6-5, 6-6		Below the water level	16
	Z12-1, Z12-2, Z12-3	Steel ATABOR	Below the water level	16
	Z013-3, Z015-3, Z016-3			14
	Z017-4			15
Circular bead weldment	9	Steel 17247.4	At the water level	16
	11		Below the water level	
U-bend	A9, B9	Steel 17247.4	At the water level	16
	A11, B11		Below the water level	
Crevice bent beam	Z040-2	Steel ATABOR	Below the water level	12
	Z017-17			15
Weld joint	Z017-4/2	Steel ATABOR	Below the water level	15
Metallographic	5-3	08CH18N10T	At the water level	16
	2-3	Steel 17247.4	Below the water level	
	Z12-1	Steel ATABOR		

TABLE 7. MEASURED CORROSION RATE OF STEELS

Material	Material Origin	Pool position	Total exposure time (years)	Average corrosion rate (μm/y)
Steel type 1.4541	Tube Ø 220 × 6.5 mm	At the water level	16	<0.1
		Below the water level	16	<0.1
Steel type ATABOR	Hexagonal tube, laser welding	Below the water level	16	<0.1
	Hexagonal tube, electron beam welding		14,16	<0.1

TABLE 8. CHEMICAL COMPOSITION OF ATABOR STEEL

Steel	Chemical Composition (wt%)								
	C	Mn	Si	Cr	Ni	Ti	P	S	B
ATABOR (AISI 304 + B)	max. 0.03	max. 2.0	max. 0.8	18.0–20.0	10.0–12.5	–	max. 0.035	max. 0.025	>110

6.1.1.1. Microbial contamination of coupons

During the handling of coupons that had been removed from the pool a 'slippery layer' was observed on their surface, and a thin film observed on the surface of the water in the corners of the pools. Recent studies carried out independently in a number of NPPs and research reactors located in different countries have revealed the presence of microorganisms in environments harbouring high radiation/low nutrient concentration levels [89]. According to Ref. [90], the pool water represents an oligotrophic environment which enables the growth of mesophilic bacteria, where the effect of radiation alters both the diversity and abundance of bacteria.

Two U-bend samples and three metallographic polished samples have been evaluated for traces of biofilm using X ray analysis. The findings are as follows:

- The presence of 'bio' elements as C and O (Fig. 36) was confirmed in deposits;
- Very significant, and important from the corrosion perspective, is the presence of Cl (see peak Cl in Fig. 37);
- Elements such as P, S, Na, Ca, and Mg were also found in deposits.

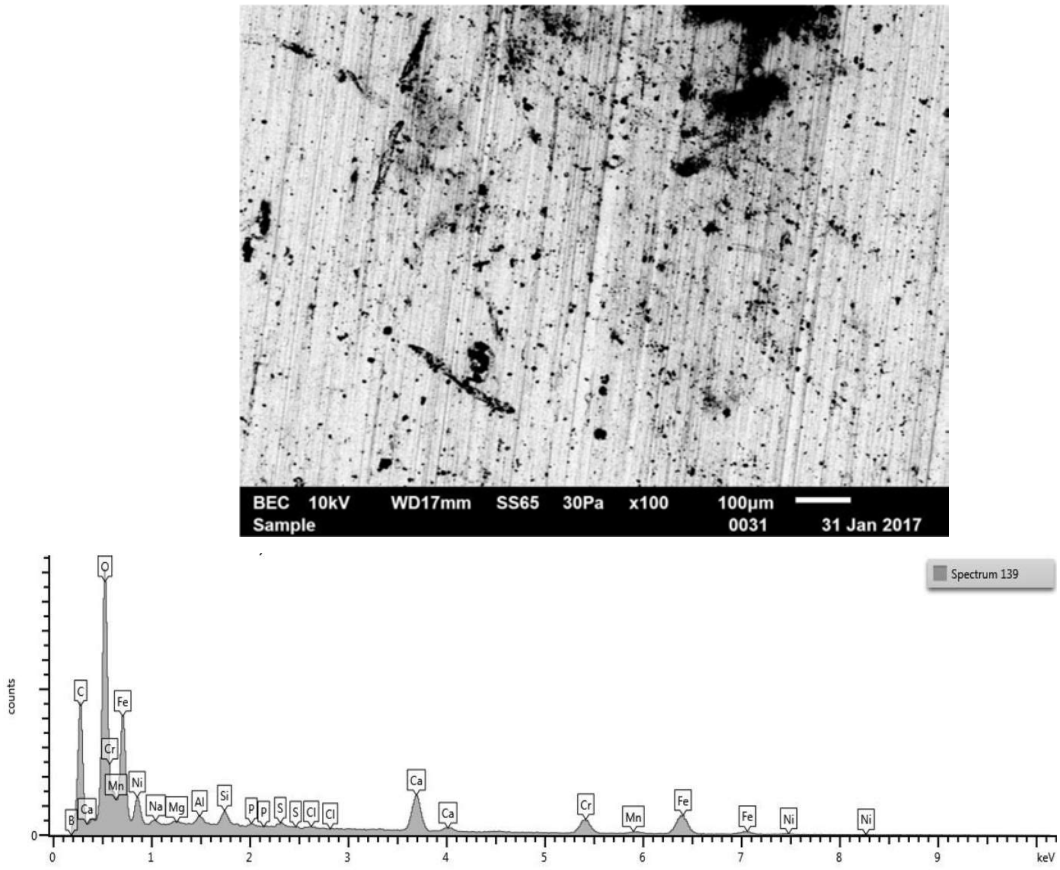

FIG. 36. U-bend sample (a) surface deposits and (b) X ray spectrum (courtesy of VUJE).

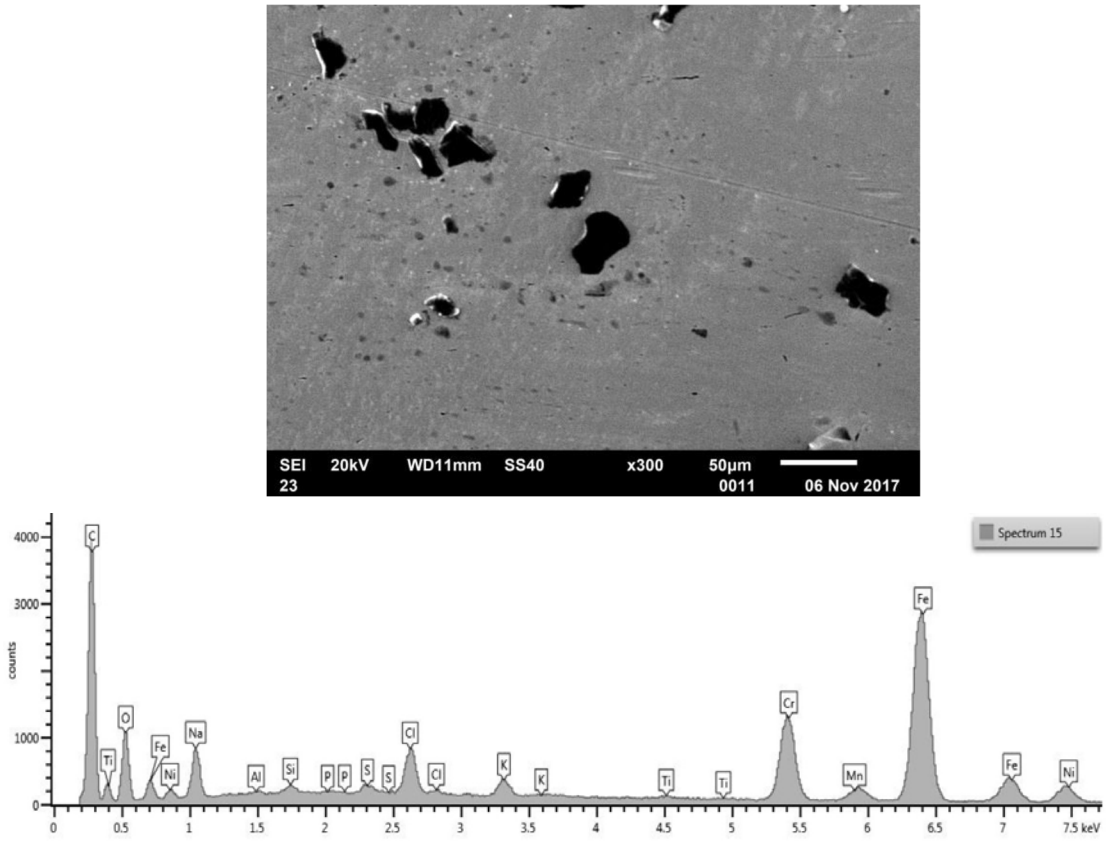

FIG. 37. Polished metallographic sample (a) surface deposits and (b) X ray spectrum (courtesy of VUJE).

Results obtained by X ray microanalysis revealed a significantly greater percentage of C, as well as other biogenic elements such as O, P, and S, on the surface of the samples that had been immersed in the pool water. All the elements detected are most likely to represent the components of bio-organic cells of the bacteria in the biofilms found on the surface of measurement samples.

6.1.2. Boral

BORAL is a neutron absorber material in common use in SFP storage racks, particularly in the USA. In addition to coupon monitoring, EPRI have also undertaken accelerated corrosion testing to evaluate the corrosion performance of BORAL over timeframes longer than 60 years.

6.1.2.1. BORAL Coupon monitoring

To monitor performance of neutron absorbers, currently, two types of monitoring programmes are typically used — coupon surveillance and in-situ measurement. Coupon surveillance uses representative coupon samples placed in the pool that are removed periodically and inspected. Since coupons are typically placed in areas of highest anticipated degradation, the performance of the coupons should provide a leading indicator of any potential degradation of the actual material in the SFP storage racks. In-situ measurements have been performed by placing a neutron source on one side of the absorber and a detector on the opposite side and measuring the neutron transmission through the absorber. However, there is fairly high uncertainty with current methods that have been used for in-situ measurements.

EPRI recently conducted an evaluation to compare the results of both monitoring methods against measurements of actual storage rack absorber panels. The Zion Power Station in the US was shut down and is undergoing decommissioning. First, the remaining coupons in the pool were removed and analysed [91]. Then, before dismantling, the panels were measured using the in-situ 'Boron-10 Areal Density Gage for Evaluating Racks' (BADGER). Finally, once all the fuel had been removed from the pool, six neutron absorber panels from each region in the SFP were selected to be extracted and destructively examined to measure the ^{10}B content. Results comparing the coupons to the actual racks shows that the coupons provide a good leading indicator of corrosion. More pits were observed in the coupons than the actual panels. Also, the key result is that the ^{10}B areal density in the coupons is representative of the areal density of the actual panels [92]. The preliminary results from the in-situ BADGER measurements indicated degradation [93]; however when the panels from the Zion SFP were removed and analysed, the analysis results showed that the panels were in very good condition and degradation indicated by BADGER was due to the accuracy of the in-situ measurements [92].

EPRI is currently working on the development of an industrywide learning ageing management programme (i-LAMP) as an alternative monitoring approach [94, 95]. In this programme, pools that do not have coupons will identify similar pools, based on absorber properties and water chemistry, and use the coupon analysis from the similar pool as part of their monitoring programme. Once the development is complete, i-LAMP will be submitted to the regulatory body for official endorsement.

6.1.2.2. BORAL accelerated corrosion testing

While limited, some degradation has been observed for BORAL in the form of blistering of the aluminium cladding on the BORAL sheet which could lead to operational issues related to fuel handling. It is important to note that the corrosion observed to date has not led to any significant loss of ^{10}B, nor have any mechanisms been identified that would lead to either of these conditions. Besides blistering of the aluminium cladding material, there were questions about potential corrosion of BORAL over extended periods of operation, given plant life extensions [96]. Given that many plants are extending their plant operating licenses, EPRI recently conducted a five-year accelerated corrosion test to evaluate the corrosion performance of BORAL over timeframes greater than 60 years.

BORAL has been manufactured since the 1970s and over that time, the manufacturing process has changed resulting in different vintages of BORAL based on the manufacturing process used at the time. As part of the accelerated corrosion test, different vintages of BORAL coupons were included to address this variation.

The test programme included BWR and PWR conditions, different manufacturing vintages of BORAL, and un-encapsulated and encapsulated coupons (simulating a wrapper plate).

The test coupons were placed in test baths simulating PWR and BWR water chemistry and monitored to be in accordance with EPRI water chemistry guidelines. The test included both bare coupons and coupons encapsulated in stainless steel to simulate the wrapper plate often used to attach the absorber plate to the storage rack. To accelerate the corrosion, the tests were conducted at an elevated temperature of 91°C (196°F) compared to a normal operating temperature range of 27–38°C (80–100°F). For the parameters included in the test matrix (manufacturing process, reactor type, encapsulation) and to provide coupons to be tested at the end of each year for five years, over 200 coupons were used for the test. To evaluate corrosion under worst conditions, the protective cladding material was intentionally removed from some

coupons directly exposing the boron carbide core material to the water at elevated temperatures [97].

Prior to the test, each coupon was characterized in detail by performing visual inspection, high-resolution photography, measurement of dimensions and weight of coupons, and areal density measurements. At the end of each year, coupons were retrieved and analysed. Blister and pit analyses were also performed for coupons that had developed blisters and/or pits.

The areal density, which is the most important parameter for maintaining criticality safety margins, did not show any statistically significant change for any of the years, including the clad removed coupons. Due to issues with the water purification system, sulphate levels in Year 1 increased to as high as an order of magnitude greater than the EPRI water chemistry guideline limit. Yet despite this significant increase in sulphate concentration, which is a known corrosion accelerator, there was no significant change in areal density values (Fig. 38). In these figures, the key for coupon labelling is: P (PWR); B (BWR); E (Encapsulated in stainless steel jacket);G (General, bare with no stainless steel jacket); A (manufacturer A); C (manufacturer C); and O (manufacturer O). Additionally, the first number indicates the designated year of the coupon analysis. For each year, three coupons of each type were immersed in test baths to identify if there are variations in degradation within the same type when exposed to the same conditions for the same amount of time. Subsequently, the last number indicates the coupon number within that batch.

The areal density results from Year 5 are shown in Fig. 39 and the areal density results for the clad removed coupons are shown in Fig. 40. As evident from the figures, there is no statistically significant change in areal density. This is especially important for clad removed coupons as this represents the most severe condition with the boron carbide material unprotected by the aluminium cladding and exposed directly to the pool water. The results from accelerated corrosion test indicates that BORAL will maintain its efficacy for a long period of time, maintaining criticality safety margins in SFPs.

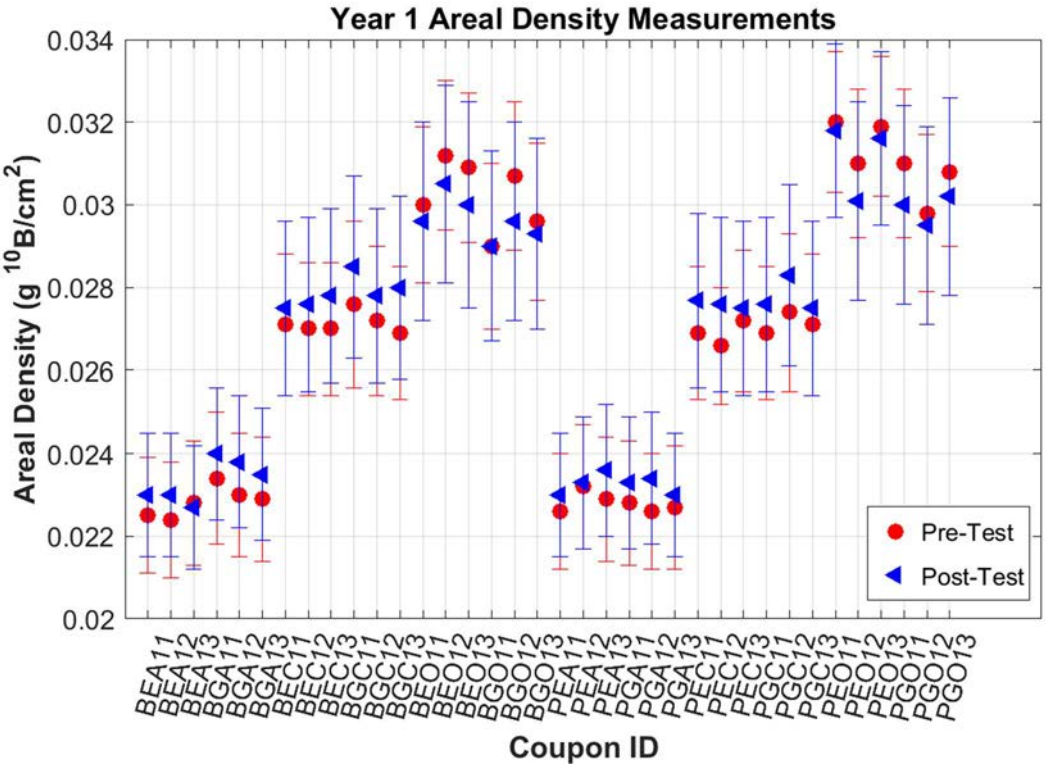

FIG. 38. Areal density results after 1 year (courtesy of EPRI).

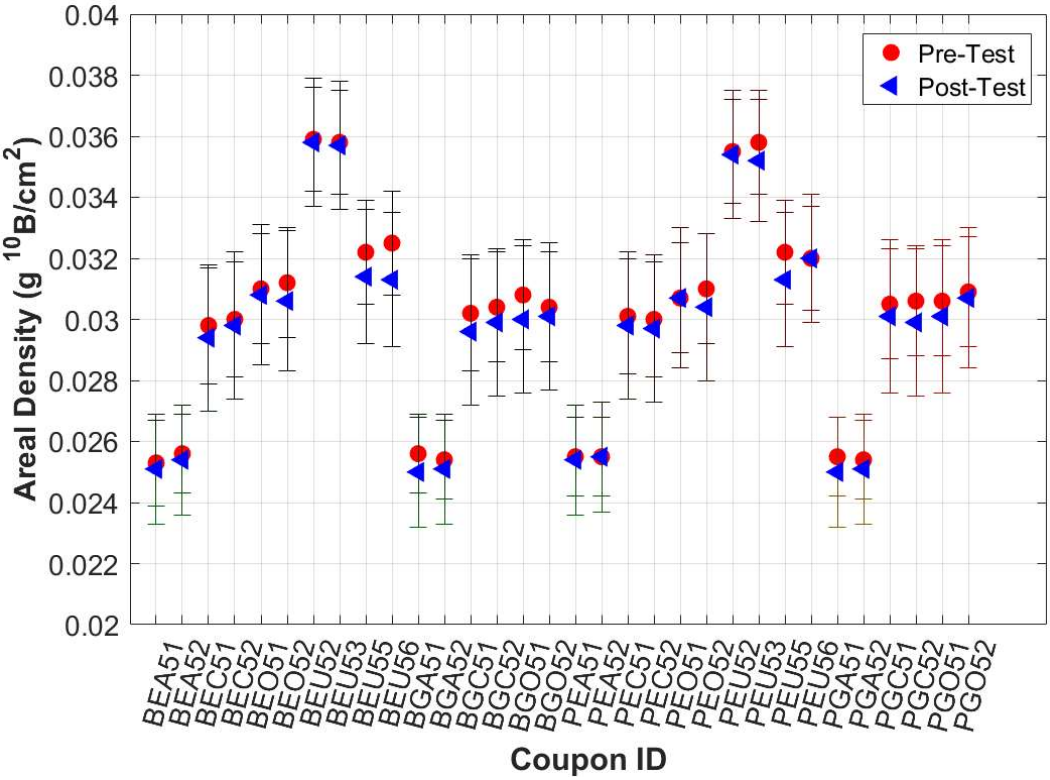

FIG. 39. Areal density results after 5 years (courtesy of EPRI).

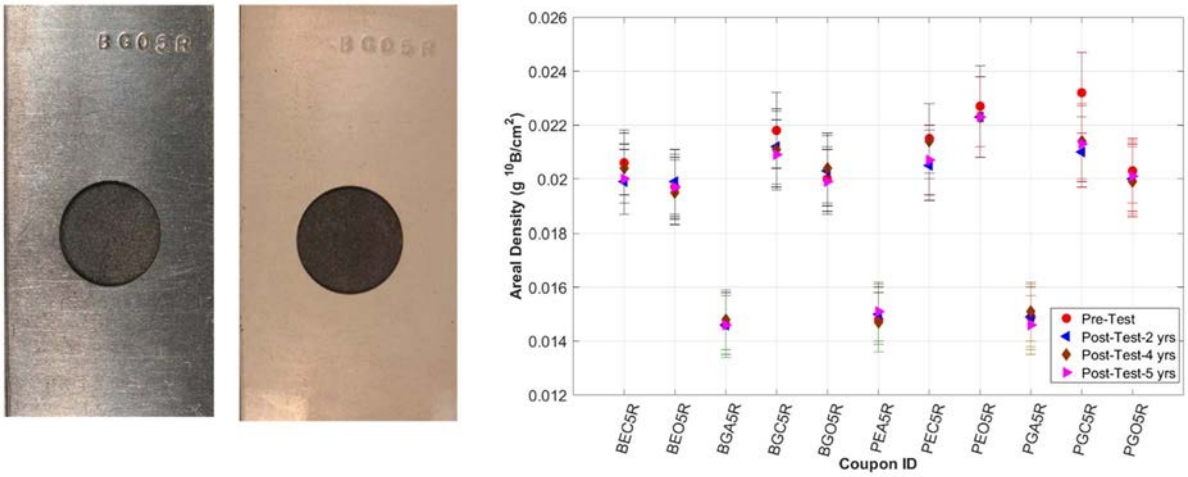

FIG. 40. Clad-removed coupon prior to the placement in a test bath (left) and the same coupon after immersion in a test bath for five years (middle). Areal density values for clad-removed coupons after immersion in PWR and BWR test baths after two, four, and five years (right) (courtesy of EPRI).

The results found blisters developed on some coupons after two years, while pitting of the aluminium cladding was observed after the first year. After five years, some pits were found to penetrate the aluminium cladding to the core material, yet no statistically significant loss of ^{10}B was observed. To evaluate the effect on reactivity from potential blisters and pits, simulations were performed to calculate the reactivity effect for a broad range of blister and pit sizes. The size of blisters and pits that would require re-evaluation of the criticality safety analysis were far beyond the size of any blisters and pits observed to date [98]. In fact, blister and pit sizes would need to be orders of magnitude larger than presently observed to result in statistically significant impacts on reactivity.

6.2. DRY STORAGE

The behaviours of dry storage systems and components over the long term have been studied to develop AMPs to ensure that the following safety functions are maintained in long term storage and subsequent transportation:

- Containment and safe enclosure of radioactive material;
- Limitation of radiation exposure;
- Sub-criticality;
- Removal of decay heat.

Several R&D programmes are performed by the industry, utilizing methodologies such as separate effect tests and small scale effect tests in order to provide information and results to develop an understanding of ageing related impacts. Accelerated tests are also important, followed by simulation and modelling to allow for prediction of degradation of materials and/or impact on safety functions. Finally, confirmatory data are provided by full scale tests, which allow for the validation and verification of the predictions.

6.2.1. Gap analysis

During SPAR-IV, Orano TN completed a gap analysis of its metal casks and horizontal silo dry storage systems. The gap analysis complements similar gap analysis which were undertaken as part of EPRI's Extended Storage Collaboration Program (ESCP) project [99] and the IAEA

CRP on Demonstrating Performance of Spent Fuel and Related Storage System Components during Very Long Term Storage (DEMO) [8]. A summary of this analysis is provided in subsections 6.2.1.1–6.2.1.6.

6.2.1.1. Containment vessel

The metal cask structural material and containment vessel is generally carbon steel that also provides gamma shielding. Temperature, gamma and neutron irradiation — the drivers for ageing — have no effect on the safety functions of the containment vessel for the storage period (even for 100 years). The risk of corrosion is minimized as a protective layer (such as ZnAl) is generally used. Water draining and drying are performed in the cask loading process, therefore the potential for oxidative conditions to develop are minimized due to the very low quantities of residual water. At the end of this operation the cavity is filled with inert gas (helium).

Concerning the degradation of closure system, lid bolts and seals, the corresponding risk is the loss of leaktightness. Corrosion and thermomechanical degradation of bolts and seals in bolted metal casks, in particular, have to be assessed. It is important to highlight that research on the metallic gaskets has been performed by CEA, focusing on the evaluation of residual seal performance and compression rate in the long term (100 000 hours = 11 years) for aluminium coated metal gaskets. Bolts could be subjected to SCC, but industrial feedback has reported no visible evidence.

The function of metallic gaskets is the confinement of radioactive material. In most cask designs, generally there are two gaskets. The environment in which the inner metallic gasket is situated is inert gas with minimal residual water and consequently, there are unlikely to be any corrosion issues or degradation. The second metallic gasket is only partially under inert atmosphere, but when correct drying is achieved, industrial feedback has shown no degradation of these gaskets.

6.2.1.2. Basket materials and neutron poison

Baskets used in metal casks are made from a variety of metals such as stainless steel, carbon steel, and aluminium alloys, and have both base metal and welds. Some basket materials, such as aluminium–boron–carbide metal matrix composite, also serve as the neutron poison material.

Temperature and stress can strongly influence creep behaviour of fuel basket material over long time periods, which would likely only be experienced in the short term (<40 years) as temperatures decrease over extended storage time. Long term exposure of austenitic stainless steel welds to elevated temperatures may result in the embrittlement of the weld metal of stainless steel baskets in dry storage systems. Both phenomena, creep of fuel baskets and embrittlement of the weld metal, may lead to a lack of geometry control, but analysis shows that control of adequate parameters can prevent such problems, with retrievability not affected and maintenance of thermal performance and subcriticality.

Corrosion of fuel baskets may occur if moisture and oxygen are present in the canister. Corrosion could lead to component failure affecting retrievability, altered thermal performance, and spent fuel configurations necessary to maintain subcriticality. Corrosion may be operative in extended storage periods but is not likely to be significant, as remaining moisture after drying is very low and the cask seals are effective at preventing moisture ingress.

Neutron poisons used in dry storage cask baskets are made primarily from borated aluminium alloys, metal matrix composites, aluminium boride carbon cermets, and borated stainless steel materials. Neutron poisons materials in dry storage casks serve a neutron absorption subcriticality function but more recently, with advancements in borated aluminium alloys and borated metal matrix composites, may also serve a load bearing structural function and facilitate

heat transfer. The major challenges related to neutron poisons in extended use of dry storage casks vary according to the material.

For load bearing alloy and metal matrix composite neutron poison materials, thermal ageing effects are observed as a result of extended time at elevated temperature, leading to space reduction with a potential impact on criticality safety functions during transportation accident scenarios.

For non-load-bearing cermet neutron poison materials, thermal embrittlement and cracking can reduce poison isotope density, whereas blistering can reduce the spacing. Wet corrosion and blistering of neutron absorbers during extended storage would only occur if undetected loss of seal or confinement failure of the casks occurred in the presence of sufficient water. In this case, possible dimensional changes may affect criticality safety, due to moderator displacement, and retrievability function.

Within the cask, the basket is submitted to various ageing conditions: loads (spent fuel), temperature, and irradiation. The main ageing effect on the basket is the decrease of typical mechanical characteristics of the borated aluminium alloy profiles used for the basket walls. Tests on aged specimens are undertaken to understand the level of mechanical degradation representing the storage period and analysed; conformity to regulatory requirements can then be confirmed.

6.2.1.3. Neutron shielding materials

To protect the public and operators from radiation exposure, neutron shielding materials are used in dry storage systems. These systems are generally made of polymer based compounds. In-service neutron shielding ageing has been addressed and safety assessment takes account of shielding degradation in the long term. The identified degradation processes are irradiation and thermal oxidation processes.

Tests carried out by Orano TN have shown that the main changes to shielding material occur in a superficial layer: hydrogen abstraction, chain scission and crosslinking.

A new methodology to predict the long term properties has been qualified through accelerated ageing tests using conservative assumptions. The ageing process is a combination of thermal oxidation, irradiation oxidation and oxygen diffusion. There is a good agreement between experimental results and simulated data (weight losses – hydrogen atoms loss – oxidation profiles) [6]. Overall, the neutron shielding degradation model, validated with sample data, shows that the long term degradation of neutron shielding materials is very limited.

6.2.1.4. Shock absorbers (impact limiters)

Before and after storage, spent fuel needs to be transported. The shock absorbers are necessary for protection in accident conditions of transport [56].

Shock absorbers are not submitted to thermal ageing since they are not permanently installed on the metal cask in storage; on-site, they are sometimes replaced by an ‘anti-crash cover’ to protect from aircraft impact. These ‘anti-crash covers’ are made of steel and are not affected by ageing.

Shock absorbers are stored in good conditions and are protected from any variation or parameter that could degrade their performance and safety functions (mechanical properties).

6.2.1.5. Coatings

The function of coatings used on metal casks is to protect against corrosion, thermal transfer (radiation) in transport and storage conditions and allow for easy decontamination. Their degradation may be operative in the short term and during extended storage.

Thermal ageing processes on cask painted surfaces are studied with a testing programme. Variations of typical properties are measured: paint adhesion, decontamination ability, corrosion and thermal coefficients.

Paint emissivity and absorptivity coefficients may change a little in storage, nevertheless, these variations have no significant impact on package temperatures.

6.2.1.6. Thermal conducting components (fins), handling means (trunnions)

These cask components are not submitted to conditions which could lead to a significant degradation in the long term.

The only potential degradation mechanism could be corrosion of trunnions, which are regularly inspected; no indication has been found so far.

6.2.2. Stress corrosion cracking of stainless steel

For welded stainless steel canisters used for dry storage of SNF, chloride induced stress corrosion cracking (CISCC) has been identified as a potential degradation mechanism for extended storage. Three concurrent conditions are needed for SCC: (i) corrosion, (ii) tensile stress, and (iii) a susceptible material. Spent fuel canisters are subject to corrosion through the deliquescence of salts on the canister surface. While the storage canisters are stored inside an overpack and are not directly exposed to the environment, the canisters are cooled by natural convection with air from the environment in direct contact with the stainless steel canister surface. The environment air can carry corrosive species, particularly chlorides for sites located near a marine coast. The chloride deposits collected on the canister surface can then absorb water from the humidity in the air (deliquesce) and create a local area for corrosion. Through the fabrication and welding of the canisters, residual tensile stress is present, primarily in the area of the welds. Spent fuel canisters are typically fabricated from austenitic stainless steels (304, 316) which are susceptible to SCC. Hence all three conditions could exist for welded stainless steel canisters. Corrosion tests performed in the laboratory have demonstrated CISCC can occur on canister materials. However, these tests are under extreme conditions that are not representative of the true conditions experienced by in-service canisters. Nevertheless, the potential for CISCC on welded stainless steel canisters was identified as a high priority gap [100], and through a systematic approach, EPRI developed an AMP to address this potential degradation mechanism.

To begin, EPRI performed a Failure Modes and Effects Analysis (FMEA) to systematically evaluate the credible degradation mechanisms affecting the confinement boundary of welded stainless steel spent fuel canisters [102]. The results concluded that CISCC was the greatest potential concern for causing penetration of the confinement boundary and that the most likely failure mode of the confinement boundary is the through-wall growth and penetration of a crack. The analysis also determined that the most susceptible locations on the canister are the cooler regions of the shell near to welds. The lower surface temperature increases the potential for deliquescence and corrosion occurring, and the area near the welds has the potential for higher residual tensile stress. Also, ISFSIs located in marine environments with breaking waves have a higher potential of chloride transport from the salt air to the canister surface.

To support the development of an AMP to address potential CISCC, information was needed on the timeframes for CISCC to propagate through-wall. EPRI performed a flaw growth and tolerance assessment [102], and using data from available literature, developed deterministic crack propagation models assuming crack initiation had already occurred. Due to the relationship between surface temperature, humidity, and deliquescence, crack growth rates are dependent on the local atmospheric conditions, and calculated through-wall crack propagation

times vary greatly among locations with different ambient conditions. In addition, the time to initiate a CISCC crack was not evaluated, yet initiation would likely require a substantial period of time due to the fact that CISCC initiation is dependent on site-specific environmental conditions and the decay heat loading of each canister. Through the flaw tolerance assessment, it was identified that canister designs are very flaw tolerant; large flaws are required before a critical flaw size is approached. Once a flaw grows through-wall, the depressurization time is calculated to be relatively short, while the time required for air to displace the inert backfilled atmosphere is months or years. A literature review was also conducted to provide supporting information for the flaw growth and tolerance assessment and development of an ageing management plan [103].

It was also important to understand the actual conditions of the stored stainless steel canisters. EPRI performed several inspections to get the first look at canisters after years of storage and to understand the environment [104–106]. Generally, the canister surface was seen to be in good condition with no signs of gross degradation and only limited surface corrosion was observed. Best estimate thermal models were able to fairly accurately predict the canister surface temperatures when details on the actual system and fuel loaded in the specific canister were modelled. For the initial six canisters inspected, some area of each canister was in the range of temperature for deliquescence to occur (<~60°C) despite the wide range of storage time (2–18 years) and decay heats (4–17 kW). The chemical analysis revealed much less chloride than expected for all locations. For Calvert Cliffs and Hope Creek, the cation/anion composition was more like inland rainwater than seawater, indicating these sites are less 'marine' sites.

The next step in development of an ageing management plan was to identify which canisters to inspect that would provide a leading indication to identify ageing related degradation, should it occur. It is important to prioritize inspections to be able to detect CISCC before it could lead to loss of confinement, thereby allowing time to identify, assess and correct the condition as commensurate with the safety significance. Hence, only a subset of canisters is likely to need inspections and monitoring in order to detect potential CISCC initiation and propagation prior to through-wall growth. To prioritize that subset of canisters to inspect, EPRI developed a set of criteria that may be used to rank canisters at ISFSIs with regard to the relative priority for inspections [107]. The criteria assess which sites have higher (or lower) susceptibility as well as which canisters at a particular site have higher (or lower) susceptibility relative to the canisters within the population at that site. For the relative susceptibility of the site, the primary factors are the distance to potential chloride aerosols and the annual average absolute humidity. For the relative susceptibility of a single canister relative to other canisters at that site, the primary factors affecting susceptibility are: the level of chloride accumulation (based on the time exposed to the conditions), the material alloy (based on its resistance to CISCC) and the regions where deliquescence could occur (based on its decay heat and surface temperature). The susceptibility assessment criteria use readily available information for implementation by industry to rank relative priority for the ageing management activities to address CISCC susceptibility primarily through assisting in choosing the canister(s) to be included in inspections. It is important that a systematic approach is used in implementing the inspection programmes to focus on inspecting the most susceptible canisters first for more efficient and practical application of resources.

Following a systematic approach over the course of a few years, the research into studying the potential for CISCC culminated in producing ageing management guidance to address the potential CISCC ageing degradation mechanism for welded stainless steel spent fuel storage canisters [108]. Guidance and recommendations for development of an AMP to address the

potential for CISCC of stainless steel welded canisters was developed and made available. An important aspect is that it should be a learning AMP to adopt and adjust as information and experience become available. Using the susceptibility criteria developed [107], the guidance reflects the susceptibility of a given site as well as the susceptibility of individual canisters at that site. The guidance is based on an inspection framework to first perform periodic visual inspections to detect signs of corrosion or degradation (a precursor to CISCC) followed by surface or volumetric examinations for the presence of cracking that is limited to areas identified as higher potential for cracking based on the initial visual inspections. A graded approach toward inspection frequency, methods, and sample size is recommended that would be adjusted based on experience and previous results. If examinations detect the presence of corrosion, guidance is provided for flaw acceptance and flaw evaluation. A probabilistic assessment was performed to provide a technically based evaluation of different inspection strategies to provide insight into the efficacy of different inspection regimes and the relative impact of inputs to modelled processes.

7. CROSS-CUTTING ISSUES

Various cross cutting issues have been investigated by the SPAR-IV participants.

The drying of spent fuel in support of transport, dry storage or disposal has previously been of interest to the SPAR CRP and is reported in Section 8 of SPAR-II [5]. The drying of failed or damaged fuel was reviewed in SPAR-II but current research on the drying of failed AGR fuel adds another dimension.

As part of preparations for the eventual transport of spent fuel from NPP sites, groups from the Republic of Korea, Spain and the USA collaborated on a project to understand the stresses spent fuel will be exposed to during transport under normal conditions. A summary of the results gained from the multimodal transportation trial were reported to SPAR-IV, in addition to other transport R&D underway in the USA.

In addition to the specific thermal modelling reported in Sections 4.3 and 5.3, some of the SPAR-IV participants have engaged in the SKB blind test benchmark; a summary is given in Section 7.3.

7.1. DRYING

AGR fuel pellets differ from LWR pellets, insofar as they have an internal bore for accommodating fission gas released during irradiation. If the fuels fail in wet storage, there is then the potential for the central bore within the fuel rod to become saturated with water. When transitioning failed AGR fuel from wet storage to either dry storage or disposal, the water within the bore may need to be removed to either inhibit co-stored intact fuel from failing, prevent canister pressurization, or limit the amount of free water going to disposal (if the quantity of failed fuel was significant).

Initial examination and assessment of the permeability of AGR fuel pellets has been undertaken as part of work on the drying of failed AGR fuel. Sequential sectioning of a fuel pellet was undertaken to provide 3-dimensional data on the fracture network within the fuel pellet. The fracture network was then analysed to produce a computational mesh, using approaches developed by Imperial College for application in geological disposal studies. Flow through the fracture network was then modelled to provide measurements of permeability in a number of directions [109]. The process is illustrated in Fig. 41.

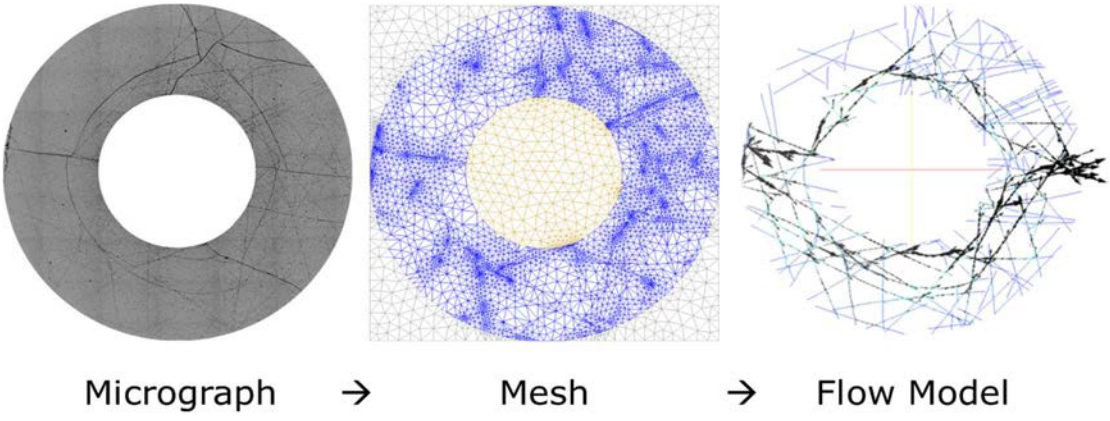

FIG. 41. Approach to modelling fuel pellet permeability (courtesy of NNL).

The modelling indicates that fractures have a larger impact on water migration in low porosity fuel pellets than high porosity pellets. Vertical permeabilities are highest due to multiple through-sample large fractures. Radial permeabilities are marginally lower than vertical permeabilities but higher than edge to edge permeabilities. Overall flow entering from a cladding defect would face substantially lower permeability if not aligned with a crack site in a pellet with fuel-clad bonding.

The best estimate permeabilities were in good agreement with measured permeability for an LWR fuel rod [110].

7.2. TRANSPORTATION R&D

7.2.1. Multimodal transportation trial

Understanding the stresses that will be induced on SNF during transport is an important facet of the High Burnup Data Project. A series of tests on surrogate PWR fuel assemblies loaded into an ENSA ENUN 32P rail cask was conducted between June and October 2017 in a collaboration between 11 organizations from the Republic of Korea, Spain and the USA. The data were collected for three different modes of transportation: road, water, and rail. Operations simulating the vertical placement of the ENSA ENUN 32P cask onto a surrogate storage pad were also conducted. In addition, eight tests (for a total of 125 test cases) were performed at the Transportation Technology Center, Inc. (TTCI), a railroad testing and training facility located in Pueblo, Colorado. TTCI tests were short duration tests with known conditions and with design parameters somewhat in excess of those expected on commercial railroads. Analysing the combination of the three modes of transportation, the special rail tests performed in TTCI and performance during handling all provide an understanding of the actual cumulative effects of transportation and handling of high burnup SNF that can be expected.

Specifically, the rail cask was transported by:

(1) Heavy-haul truck within northern Spain;

(2) Vessel first from Port of Santander to Port of Zeebrugge and then from Port of Zeebrugge to Port of Baltimore;

(3) Rail to the TTCI near Pueblo Colorado.

Additional testing was conducted at the TTCI using the same railcar. See Fig. 42 for a visual representation of the transportation test route.

FIG. 42. Route for ENSA ENUN 32P cask transportation tests (based on UN World Map, No. 4170, Rev. 19, October 2020).

The basket was populated with three surrogate PWR assemblies from Sandia National Laboratories (SNL), ENRESA in Spain, and a Korean reactor, along with 29 dummy assemblies which simulated the fuel assemblies' actual mass (Fig. 43). The loaded mass of the carbon steel cask was 120 t without impact limiters (the configuration used for this test) and 137 t with impact limiters.

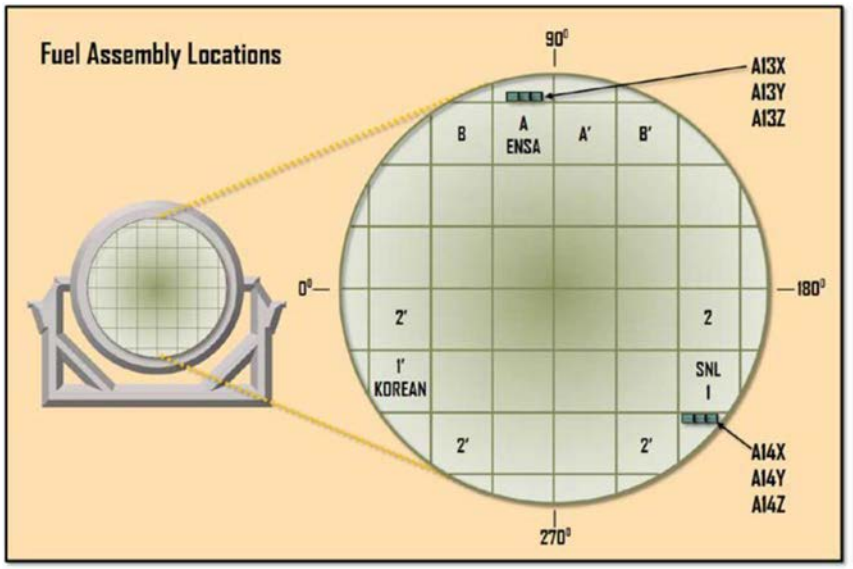

FIG. 43. Locations of the dummy assemblies in the transport cask (courtesy of ENSA).

The primary objective in conducting these tests was to measure strain and acceleration on surrogate fuel rods when the assemblies were subjected to normal conditions of transport within the ENSA ENUN 32P cask (Fig. 44). Accelerations on the cask basket, the cask, the cask cradle, and the transport platforms were also measured. Many hours of data (about 6 TB of information) were recorded by 40 accelerometers, 37 strain gauges, and 3 global positioning system (GPS) channels. The data collection frequency was 10 240 Hz for the short duration tests and 512 Hz for the long duration tests, respectively. The major purpose of the data analysis was to envelop the responses of the different transportation system elements, such as the cask, the cradle, the basket, and especially the assemblies. Therefore, the data were not filtered, with a few exceptions. The maximum accelerations and strains were determined for each of 125 TTCI tests, 10 handling tests, and shock events observed during the rail, heavy-haul, and vessel transport.

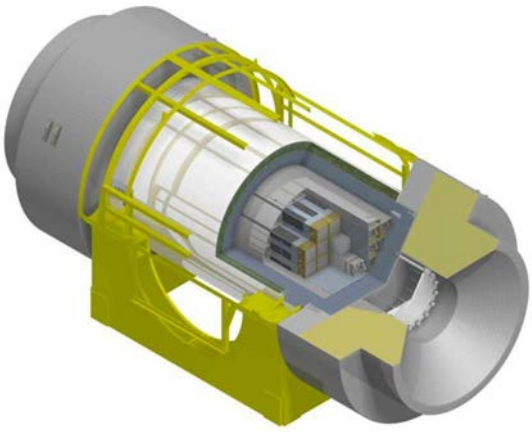

FIG. 44. Cross section schematic of ENSA ENUN 32P cask (courtesy of ENSA).

The data analysis indicated that the elements of the transportation system respond differently to the transient inputs. There was significant attenuation from the transportation platform to the cask and the basket. Smaller, but noticeable, attenuation was observed from the transportation platform to the cradle and the assemblies, except in the low frequency band (up to 4 Hz). The low frequency peak (2.5–3 Hz) in accelerations and strains of all the elements, except in the transportation platform, is related to the suspension resonance frequency. The accelerations and strains on the surrogate assemblies showed a distinct peak around 45–50 Hz related to the assembly resonance frequency. Some amplification from the transportation platform to the assemblies within the low and high frequencies was observed only in coupling at high velocities (greater than 2.7 m/s (6 mph), which are not expected to occur during the transport of SNF [111].

The analysis provides the probability distribution functions describing the shock events that occurred during ~3100 km rail transport from the Port of Baltimore to Pueblo, Colorado, and the ~400 km heavy-haul truck transport in Spain. The shock events during the ship transport were very small. The coupling events that occurred during rail transport from Pueblo, Colorado, to St. Louis, Missouri (the last point of the data collection) were also analysed. These results are important for understanding the shock environment during the different modes of transport [111].

The strains were exceedingly low on the surrogate fuel rods during the rail cask tests for all the transport and handling modes. The test results provided a sound technical basis for the safe transport of SNF.

7.2.2. Transportation equipment and logistics R&D

Regarding transportation, the USA is actively pursuing research activities in a number of areas, including:

- Development of railcars for the transport of SNF;
- Investigation of the conditions at the 14 shutdown NPP sites, along with the logistical complexity of shipping SNF from the sites;
- The conditions to be encountered by transportation casks loaded with SNF during transport activities in all transportation modes (road, rail, and water).

7.2.2.1. Railcar Development

It is anticipated that the primary mode of transport of SNF will be via rail, especially as significant amounts of SNF has been loaded into canisters for dry storage of the type associated with rail-size transportation overpacks. The efficient transportation of SNF and HLW will require the development of a specialized cask (Fig. 45) and buffer railcars to be approved by the Association of American Railroads (AAR) under Standard S-2043 [112], which defines the performance specification for trains used to carry SNF and HLW.

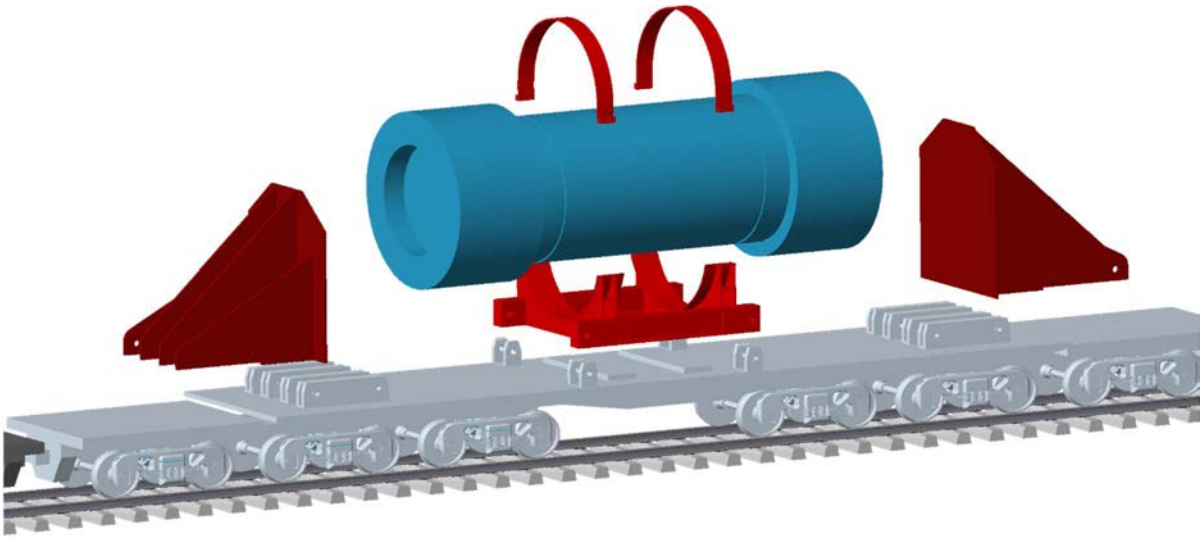

FIG. 45. 12-Axle cask railcar with simulated payload including cask, cradle, and endstop (courtesy of USDOE).

The USA has completed the initial contract in this process, which included three specific phases:

- Phase 1, Mobilization and Conceptual Design;
- Phase 2, Preliminary Design;
- Phase 3, Prototype Fabrication and Delivery.

Additionally, the USA has initiated a second contract for the final two phases of the development processes which include:

- Phase 4, Single-Car Testing;
- Phase 5, Multiple-Car Testing.

Phase 4 activities started in 2018 and included preparations for testing, such as procuring long-lead-time items such as instrumented wheel sets and fabrication of test weights that are being used to mimic the transportation casks during the testing process, as well as the single car testing of the Atlas railcar and buffer railcars. Phase 5 planning activities began in 2020 and multiple-car testing is anticipated to begin in 2021, which includes testing of the complete rail system and testing of the safety monitoring system. Completion of the project, which will include certification of the railcars as meeting S-2043 requirements, is anticipated in late 2022 or early 2023.

7.3. THERMAL MODELLING

During dry storage, in particular during the fuel drying process, fuel cladding temperature will initially increase, bringing a higher amount of hydrogen in solution out of existing hydrides, when a threshold is reached. Therefore, the determination of fuel cladding temperature is a key point for SNF safety assessment during dry storage. Because uncertainties in decay heat evaluation directly affect the determination of fuel temperature, an experimental evaluation of SNF decay heat is extremely valuable.

The Swedish Nuclear Fuel and Waste Management Company (SKB) is conducting an programme consisting of measuring the decay heat of individual spent fuel assemblies [113]. The measurements are performed at the Central Interim Storage Facility for Spent Nuclear Fuel

(Clab)[12] in Sweden, where SKB can perform calorimetric measurement of full-length fuel assemblies in addition to gamma spectroscopic measurements.

A blind test benchmark was initiated by SKB, with the support of OECD-NEA, as a contribution to the broad international cooperation aiming to increase spent fuel characterization knowledge. The blind test benchmark comprises of five PWR fuel assemblies each with different mechanical design, operational history, and cooling time from the Ringhals 4 NPP in Sweden. The peculiarity of the blind test benchmark is to have a comparison between results obtained using different simulation codes and new measured values, without having prior knowledge of the measurement data. This approach was to ensure the absence of any bias on the calculation path, with the intention of addressing which of the input parameters have the most effect on the results.

Each of the 18 different organizations participating has to report their results before being informed of the decay heat value determined by the calorimetric measurements. The benchmark involved several fuel depletion and/or decay codes and cross section libraries.

The main target of the collaboration is to assess the accuracy of the state-of-the-art simulation codes in predicting the decay heat, as well as to investigate the differences in performance between different codes. Furthermore, the programme aims to study the impact of different levels of details in the operational history on the decay heat prediction.

[12] Clab – Central Interim Storage Facility for Spent Nuclear Fuel, is a wet storage facility which has a current capacity to store 8000 tonnes of SNF. An application has been submitted to increase Clab's storage capacity from 8000 tonnes to 11 000 tonnes.

8. CONCLUSIONS

8.1. SPENT FUEL PERFORMANCE IN WET AND DRY STORAGE

Since SPAR-III, the reporting by CRP participants has not identified any new degradation mechanisms for commercial spent fuel in storage. The ongoing performance of LWR and PHWR fuel in high quality demineralized and boronated water remains excellent with storage experience spanning 60 years; there is ~35 years dry storage experience. In the case of AGR fuel, recent fuel examinations have shown that the fuel remains in excellent condition after 25 years of wet storage in sodium hydroxide dosed water. Ongoing AGR wet storage experience in dosed water now spans some 40 years.

8.2. SPENT FUEL DEGRADATION MECHANISMS (WET AND DRY)

None of the potential degradation mechanisms identified that may affect zirconium based clad integrity in wet storage has been demonstrated to be significantly involved under wet storage conditions as deducible from the studies undertaken by BEFAST and SPAR participants to date. It can, therefore, be concluded that there is no evidence available to date or a theoretical mechanism has not been identified so far that would limit the dwell time of zirconium alloy clad fuel in wet storage; provided the pool water chemistry is maintained within specified limits.

Under normal dry storage conditions the mechanisms which are currently receiving interest from CRP participants are thermal creep (although this is not considered as an issue in the USA), hydriding issues (DHC was an issue being investigated in SPAR III and related work is ongoing in some countries), and the effect of hydrogen reorientation on the behaviour of zirconium clad. The latter is an area which is still under investigation and is potentially an issue under given operating and handling conditions.

Improving the knowledge base on spent fuel behaviour for retrieval and transport situations has been investigated. A programme to experimentally verify the response of spent fuel rods to mechanical stresses was carried out using mainly PWR UO_2 spent fuel rod segments varying from low (18 GWd/tHM) to very high (100 GWd/tHM) burnup. The observed fuel masses releases from bending and impact tests were significantly less than the mass of a single fuel pellet.

For stainless steel clad fuels, the position is slightly different. The cladding is not affected by hydriding, however, other mechanisms become dominant. Where material has experienced reactor operating temperatures between 350 and 520°C, it is susceptible to inter-granular attack in storage (both wet and dry). Mitigation is through adjusting the storage chemistry in terms of pool storage or total exclusion of moisture for dry storage. Work in support of AGR fuel technology included evaluation of the effects on higher fuel burnup, modelling of the potential for creep failure during either drying or storage and assessing the difficulty of removing water from the fuel deposits.

Microstructural examination of higher burnup AGR cladding has shown that the level of precipitation and extent of grain-boundary segregation are not significantly greater in modern fuel with a peak burnup around 43 GWd/tU than those observed in the 1990s on fuel with a lower peak burnup around 21 GWd/tU.

With regard to cladding creep, there was a need to address the effects of long term fuel swelling that occurs due to the build-up of interstitial helium produced by alpha decay in the fuel matrix and its interaction with defects in the lattice structure. It was concluded that the majority of the

risk from creep failure was related to damage occurring during in-reactor operations; additional failure probability due to post-irradiation helium lattice swelling over 250 years was not significant compared to the effects of irradiation.

Since a small proportion of the fuel discharged from AGRs is sensitized to localized corrosion, it was necessary to predict whether the environment within a dry storage system could support localized corrosion. Scoping tests have shown that the majority of deposits should dry readily in any industrial drying process with minimal heating.

R&D specific to dry storage covered a range of investigations focused on:

- Spent LWR fuel: zirconium-based alloy thermal creep, hydriding issues, assessment of consequences of fuel rod breaks; mechanical testing of fuel assembly hardware components.
- Thermal modelling
    - Development of an iterative methodology for calculating the temperature of WWER fuel in VSC-24 container types;
    - Results from the HBU Demo Cask project being conducted at the North Anna site, including the insights deriving from a blind thermal benchmark.

Investigations related to hydride reorientation covered a range of topics from fundamental studies of hydride dissolution and precipitation to the development of a technical guide for safety assessment purposes. A study, unusual in terms of the time committed for performing such an investigation, involved cooling various unirradiated Zry-4 with a hydrogen content of either 200 ppm or 400 ppm from 400°C down to 100°C over periods of 1, 3, 6, and 12 months. The applied hoop stresses varied from 70 to 110 MPa. The specimens were tested at room temperature for ductility by RCT prior to and after long duration cooling. Results appear to show a variety of behaviours that are still being evaluated. Overall, very low cooling rates may further result in ductility reduction compared to results from laboratory experiments performed at high cooling rates.

Investigations devoted to areas of fuel performance concerns during dry storage involved the impact of spalling and hydride blisters on fuel performance. Spalled oxide fuels were metallographically and mechanically examined. Results from three-point bending tests on fuel rod segments with pellets inside showed the margin that the fuel column provides to the fuel rod under bending, even with a blister present in the cladding. The possibility of enhanced radial hydride precipitation was also examined. Blisters are characterized by their depth and by radial hydrides that naturally form perpendicularly to the blister due to the blister-generated tensile stresses in the surrounding cladding. For blisters deeper than ~230 μm, these naturally occurring radial hydrides reach the inner surface of a 570 mm thick cladding. After reorientation tests limited to temperatures equal to, or less than 200°C, there was no enhanced increase in radial hydride length for blisters with depth less than ~230 μm.

Results from the HBU Demo Cask project being conducted at the North Anna site provided temperature and gas sample data, which were collected at the time of cask loading in November 2017. Measured thermocouple temperatures were significantly lower than predicted. The measured PCT was ~240°C. Prior to the release of the temperature data, a blind thermal benchmark was set up. Results from best estimate thermal calculations were then compared to measured temperatures. Overall, the results from this exercise highlighted the need for research

to assess the knowledge levels needed to have confidence in best estimate thermal models. The quantity of residual water after drying was estimated to be ~100 g.

Based on good storage parameters, the evidence to date supports that transport following storage should not pose any safety concerns.

8.3. STRUCTURES WET AND DRY STORAGE

Knowledge of the long term performance of materials used in spent fuel storage systems is required for continued operations, storage system relicensing, and the development and implementation of AMPs. A number of studies on the behaviour of materials have continued or been initiated during this phase of the SPAR project.

There are many materials in use in fuel storage, for example metals, concrete and polymers.

Accelerated corrosion testing of BORAL coupons over a five year period found there to be no statistically significant loss of ^{10}B nor reactivity based on the observed results. The results imply that BORAL will maintain its efficacy and remain within SFP criticality safety margins for many years.

Areas which have been identified to date as requiring further consideration are ageing management and issues related to SCC in dry storage systems.

8.4. GENERAL CONCLUSIONS

A wealth of data to support the ongoing safe storage of spent fuel in both wet and dry storage systems has been generated by work underway in Member States. As storage durations extend, in addition to the issues directly relevant to storage, research programmes relating to the transition between nuclear fuel cycle steps such as transportation and disposal are being developed and implemented.

For more than 20 years, the IAEA's SPAR CRPs have reported the results of participating Member States' research programmes in support of wet and dry storage and the ongoing performance of spent fuel in storage. Feedback from participants and through vehicles such as IAEA advisory groups (e.g. the Technical Working Group on Nuclear Fuel Cycle Options and Spent Fuel Management, TWG-NFCO) have voiced the benefits of the CRPs to the wider international community to inform their national programmes, through the timely reporting of topical issues and developments and being a source of technical information to support safety cases.

APPENDIX I – HYDRIDE REORIENTATION AROUND BLISTERS DURING LONG INTERIM DRY STORAGE (ARGENTINA)

The possibility of radial hydride precipitation, affected by residual stress around a blister, has been analysed under conditions similar to those existing during dry storage of CNA-1 SNF. The material used was Zry-4 Atucha non-irradiated cladding section, with an external diameter of 11.9 mm and a wall thickness of 0.55 mm. From this, lengths of 50–120 mm were cut and subjected to the following tests:

- Gaseous hydrogen charging with gaseous pure hydrogen in a Sieverts device. During the whole process the specimen temperature did not exceed 38°C to avoid altering the residual stress state of the cladding. The total hydrogen concentration (initial plus charged hydrogen) was 110–140 wt. ppm, considering that the final concentration of CNA-1 claddings is in the order of 100 wt. ppm.
- Heat treatment for hydrogen homogenization at 370°C during 24 h.
- Blister formation: Each specimen was placed over an aluminium block heated in an electrical furnace (Fig. 46); in order to optimize the thermal conductivity and to produce uniform temperature along the tube, aluminium powder or a stainless steel block was introduced in the tube. The temperature of the specimen was measured with a J-type sheathed thermocouple, spot welded onto one extremity of the tube. The thermal gradient was obtained by pressing an aluminium or stainless steel, water refrigerated cold finger onto the upper surface of the tube. The cold finger contact area was circumferential, with different materials, sizes and shapes as detailed in Tables 9 and 10.
- Hydride Reorientation Test (HRT): To carry out these tests, dry storage conditions were taken into account: a maximum SNF cladding temperature of 200ºC and a maximum silo unit wall temperature of 70ºC. The tube section was pressurized with argon at temperature for a period of time (see Table 9); the pressure was calculated considering the extreme value at the end of operation life (100 bar at 350°C). Three different conditions were applied during HRT:
    1. Heating up to 200°C, pressurization of the tube at 75 bar, holding at this temperature/pressure for 30 days, removing the pressure and cooling to room temperature;
    2. Heating up to 90°C, pressurization of the tube at 59 bar, holding at this temperature/pressure for 30 days, removing the pressure and cooling to room temperature;
    3. Heating up to 190–200°C, pressurization of the tube at 75 bar, holding at this temperature/pressure for 4 hours, and cooling to room temperature at a rate of 0.24°C/h under inner gas pressure.
- Finally, the tubes were metallographically analysed looking for the presence of reoriented radial hydrides around the blisters. The specimens were progressively ground with SiC paper on the radial–circumferential plane and then etched in a solution of 45 ml HNO_3, 45 ml lactic acid and 6 ml HF (see Fig. 47). Some blisters were sectioned without HRT in order to compare with the reorientation of hydrides in samples subjected to HRT.

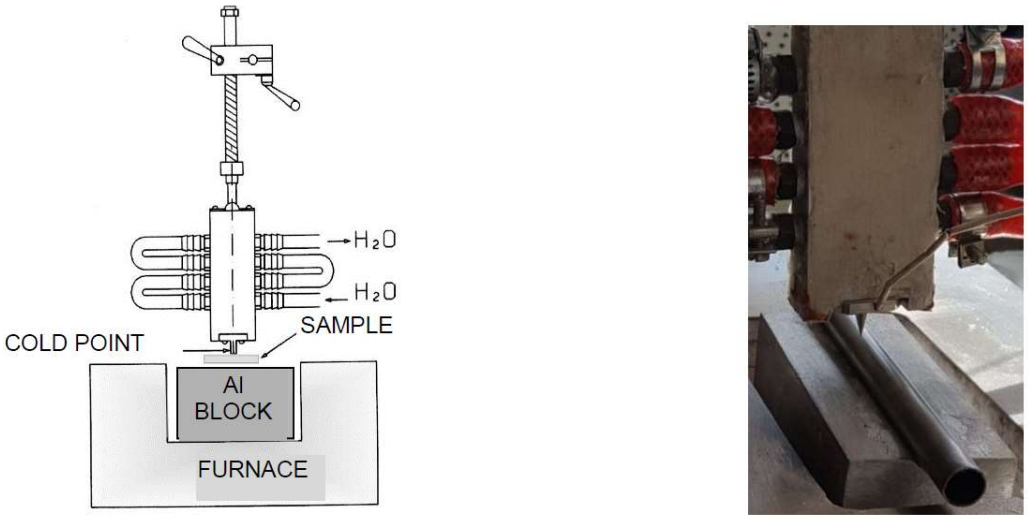

FIG. 46. Device used for Blister formation (courtesy of CNEA).

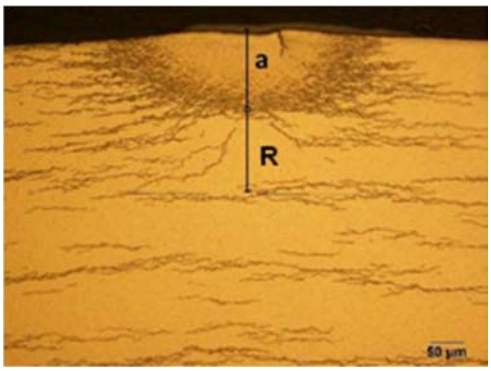

FIG. 47. Optical micrograph of a blister (20-2) showing depth (a) and reach (R) (courtesy of CNEA).

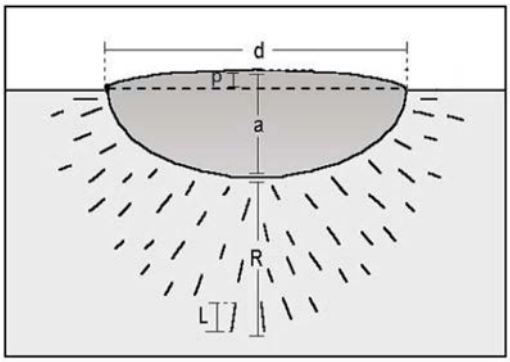

FIG. 48. Description of the parameters used to characterize the blister and radial reoriented hydrides (courtesy of CNEA).

Figure 48 is a scheme of the metallographic section (radial– circumferential plane) of a blister showing its depth (*a*), diameter (*d*), protrusion (*p*) produced by the increase in volume associated with the lower density of zirconium hydride in comparison to the zirconium matrix. The distribution of the reoriented hydride particles grown in the radial direction of the blister was characterized by the reach (*R*) which is the distance from the blister–matrix interface to the farthest radial hydride. The values corresponding to the middle section of the blister are reported in Table 9.

TABLE 9. SUMMARY OF THE CONDITIONS OF TESTS PERFORMED ON EACH SPECIMEN AND CHARACTERISTICS OF THE BLISTERS.

Blister	Blister growth condition				HRT Condition	Blister Characteristics			
	Cold finger diameter (mm)	Contact	Temp. (°C)	Time (days)		d (μm)	a (μm)	R (μm)	p (μm)
8-1	0.3	Al powder	327–330	4	No HRT	694	245	279± 74	28
8-2	0.2	Al powder	320–330	4	No HRT	843	320	215± 65	30
15-1[a]	0.2	---	306	4	No HRT	662	268	248± 30	28
15-2[a]	0.2	---	304	2	No HRT	308	117	227± 40	21
18-1	0.3	---	354	1	No HRT	388	117	127± 35	17
18-2	0.3	---	355	3	No HRT	458	144	173± 50	26
18-3	0.3	---	347	6	No HRT	590	162	260± 70	19
20-2	0.6	Alumina powder	376	4	No HRT	321	117	98± 20	6
21-1	0.6	Alumina powder	334	4	No HRT	567	158	117± 20	5
11	5.5 curved	Refractory powder	360	4	No HRT	265	76	64± 20	7
22-1	0.8	Alumina powder	337	6	No HRT	1080	445	162± 20	40
22-2	0.8	Alumina powder	336	4	No HRT	850	296	279± 31	32
23-1	0.8	Alumina powder	337	2	No HRT	675	234	336± 20	28
23-2	0.6	Alumina powder	335	6	No HRT	762	235	330± 20	24
29	0.6	Alumina powder	340	1	No HRT	368	95	125± 30	6
30-1	0.8	Alumina powder	370	4	No HRT	700	216	243± 50	17
30-2	0.8	Alumina powder	370	2	No HRT	525	138	142± 40	4
31	0.6	Alumina powder	370	2	No HRT	399	77	107± 20	5

TABLE 9. SUMMARY OF THE CONDITIONS OF TESTS PERFORMED ON EACH SPECIMEN AND CHARACTERISTICS OF THE BLISTERS (cont.)

Blister	Blister growth condition				HRT Condition	Blister Characteristics			
33	Cold finger diameter (mm)	Contact	Temp. (°C)	Time (days)	No HRT	d (μm)	a (μm)	R (μm)	p (μm)
14-1	0.37	---	325	4	90°C, 59 bar, 30 days	529	237	292± 45	19
14-2	0.37	---	331	3	90°C, 59 bar, 30 days	492	191	307± 72	33
14-3	0.37	---	331	2	90°C, 59 bar, 30 days	360	143	193± 20	20
16-1[b]	0.3	---	340	4	200°C, 75 bar, 30 days	680	250	180± 20	14
16-2	0.3	---	344	3	200°C, 75 bar, 30 days	666	255	302± 35	29
16-3	0.3	---	345	2	200°C, 75 bar, 30 days	424	134	306± 40	26
10	5.5 curved	Refractory powder	321	4.6	200°C, 75 bar, 30 days	227	77	71± 10	15
19-5	0.6	Alumina powder	360	4	200°C, 75 bar, 4 h, 0.24°C/hr cooling	818	270	283± 35	31
19-6	0.6	Alumina powder	350	2	200°C, 75 bar, 4 h, 0.24°C/hr cooling	700	230	285± 50	26
28-4	0.6	Alumina powder	340	2	200°C, 75 bar, 4 h, 0.24°C/hr cooling	477	123	121± 23	20
27-1	0.6	Alumina powder	345	5	190°C, 75 bar, 4 h, 0.24°C/hr cooling	735	256	288± 26	25
27-2	0.6	Alumina powder	343	3	190°C, 75 bar, 4 h, 0.24°C/hr cooling	606	181	347± 30	16
27-3	0.6	Alumina powder	334	10	190°C, 75 bar, 4 h, 0.24°C/hr cooling	443	106	226± 50	9

[a] Blister formed at lower temperature than the others

[b] Blister partially dissolved

In Fig 49, the reach of radial hydrides added to the blister depth is presented as a function of the blister's depth; the protrusion *p* has been subtracted. The figure also shows that, considering the error bars, there is no evident increase of the radial hydride reach after the reorientation tests. It is clear that the effect of the stresses surrounding the blister increases with the depth of the blister.

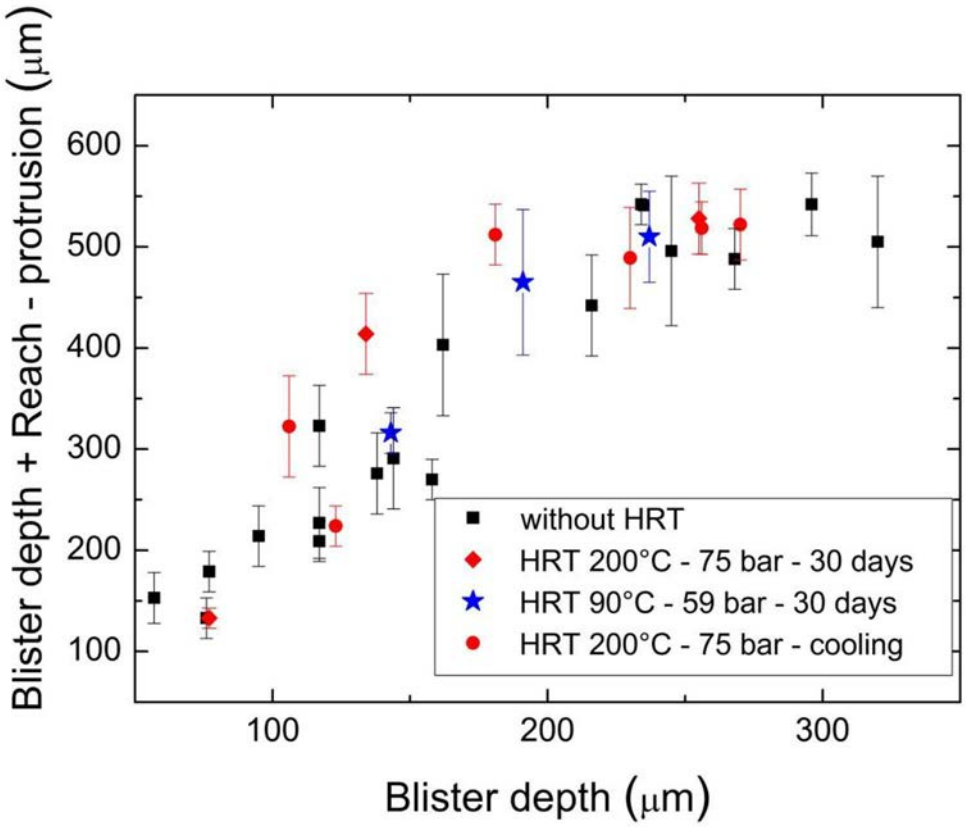

FIG. 49. Reach of radial hydrides added to the blister depth vs. the blister's depth (courtesy of CNEA).

For blisters deeper than 230 μm, radial hydrides reach the inner surface of the cladding (Fig. 50). No difference was observed between the HRT at 200°C over one month and cooled without pressure, and HRT at 200°C for 4 hours and cooled with pressure. No cases of hydride cracking were observed.

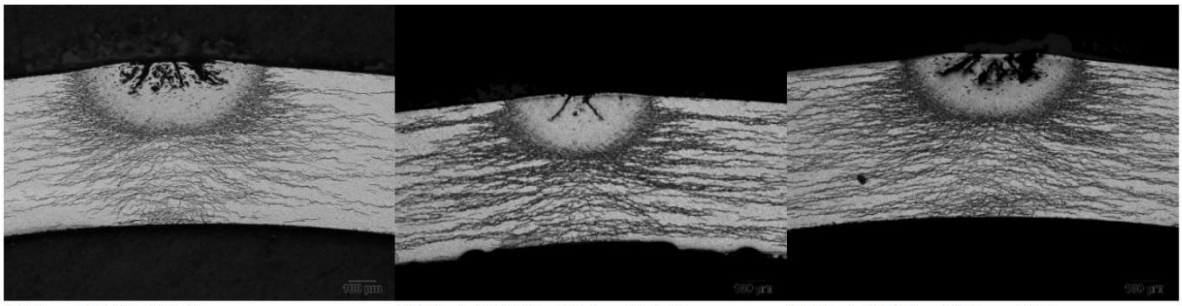

Without HRT- (15-1) *HRT at 200 °C – 75 bar (14-1).* *HRT at 90 °C – 59 bar- 16-2.*

FIG. 50. Blisters with depth greater than 230 μm: radial hydrides reach the inner surface of cladding (courtesy of CNEA).

During blister formation at a temperature of 350°C, the hydrogen concentration in solution is 102–132 ppm (terminal solid solubility according to different authors); this concentration and the stress around the blisters promotes the precipitation of radial hydrides as the blister is slowly cooled down to room temperature (10°C/h approximately). During HRT at 200°C, the cooling rate is slower (0.24°C/h) but the hydrogen concentration is only 11–19 ppm; the stress gradient might impulse hydrogen diffusion from the compressive to the tensile zone. According to the obtained results, the stress concentrator effect of the blister under the hoop stress (82 MPa at 200°C), would not seem have promoted enough hydrogen diffusion to enlarge radial hydrides, at least in a period of 30 days at temperature.

Comparison of blisters 15-2, 18-1 and 20-2, which have the same depth but were grown at different temperatures (302°C, 354°C and 376°C, respectively), shows that the reach of radial hydrides is higher at lower temperature of formation (Fig. 51). This is in agreement with the results obtained in pressure tubes reported in Refs [43, 44] and may be attributed to the decrease in alloy yield stress as temperature increases, and consequently to a decrease in tensile stresses produced by the blister.

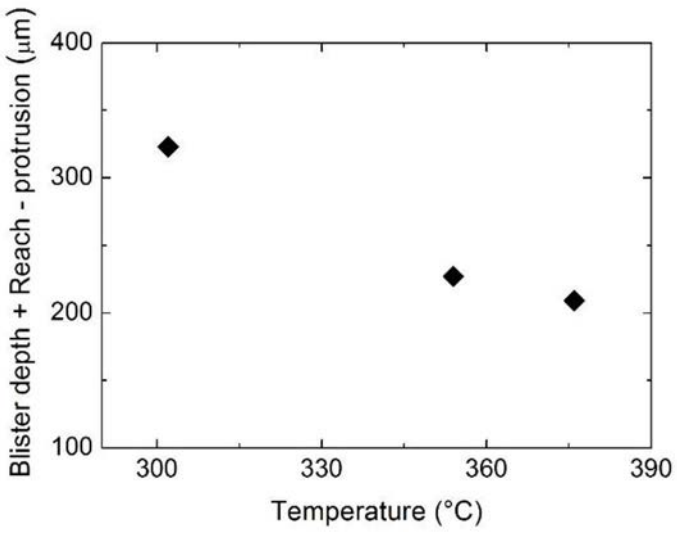

FIG. 51. Effect of the temperature during blister formation on the reach of radial hydrides, depth of the blister 117 μm (courtesy of CNEA).

Blisters reported in Table 10 and shown in Fig. 52 cross the cladding thickness, thus they are not useful for analysis of hydride reorientation. Nevertheless, it was observed that the blisters not subjected to HRT (Fig. 52(a) and (b)) present cracks that remain inside the blister, while in blisters subjected to HRT at 90°C and 59 bar or at 200°C and 75 bar (Fig. 52(c) and (d), respectively), the cracks have attained the blister–matrix interface. It is expected and usually observed in blisters reported in literature that cracks remain inside the blisters due to compressive stresses inside them. Thus, in the current HRT it is likely that hoop stress, during HRT, has surpassed those compressive stresses, favouring crack propagation.

TABLE 10. SUMMARY OF THE CONDITIONS OF TESTS PERFORMED ON EACH SPECIMEN AND CHARACTERISTICS OF THE BLISTERS

Blister	Blister growth condition				HRT Condition			Blister Characteristics	
	Cold finger diameter (mm)	Contact	Temp. (°C)	Time (days)	Temp. (°C)	Pressure (bar)	Time (days)	d (µm)	a (µm)
9	0.8	Alumina	345	7	No HRT			1300	584
24	0.8	Alumina	340	10	No HRT			1129	577
3	0.8	Ultra copper	339	14	90	59	30	1325	563
4	0.8	Ultra copper	334	14	200	75	7	1364	452

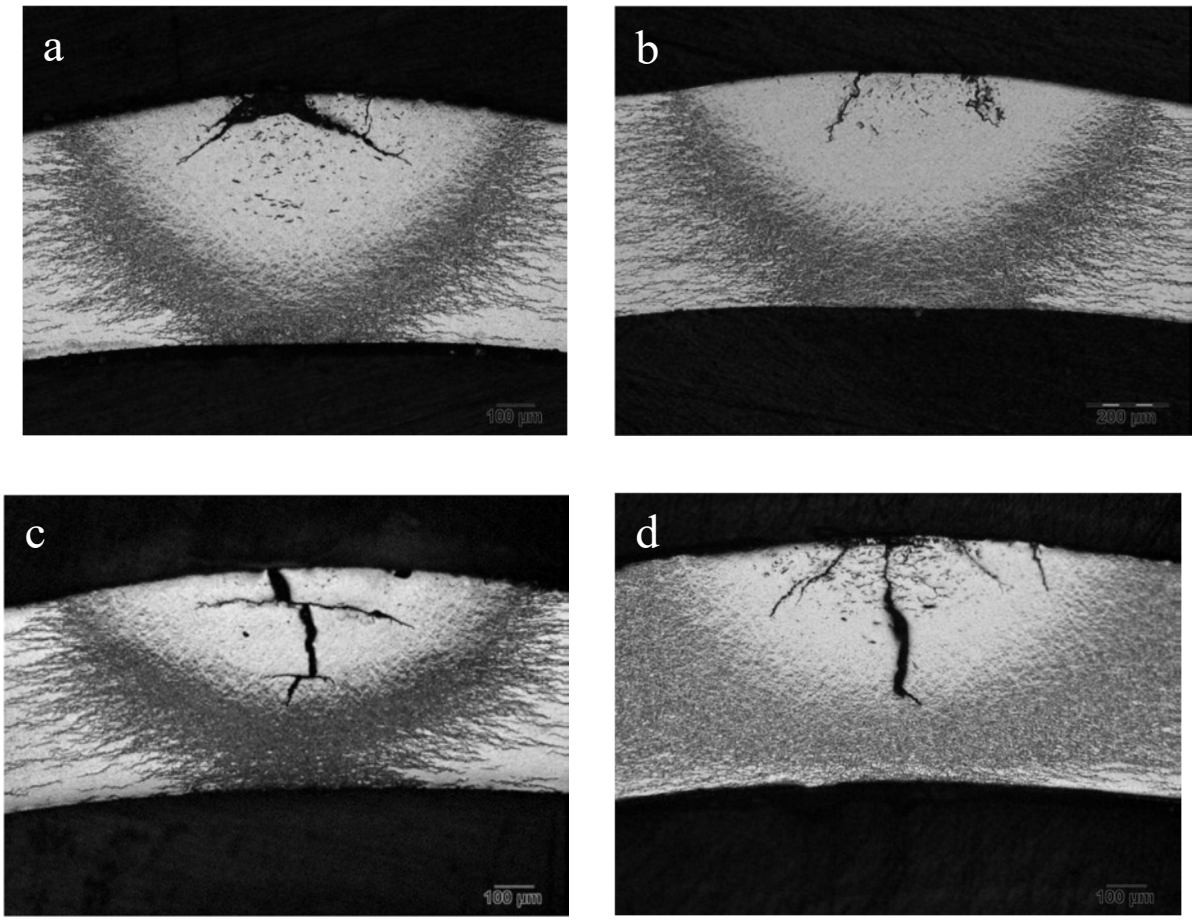

FIG. 52. Optical micrographs of blisters (from top): a) 9 (without HRT); b) 24 (without HRT); c) 3 (HRT at 90°C & 59 bar); d) 4 (HRT at 200°C & 75 bar) (courtesy of CNEA).

Some blisters have been dissolved under the conditions presented in Table 11. After that, they were subjected to HRT at 200°C and 75 bar during 4 hours followed by cooling at 0.25°C/h.

TABLE 11. CONDITIONS OF GROWING AND DISSOLUTION OF BLISTER AND LENGTH OF CRACKS AND HYDRIDES AFTER HRT AT 200 °C

Blister	Blister growth conditions				Blister dissolution		Crack length (μm)	Hydride length (μm)	Hydride growth rate (m/s)
	Cold finger diameter (mm)	Contact	Temp. (°C)	Time (days)	Temp. (°C)	Time (days)			
19-1	0.8	Alumina powder	360	4	345–370	18	166	100	3.9E-11
19-2	0.8	Alumina powder	360	2	345–370	16	147	81	3.1E-11
19-4	0.4	Alumina powder	355	4	345–370	12	102	29	1.1E-11
28-1	0.8	Alumina powder	340	10	340–355	8	117	48	2.4E-11
							86	31	1.6E-1
28-2	0.6	Alumina powder	340	4	345–355	4	38	9	4.5E-12
17-4	0.4	No	337	5	330-370	10	47	20	4.3E-12

The metallographic analysis showed that hydrides grew at the crack tip (Fig. 53). The length of cracks and hydrides are reported in Table 11. Figure 54 shows the hydride growth rate (calculated as hydride length / HRT duration) as a function of crack length. In these HRTs, two effect are superposed: the diffusion induced by the stress concentration effect of the crack and the precipitation accelerated by the cooling at 0.24°C/h, which is much higher than cooling in a silo. Considering a crack of 166 μm and a cladding thickness of 0.55 mm, hydride growing at a rate of 3.9×10^{-11} m/s would cross the entire thickness in 163 days.

FIG. 53. Hydrides precipitated during HRT at crack tips in dissolved blisters (courtesy of CNEA).

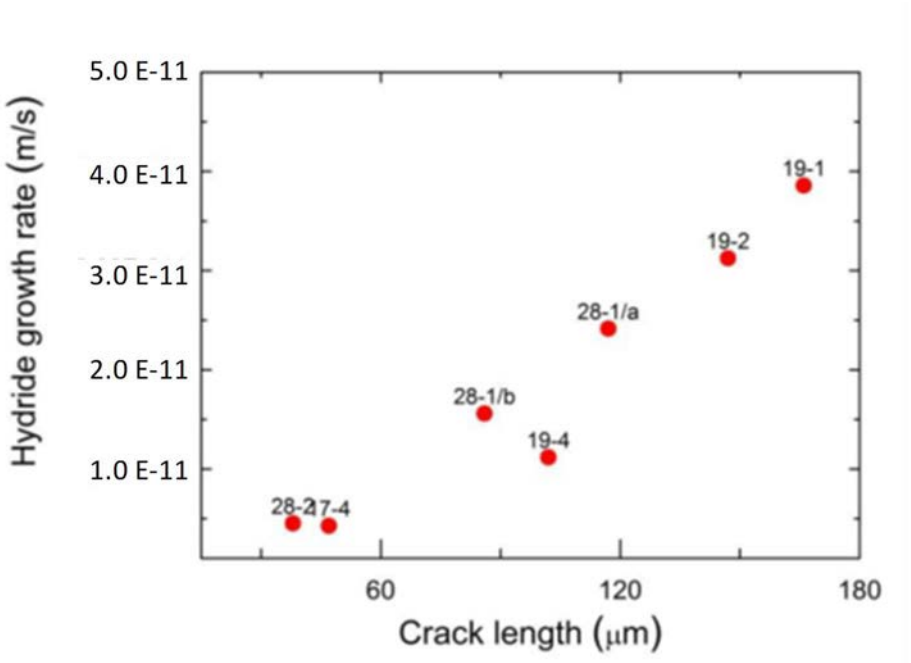

FIG. 54. Hydride growth rate at cracks tip in dissolved blisters during HRT at 200 °C – cooling with pressure (courtesy of CNEA).

APPENDIX II – SPENT NUCLEAR FUEL MECHANICAL TESTING AT JRC (SWITZERLAND)

In line with the decision by the Swiss Federal Council and the ENSI Guideline [60], Nagra initiated several studies and research, development and demonstration activities aimed at assessing spent fuel mechanical performance (response of spent fuel rods to mechanical stresses), and also at developing concepts for handling of consequence scenarios [114].

The main experimental campaign is conducted in JRC Karlsruhe exploiting the hot cell facilities and past experience on mechanical testing of SNF [61]. The focus of the experimental studies is on the effect of hydrogen load, hydride distribution and fuel–cladding interaction on the cladding integrity. The campaign is carried out using spent fuel rods and segments with different burnup levels (from low to ultra-high burnup) mainly originating from Gösgen NPP, with the focus on the effect of hydrogen load, hydride distribution and pellet–cladding interaction on the cladding integrity. Impact and bending tests on several samples have been already performed whilst post irradiation examination are currently under development and/or in a post processing phase.

A description of the experimental campaign is given in the following sections, starting with the description of samples preparation and experimental devices, followed by the cold test campaign.

II.1. TEST MATERIAL AND SAMPLE PREPARATION

The experimental campaign was divided in two phases, namely the ‘cold’ or analogue experiments and the hot cell campaign. The analogue studies were performed before testing on the spent fuel rods to test and further optimize the equipment, as well as to obtain indicative data for the performance tests in the hot cells.

The cold samples consisted of cladding tubes filled with high purity aluminium oxide pellets of known mechanical properties with a diameter of 9.27 mm and length of 10 mm. The cladding material used was a conventional Zircaloy-4 (ZY-4 PCA-1 FFQ) tube with known impurity concentrations. The Zry-4 tubes had an outer diameter of 10.75 mm, wall thickness of 0.725 mm and a total length of 298 mm, giving a radial gap between the cladding and the pellets of 0.015 mm.

PWR spent fuel rods available to JRC-Karlsruhe were used for the hot test campaign. The samples were selected on the basis of consistent fuel (UO_2) and cladding type (DX-D4) and burnup variation (from 18–100 GWd/tHM). The 100 GWd/tHM rod represents a very special case, as standard SFA-averaged burnups from Swiss NPPs are below 80 GWd/tHM. The DX-D4 was chosen as it is representative of the PWR cladding type employed in Swiss NPPs and, furthermore, conservative in terms of hydrogen uptake of the cladding when compared to the other available cladding type (i.e. the M5 – enhanced cladding designed for high burnup [115]).

The dummy samples were pressurised up to 40 bars with helium. The selection of this internal pressure is typical of irradiated commercial fuel rods, representative of a burnup value of around 50 GWd/tHM [99]. The hydrogenated cladding samples were provided by the Institute of Applied Materials (IAM) of the Karlsruhe Institute of Technology (KIT). The hydrogenation method is described in Refs [115, 116]; the samples were hydrogenated at temperatures of 550°C, 650°C and 750°C, respectively. Different hydrogenation temperatures result in different zirconium hydride orientation, where the higher the temperature is, the more randomly oriented hydrides are created. The treatment resulted in a hydrogen concentration distribution along the axis that was determined by measuring diameter variations.

Each spent fuel rod was segmented into pieces of ~480 mm and the segments pressurized to their corresponding internal pressure (typically ~30–70 bar at room temperature), as measured at the end of in-pile service. These segments, with basically similar characteristics within a rod, can have significant differences, e.g. burnup, if from the top and/or bottom of the rod. Further details on sample preparation, device specific characteristics and results with the use of surrogate rods, have been reported in Ref. [114].

II.2. THREE-POINT BENDING TEST DEVICE

The experimental apparatus, which follows the prerequisites of a standard bending test as specified in the ISO 7438 standard, is shown in Fig. 55. The device consists of a step-motor which drives a loading column along a vertical axis, perpendicular to the sample orientation. The loading column has a concave contact surface which is adjusted to the cladding surface of the fuel rod sample. The modular design of the device allows the use of different loading contact components. A load sensor measures the load applied to the cladding surface. The sample supporting points could be placed at different distances. This provides a great flexibility for measuring samples of different lengths. The minimum distance between the centres of the supports is 140 mm and the maximum deflection that can be achieved is 75 mm. Data acquisition is performed by using three different sensors to measure the applied load, the deflection, and the internal pressure of the segment.

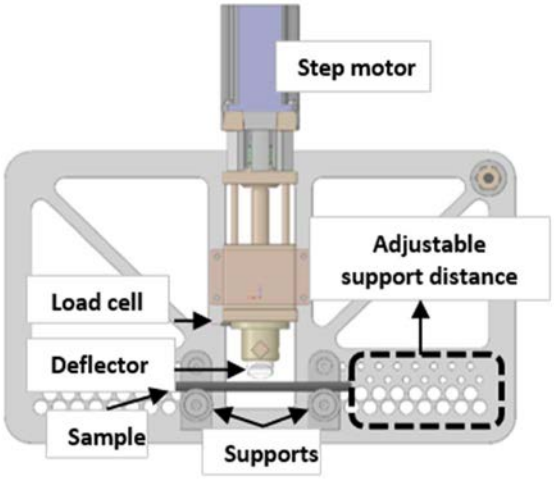

FIG. 55. Overview of the three-point bending device (courtesy of JRC-Karlsruhe).

II.3. IMPACT TEST DEVICE

An impact load device was built for hot cell testing of spent fuel rodlets and was used to perform a new campaign of measurements. This advanced setup, shown in Fig. 56 (left), presented several improvements compared with the device operating in the previous tests [117]: the impact takes place in a closed chamber in order to contain all released material; the chamber is connected to an aspiration system through a particulate filter; the heavy fragments after fracturing fall in a collection chamber at the bottom of the device, to allow for their characterisation.

The impact is recorded by a high-speed camera mounted on the device (instead of outside the hot cell window); the rodlet mount allows rigid or loose support of the rodlet; special impact

modes are possible. Figure 56 (right) shows the device in its current location in the hot cell. The test procedure consists of releasing the free-falling impactor from the top end through a vertical guide column, which impacts the sample laterally. The height of the column (total height is 69 cm) and the mass of the impactor determine the load on the sample. Rounded support holders are used to allow the free upward movement of the rod during the test.

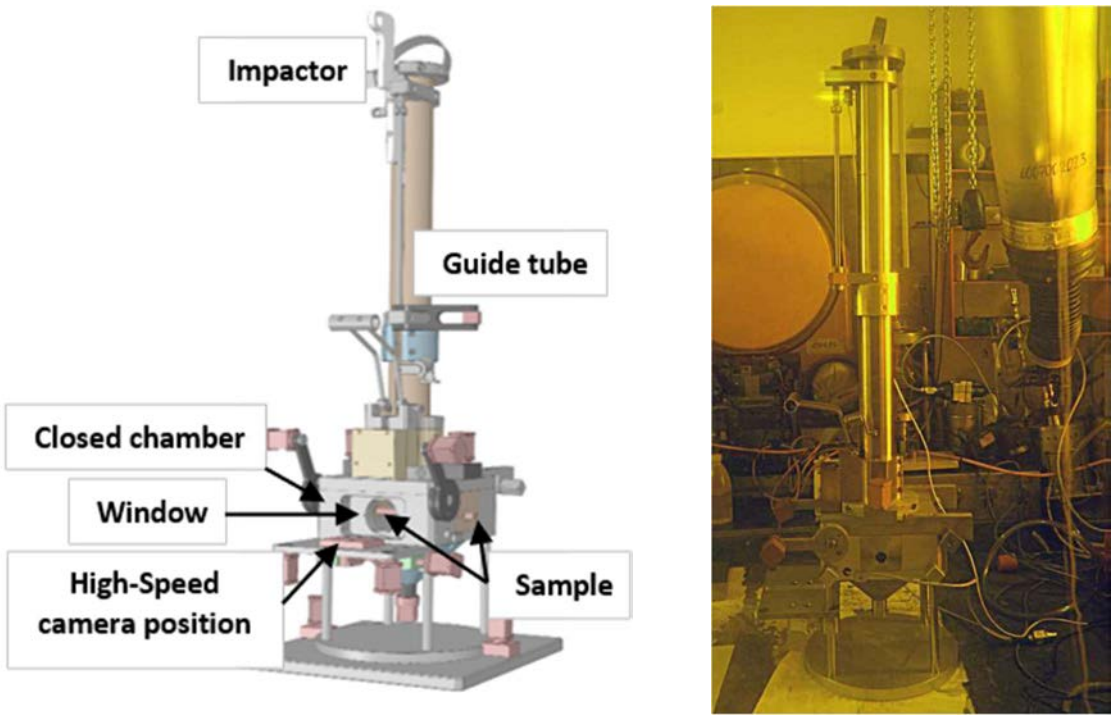

FIG. 56. Impact test device design (left), impact test device installed in the hot cell (right) (courtesy of JRC-Karlsruhe).

The determination of the amount of fuel released during the impact is carried out by the accurate weighing of the samples before and after the test, while the heavy fragments are collected at the bottom of the testing chamber and weighed after sieving into different size groups. A pump coupled with micro-filters samples the gas from the impact testing chamber to collect aerosols and fine particulates fraction (see Fig. 57). These particles will be analysed in terms of size distribution and elemental composition. This type of information can be extremely useful for DPC cavity decontamination and/or to set-up inspections. Moreover, it can help in the phase of development of concepts about the safely handling of damaged fuel, where real data can replace (or validate) theoretical assumptions (e.g. fuel powder and gases released outside the DPC).

FIG. 57. Big fragments are collected in the container placed at the bottom of the funnel (left), fine fragments/aerosol particles are collected on the metallic filter (right) (courtesy of JRC-Karlsruhe).

II.4. COLD CAMPAIGN: ANALOGUE BENDING TESTS

The first phase of the experimental campaign consisted of analogue experiments conducted in cold laboratories with dummy rods (as previously illustrated), where the devices and the acquisition capabilities could go through an optimization procedure.

Results from the cold test campaign aimed to provide valuable input on finite element analysis of mechanical tests, highly important for validating the models of spent fuel rod mechanical behaviour as well as to provide the necessary experience to test the device [118].

It is well known that the hydrogen content and distribution in spent fuel cladding is a key factor affecting the response of the fuel rod to mechanical stresses and loading that may occur during the various stages of spent fuel management. To verify the effectiveness of the bending setup in characterizing such effects, the cold test campaign covered a wide range of local hydrogen concentration levels, from very low (including untreated cladding) to extremely high (>2000 ppm). Hydride reorientation phenomena have been not induced and have been not observed.

In total, 20 experiments have been conducted on hydrogenated samples for the present cold test campaign. The pressure, the applied load, and the deflection of the sample at the loading point were acquired for each experiment. Typically, a constant displacement rate of 1 mm/min was used. The evolution of the data acquired during the test provided information from the first contact to the point when the cladding cracked and the pressure and applied load dropped. Figure 58 illustrates the typical results of one such experiment performed on a sample with a local hydrogen content of 230–240 ppm. In the graph, load and internal pressure are plotted as a function of deflection. The pressure decreases slowly during the bending of the rod (gradual volume increase), dropping once the cladding tube cracks; the elastic and plastic deformation regions can be easily distinguished. The strain energy transmitted by the loading device to the sample can be calculated by integrating the area under the curve; the critical energy until fracture can be also estimated. Furthermore, the ultimate and fracture strength can be calculated. Details of small discontinuities observed in the plastic deformation region of the load vs. deflection curve are highlighted in the inset shown in Fig. 58. The small drops of the load can be attributed to cracking occurring in the alumina pellets under the load applied during the experiment. Such cracking of pellets was audible during the test.

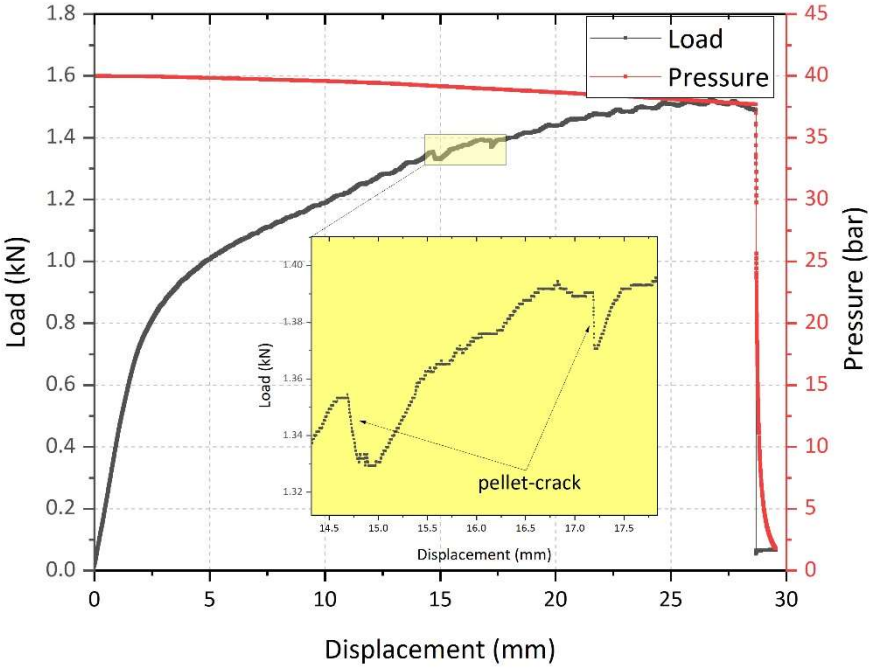

FIG. 58: Load/pressure vs. displacement during a 3-point bending test (courtesy of JRC-Karlsruhe/Nagra/EPFL).

In Fig. 59, the deflection corresponding to the sample fracture is plotted as a function of the local hydrogen content for all the experiments performed on hydrogenated samples. The effect of varying hydrogen concentration is clearly visible. Black, orange and red dots correspond to samples having experienced hydrogenation temperatures of 550°C, 650°C and 750°C, respectively. The maximum load persists in a very narrow range between 1.3 and 2.1 kN.

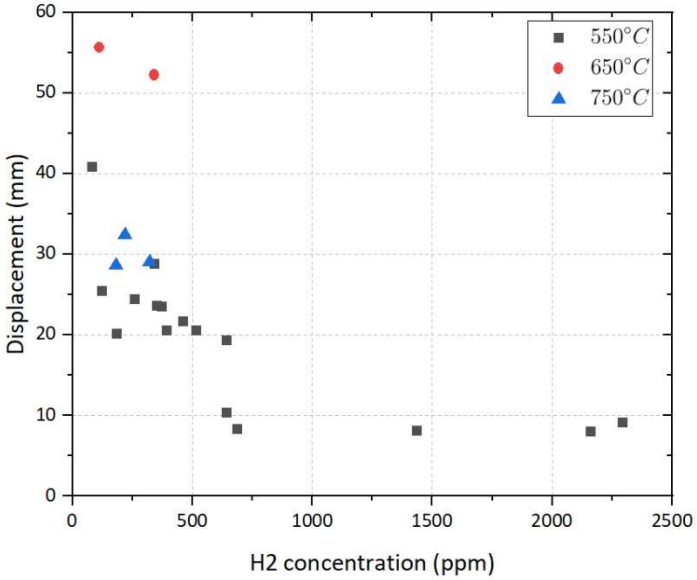

FIG. 59: Deflection to fracture as a function of hydrogen concentration. Black, orange and red dots correspond to samples having experienced hydrogenation temperatures of 550°C, 650°C and 750°C, respectively (courtesy of JRC-Karlsruhe/Nagra/EPFL).

As a first outcome of these tests, it can be seen that the cladding has preserved its ductility at very low hydrogen content (≤100 ppm) and it requires a large deflection in order to become fractured. In this case, the presence of the dummy alumina pellets inside the samples seems to contribute to the fracturing (see Fig. 60(b)). Zry-4 cladding tubes with the same hydrogen content but without pellets inside did not fracture. Also, no fracture was observed in non-hydrogenated cladding tubes (see Fig. 60(a)), highlighting both the high ductility of the material and the deteriorating effect of the hydrogen content (even at low concentration) on its mechanical strength. A nearly linear correlation between the local hydrogen content and the deflection range can be observed for a hydrogen content above 100 ppm and up to around 700 ppm. Figure 60(c) shows the fracturing of the rod for an intermediate Zr hydride range. This region includes the hydrogen content range to be expected in commercial spent fuel cladding after discharge from reactor. At higher hydrogen content (by no means representative of real conditions during dry storage), the samples break at the same deflection level independent of the local hydrogen content. The cladding material in this range can only withstand a deflection of ~9 mm until cracking, as shown in Fig. 60(d). The fracturing of the sample occurs more abruptly than for the more ductile samples. Post-test examinations were performed on the samples. Examination of the fracture indicated, as expected, that the samples cracked preferentially at the pellet–pellet interface nearest to the loading point and not exactly at the point of the theoretical maximum applied load, i.e. at the axial position under the loading contact point. This confirms the high significance of the presence of the fuel pellets, which affects the response to the mechanical load of the composite fuel–cladding system.

Hydrogen measurements using the method of hot gas extraction have been carried out on selected samples at the point of fracture to determine the local hydrogen concentration to confirm the nominal content and support the conclusions from the observed trends.

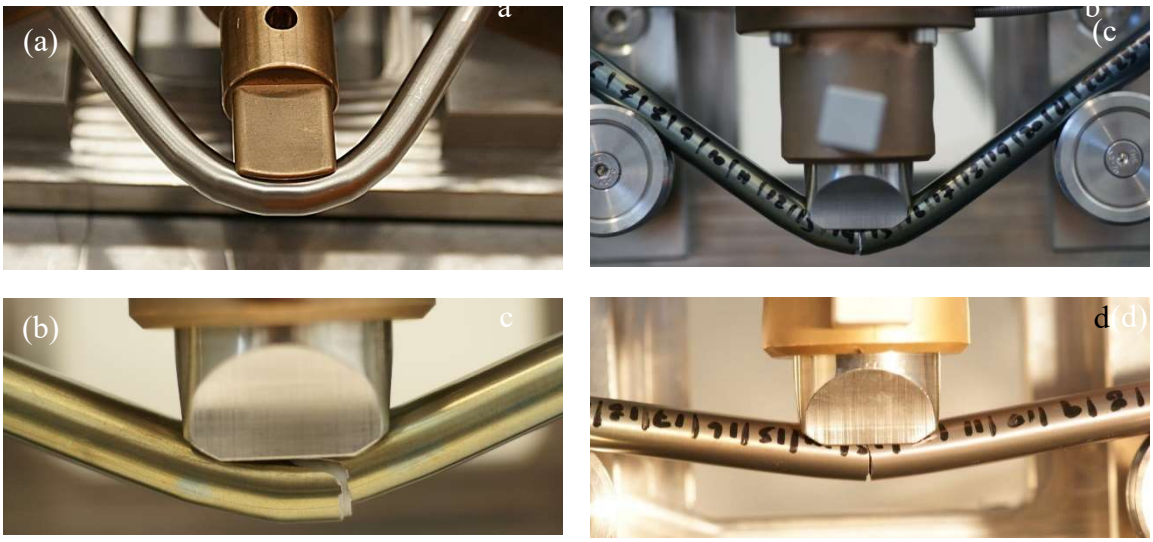

FIG. 60: Analogue bending tests; a) Bending test in non-hydrogenated sample. The rod shows high ductility; b) Bending test in sample with intermediate zirconium hydride content; c) Importance of the presence of pellets during the test. The sample breaks under the influence of the pellets, always at the pellet-pellet interface; d) Bending test in high Zr hydride content (>700 ppm) sample. The rod shows brittle behaviour when compared to the other rods (courtesy of JRC-Karlsruhe/Nagra/EPFL).

II.5. MECHANICAL BEHAVIOUR OF SPENT FUEL RODS: THE BENDING EXPERIMENTS

Three-point bending tests were carried out to study the mechanical response of the sample by derivation of load-deflection curves, as shown in Fig. 61(a) (*in arbitrary units*: a.u.) for two samples of different burnup. A constant displacement rate of ~1 mm/min was applied. The load drops instantly at the point of fracture when the crack initiates. Both samples experience plastic deformation, but the low burnup segment (black line in Fig 61) preserves ductility. The high burnup sample (red line in Fig 61) exhibits greater strength indicated by the fracture load comparison. The rupturing load for the high sample is not that much higher with respect to the lower (~20%). In addition, it has slightly higher stiffness as observed in the slope at the elastic region. The related displacement is ~2.5 times longer for the lower burnup sample. The stiffness of the rod is basically a response of the system 'Cladding' + 'Pellets', therefore the higher stiffness of the high burnup fuel rod should be mainly caused by the strength of the interface pellet–cladding inner surface, i.e. at lower burnup this interface is either not yet formed (no complete closing of the gap) or at least mechanically not as stable as in the case of high burnup rods.

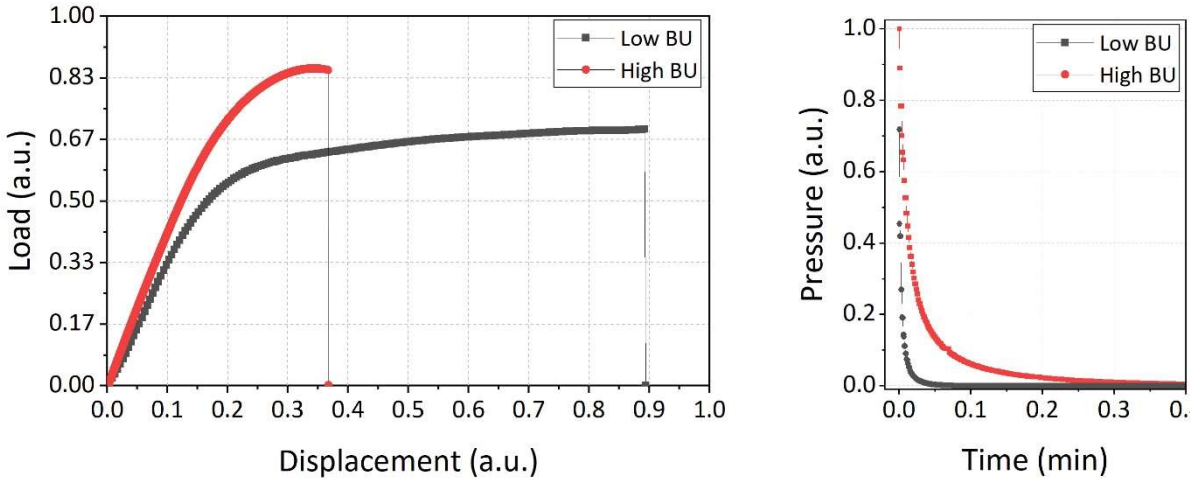

FIG. 61. (a) Load deflection curve of high and low burnup (BU) samples during the 3-point bending test; (b) segment pressure drop after fracture vs. time (a.u. = arbitrary units) (courtesy of JRC-Karlsruhe/Framatome/Nagra/EPFL).

The pressure drops after fracture, shown in Fig. 61(b), provide information on the gas permeability through the SNF rods. As expected, the depressurisation of the high burnup sample is slower due to the closed gap between the cladding and the pellets. In both cases, the time to ambient pressure is in the order of seconds. The permeability data can be used in other assessments concerning the safety of spent fuel rods, e.g. in the assessment of drying procedures of defect pins. Figure 62 shows the 67 GWd/tHM spent fuel rod, pressurized at 70 bar, at the breakage after the bending test. Figure 63 shows the related post irradiation examination and the morphology and location of the hydrides in the duplex cladding, respectively to the left and right of the figure.

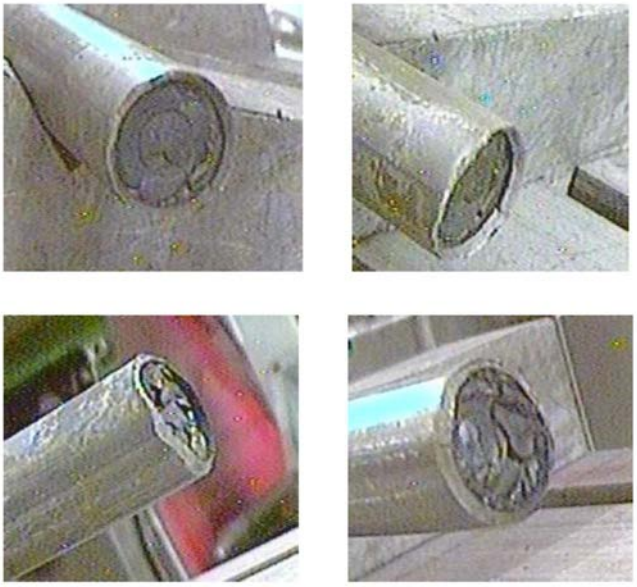

FIG. 62. Several views of the SNF rod at the breakage after bending test (courtesy of JRC-Karlsruhe/Framatome/Nagra/EPFL).

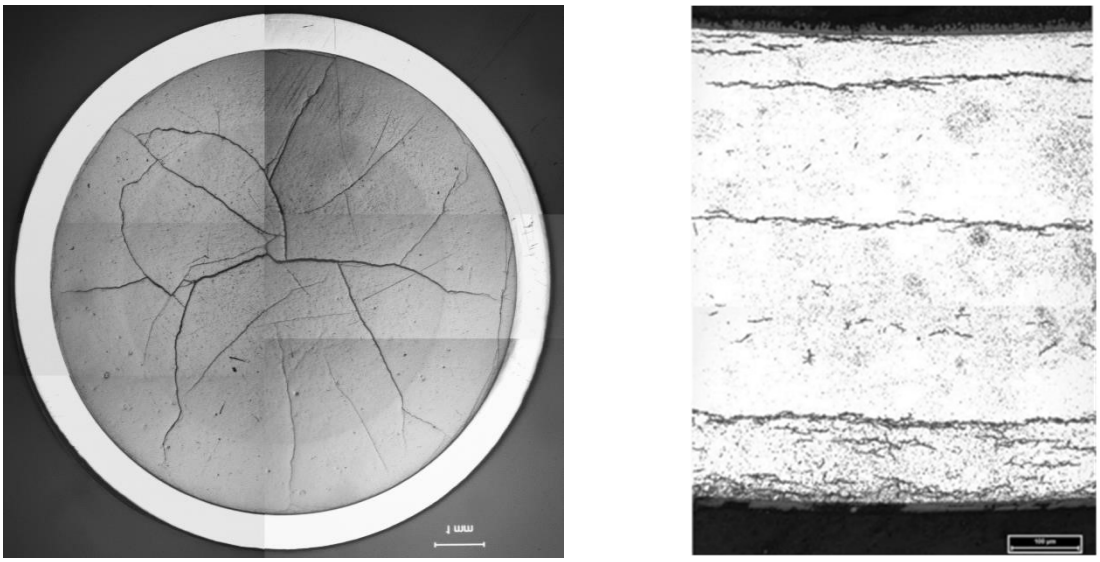

FIG. 63. Post irradiation Examination of the 67 GWd/tHM SNF rod (left); Morphology (left) and location of the hydrides in the duplex cladding (right) (courtesy of JRC-Karlsruhe/Framatome/Nagra/EPFL).

II.6. IMPACT TESTS AND SPENT FUEL RELEASE

The fuel rod samples are mounted on a stable metallic block near the column bottom end. To prevent the impactor from bouncing onto the sample, brakes are placed at the bottom end of the column to block the impactor after its first impact. The experiment is recorded by a high-speed camera (2000/4000 frames/sec) connected to the testing chamber inside the hot cell. An example of an image sequence is shown in Fig. 64 where a set of frames are selected to illustrate the deflection and fracture of an SNF rod segment [119]. The visual inspection of the impact provides extremely valuable insight of various phenomena occurring. The image on frame 1 of

Fig. 64 shows the hammer just before touching the specimen, while frame 2 shows the moment of contact between hammer and specimen. In frames 5 and 6, the spallation (ejection) of the outer oxide layer on the Zircaloy cladding is clearly seen in areas at the vicinity of the applied load as soon as impact occurs. In addition, the position of the crack initiation as well as its propagation and morphology are revealed, providing important information on the type of fracture and the critical regions where maximum stresses occur. Moreover, the progression of the released fuel fragments at the opening of the crack can be observed. The experience gained in the development phase of the device showed that the velocity of the fragments could be correlated to the depressurisation which in turn could potentially influence the amount of the total released fuel mass.

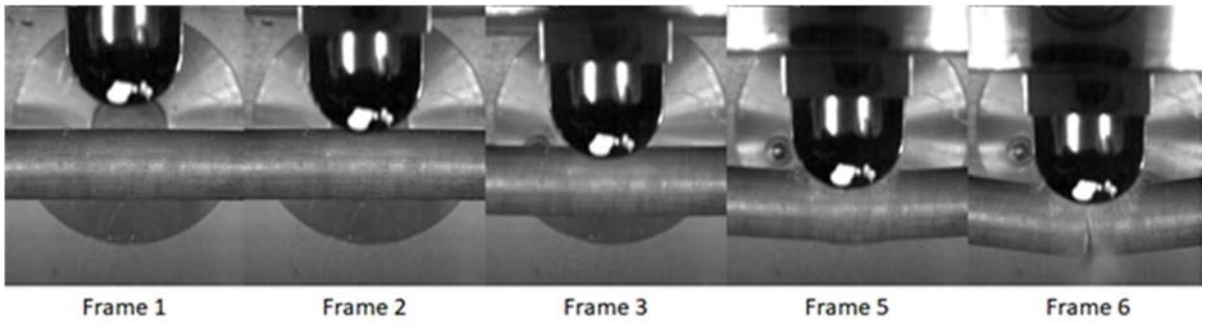

FIG. 64. Representative selected frames of the image sequence during an impact test (courtesy of JRC-Karlsruhe/Framatome/Nagra/EPFL).

Some impacted rodlets exhibit additional cracking at the sample holders under the impactor. No excess release of fuel was observed, even with high burnup samples. Figure 65 shows the image at the point of rupture for three different fuel segments, with increasing burnup (BU in figure) from left to the right. These results are in absolute conformity with the bending tests. By considering the initial horizontal position of the sample, denoted by the red line in Fig. 65, the displacements at the moment of rupture can be determined. This decreases with increasing burnup for fuel rods having the same cladding material. As with the bending results presented above, the deformation from the initial (horizontal) state depends mostly on the hydrogen content in the cladding, which usually follows the burnup.

Only the volume affected by the fracture was released. Moreover, no additional fuel was released upon tapping the two fractured segments as the fuel was solidly bonded in the fractured segments. The aerosol and fine particulate fraction were collected. Particulate size distribution on the filter indicates a log-normal distribution with a certain size and standard deviation.

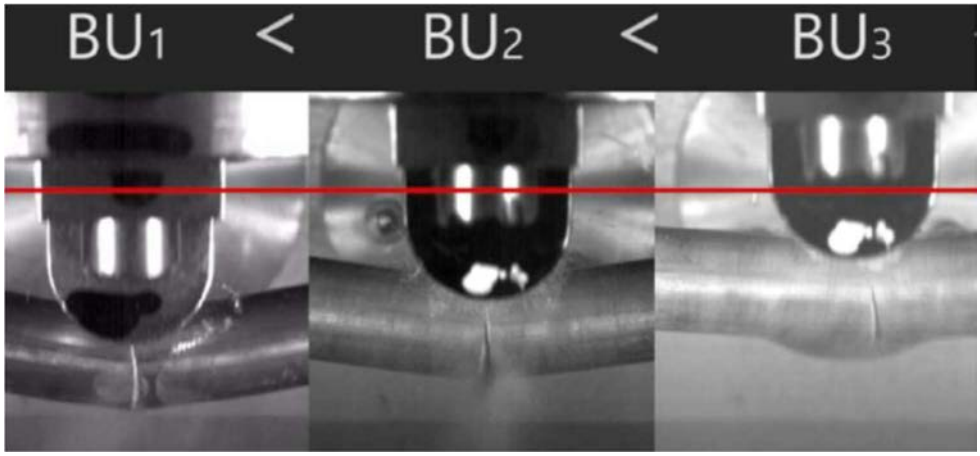

FIG. 65. High speed camera videos from different impact tests showing the aerosol release and total deflection from the initial horizontal position (red line) at the rupturing moments (courtesy of JRC-Karlsruhe/Framatome/Nagra/EPFL).

II.7. IMAGE ANALYSIS

A dedicated effort has been given to develop an image analysis procedure to convert the obtained impact sequence images into useful data, namely the instantaneous sample deflection and impactor velocity per frame, and also acceleration and impact loads can be achieved. In fact, the process converts the obtained impact sequence images into an instantaneous sample deflection and hammer velocity. Thus, the kinetic energy transmitted by the hammer to the specimen can be calculated from the observed velocity reduction upon impact, as illustrated in Fig. 66. The quantification of the uncertainty associated with the derived image analysis methodology has not been evaluated at this stage. A direct estimation of this uncertainty is very challenging, since it is depended on the minimum detectable displacement and applied object tracking algorithms, which can differ for each case.

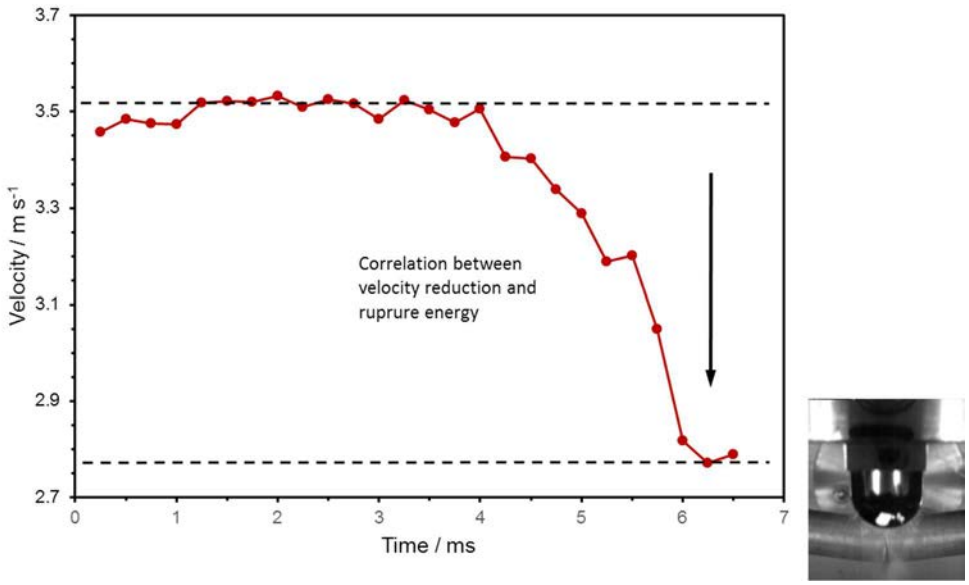

FIG. 66. The hammer velocity change is used to calculate the transmitted energy caused the specimen rupture (courtesy of JRC-Karlsruhe/Framatome/Nagra/EPFL).

II.8. FUEL RELEASED AFTER IMPACT

The results from impact test on the 67 GWd/tHM SNF rod show that a total of 2.33 g of material was released upon fracturing, predominantly fuel, but also some fragments from the cladding oxide. The specimen, fixed on the chamber walls, was impacted by an 8.5 kg hammer and broke in two parts via three breakages with an overall mass release of 2.44 g, i.e. 0.81 g per breakage. The majority of the released material was collected as coarse fragments, whereas ~0.05 g (2% of the total mass released) consisted of fine particles deposited on the inner walls or collected on the aspiration system of the testing chamber. The results of this previous experiment were reported in Ref. [116].

A classification of the fuel particles released after the impact test is given in Fig. 67 for large fragments, where the weight fraction of the particles is shown as a function of particle size. Roughly 98% of the released mass collected at bottom of the test chamber, where almost half had a size larger than 1000 µm.

It is worth noting that for both the high burnup case and the low burnup case, the total mass of fuel released upon fracture did not exceed one pellet per fracture. On the basis of these results, and supported by fracture surfaces analysis, the unzipping of fuel material from cladding tubes of SNF during handling accident scenarios (fuel crash) can be excluded with very high probability.

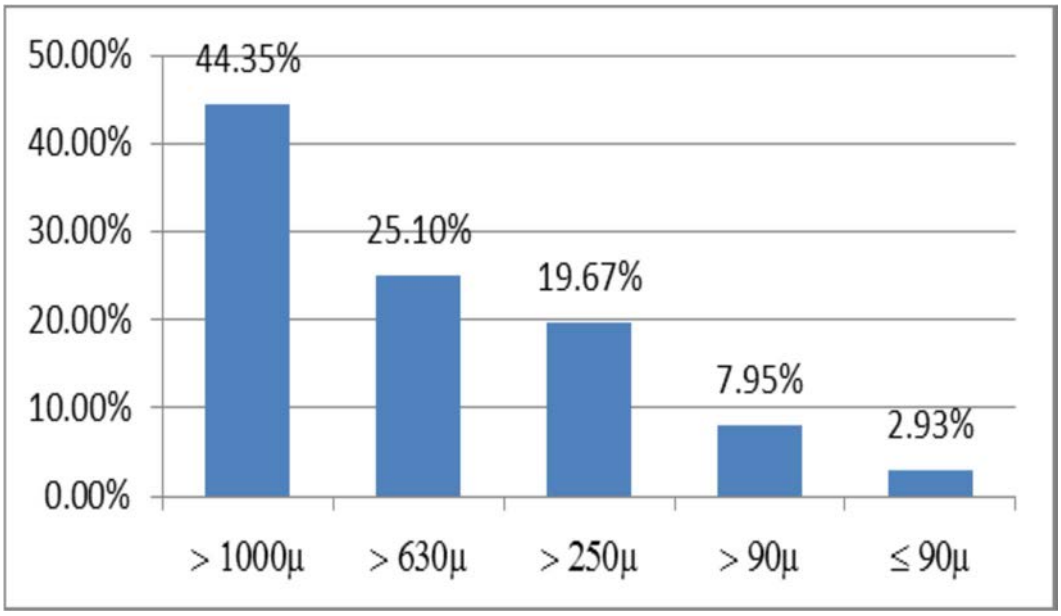

FIG. 67. Classification of the fuel particles released – large fragments: weight fraction as a function of particle size (courtesy of JRC-Karlsruhe/Framatome/Nagra/EPFL).

Additionally, a swipe test using a carbon filter was performed at the surface of the closed chamber to collect and examine the remaining particles in order to determine size distribution and elemental composition. The released particles were also photographed on a scanning electron microscope (SEM). The fuel particles reveal a variety of morphologies, as they originate from different radial locations of the fuel pellet. The presence of relatively large (up to tens of microns in size) particles with the typical morphology of the high burn-up structure (HBS) confirms that recrystallised particles in HBS areas do not necessarily fragment into individual grains, but rather follow discrete cracking patterns. However, numerous sub-micron grains were also found. Cladding oxide particles were also detected but excluded from the

analysis, as they were distinguished in the micrographs with the back-scattered technique. The micrographs were processed to classify the particles according to their equivalent circle diameter. Indicatively, five of the processed SEM micrographs and the resulting histogram are presented in Fig. 68. The histogram represents the average number of particles in each class found in all processed images. The red squares in the same plot are the average equivalent circle diameter in each class.

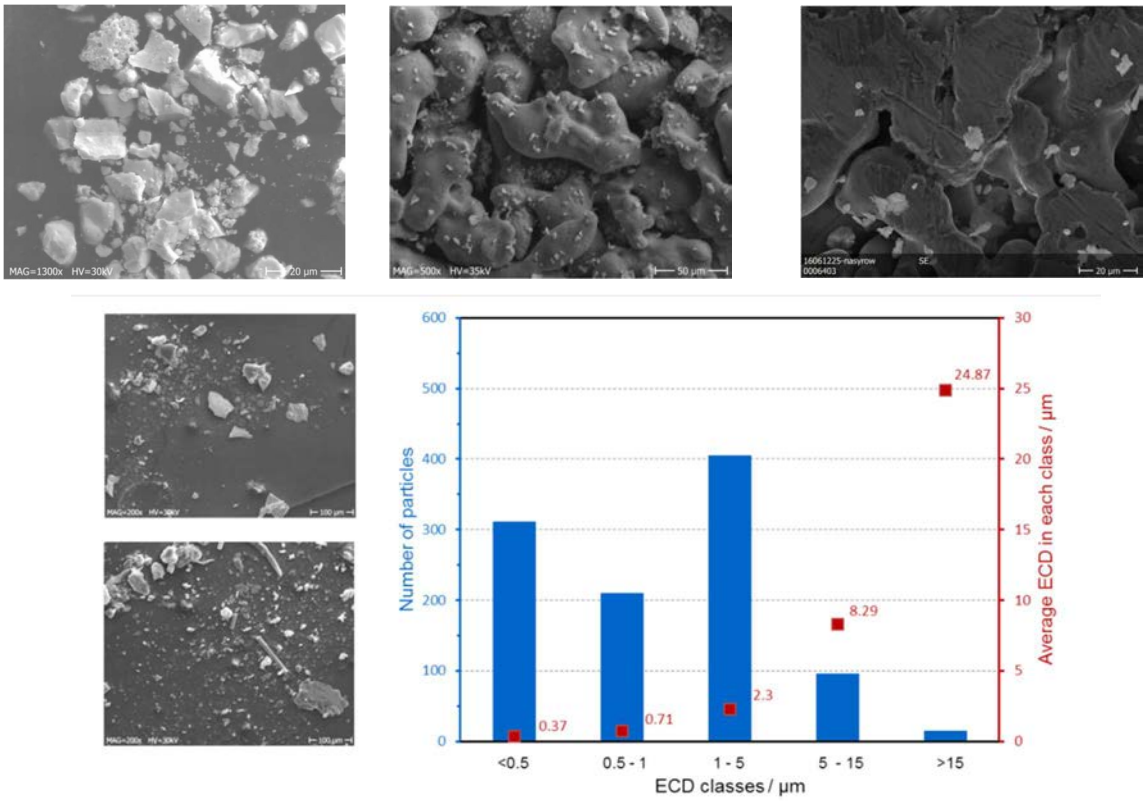

FIG. 68. SEM micrographs of particles released after bending and histogram with their average population of each size class (courtesy of JRC-Karlsruhe/Framatome/Nagra/EPFL).

II.9. NUMERICAL ANALYSIS OF THE TESTS

Numerical investigations via finite element analysis were performed to contribute towards a better understanding of the SNF rod mechanical response under bending stresses. The main objective of this activity is the development and calibration of finite element models against the experimental results to derive effective mechanical properties of the SNF rods. The final product of this study would be the development of a macroscale fuel assembly, including its structural parts, to investigate its mechanical integrity in various loading conditions (normal and/or accidental scenarios) for different fuel cycle back-end activities, namely fuel storage, transportation, handling and encapsulation in final disposal canisters.

A stepwise approach was followed to derive the effective mechanical properties of the composite fuel–cladding system. Therefore, the rod has been modelled initially as 1) a simple beam element and then 2) integrating an explicit description of fuel and cladding. Since the experimental results describe macroscopically the mechanical behaviour of the rod, the simple beam element directly simulates the experimental results and the model can be calibrated against them. The mechanical properties derived are restricted to the specific type of fuel rod

used in the experimental tests. To broaden the numerical results to different types of fuel design, the tests were simulated and validated again by considering explicitly the cladding and the fuel pellets. A sensitivity analysis was performed to identify the driving parameters and the relative influence of different phenomena to the rod's mechanical response, such as pellet-clad gap size, clad thickness, and pellet positioning.

The ANSYS mechanical tool is used for the development of the finite element models. Due to the difference in strain rate and boundary conditions (load application) between the three-point bending and the impact test, two different models were created for the simulation of the two mechanical tests. For the displacement driven three-point bending test, a step-motor is used to slowly drive the former onto the sample by applying quasi-static loads, whereas in the gravitational impact test dynamic loads are applied to the sample by the free-fall movement of the hammer. Therefore, 3D static structural models have been developed using the implicit and transient analysis (including inertia effects) for the bending and impact case, respectively.

The analogue studies with the use of the unirradiated but hydrogenated sample rods are used as the basis for the development and calibration of the finite element models. The highly inhomogeneous material properties and geometrical configuration of SNF rods do not enable a direct investigation of individual phenomena (e.g. pellet–cladding mechanical interaction (PCMI), zirconium hydride orientation and/or concentration). In contrast, the 'cold-test' campaign is conducted with materials having well-known properties, which facilitates a deeper understanding of the phenomena involved during the tests governing the mechanical response of the rodlets.

The model involves large deformation effects and it is highly non-linear. As seen from the three-point bending test results, even the SNF rods with high burnup experience plastic deformation. In this situation, the analysis evolves from linear (elastic behaviour) to non-linear (elastoplastic behaviour). Therefore, the selection of various model parameters might introduce numerical uncertainties that could potentially influence the results. For the derivation of a final model, a sensitivity analysis was performed to address the importance of different parameters, such as the contact method, the element type and mesh quality, the friction coefficient, the material laws, the boundary conditions, and many others. The numerical results are compared against the experiment and the focus was on specific outcomes, such as the CPU time, maximum stresses at cladding and pellets and maximum contact pressure and penetration. The final model is derived as the best compromise between the simulation time and the numerical accuracy. As a result, the pellets are modelled as cylindrical solid elements with flexible behaviour.

Quasi-static loads were applied by assigning a maximum deflection to the former in accordance with the experimental results. The model was calibrated against the experimental results with the use of the optiSLang tool, an ANSYS integrated software package for sensitivity analysis and optimisation.

Figure 69 provides the pellet–cladding equivalent (von-Mises) stresses for a deflection of 15 mm (right) at the symmetry z-plane, where a snapshot of the rod bending is shown on the left. It is noticed that the maximum stresses are developed at the inner cladding surface subjected to tension (opposite to the deflector) and the pellet-pellet interphase closest to the applied load (symmetry z-plane). This explains the importance of the pellets position in conjunction to crack initiation and demonstrates the weakest points that might endanger the cladding integrity.

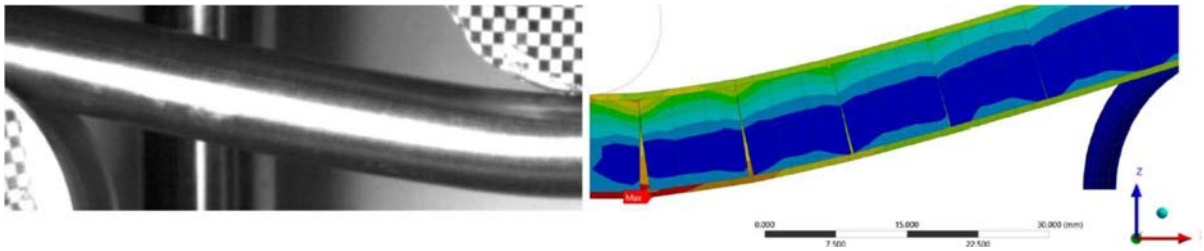

FIG. 69. Equivalent (von-Mises) stresses at a rod displacement of 1.5 mm at the symmetry z-plane. Maximum stress indication at the inner clad surface subjected in tension and at the closest pellet–pellet interphase to the theoretical maximum applied load (symmetry plane) (courtesy of JRC-Karlsruhe/Framatome/Nagra/EPFL).

REFERENCES

[1] INTERNATIONAL ATOMIC ENERGY AGENCY, Behaviour of Spent Fuel Assemblies During Extended Storage (Final Report of a Co-ordinated Research Programme on Befast, Phase 1, 1981-1986), IAEA-TECDOC-414, IAEA, Vienna (1987).

[2] INTERNATIONAL ATOMIC ENERGY AGENCY, Extended Storage of Spent Fuel (Final Report of a Co-ordinated Research Programme, (BEFAST-II), 1986–1991)), IAEA-TECDOC-673, IAEA, Vienna (1992).

[3] INTERNATIONAL ATOMIC ENERGY AGENCY, Further Analysis of Extended Storage of Spent Fuel, BEFAST-III, IAEA-TECDOC-944, IAEA, Vienna (1997).

[4] INTERNATIONAL ATOMIC ENERGY AGENCY, Spent Fuel Performance Assessment and Research, IAEA-TECDOC-1343, IAEA, Vienna (2003).

[5] INTERNATIONAL ATOMIC ENERGY AGENCY, Spent Fuel Performance Assessment and Research: Final Report of a Coordinated Research Project (SPAR-II), IAEA-TECDOC-1680, IAEA, Vienna (2012).

[6] INTERNATIONAL ATOMIC ENERGY AGENCY, Spent Fuel Performance Assessment and Research: Final Report of a Coordinated Research Project on Spent Fuel Performance Assessment and Research (SPAR-III) 2009-2014, IAEA-TECDOC-1771, IAEA, Vienna (2015).

[7] INTERNATIONAL ATOMIC ENERGY AGENCY, Behaviour of Spent Power Reactor Fuel during Storage, Extracts from the Final Reports of Coordinated Research Projects on Behaviour of Spent Fuel Assemblies in Storage (BEFAST I–III) and Spent Fuel Performance Assessment and Research (SPAR I–III) 1981—2014, IAEA-TECDOC-1862, IAEA, Vienna (2019).

[8] INTERNATIONAL ATOMIC ENERGY AGENCY, Demonstrating Performance of Spent Fuel and Related Storage System Components during Very Long Term Storage, IAEA-TECDOC-1878, IAEA, Vienna (2019).

[9] OFFICE PARLEMENTAIRE D'ÉVALUATION DES CHOIX SCIENTIFIQUES ET TECHNOLOGIQUES, The 2006 programme act on the sustainable management of radioactive materials and wastes, Programme Act No. 2006-739 of 28 June 2006, Assemblée Nationale, Paris (2006).

[10] BUNDESGESETZBLATT, Act on the Peaceful Utilisation of Atomic Energy and the Protection Against its Hazards (Atomic Energy Act), BGBl. I 2002, Bundesgesetzblatt 26 (2002) 1351–1359.

[11] BUNDESMINISTERIUM FÜR UMWELT, NATURSCHUTZ UND NUKLEARE SICHERHEIT, Joint Convention on the Safety of Spent Fuel Management and on the Safety of Radioactive Waste Management, Report of the Federal Republic of Germany for the Sixth Review Meeting in May 2018, BMU, Berlin (2017).

[12] BUNDESGESETZBLATT Gesetz zur Neuordnung der Verantwortung in der Kerntechnischen Entsorgung vom 27. Januar 2017, BGBL. I 2017, Bundesgestezblatt 5 (2017) 114–129.

[13] ENTSORGUNGKOMMISSION, ESK Guidelines for Dry Cask Storage of Spent Fuel and Heat-Generating Waste, Recommendation of the Nuclear Waste Management Commission (ESK), revised version of 10.06.2013.

[14] ENTSORGUNGKOMMISSION, ESK Guidelines for the performance of periodic safety reviews and on technical ageing management for storage facilities for spent fuel and heat-generating radioactive waste, Recommendation of the Nuclear Waste Management Commission (ESK) of 13.03.2014, (2014).

[15] ENTSORGUNGKOMMISSION, ESK Discussion paper on the extended storage of spent fuel and other heat-generating radioactive waste, Discussion paper of the Nuclear Waste Management Commission (ESK) of 29.10.2015, (2015).

[16] WORLD NUCLEAR NEWS, Expansion of Wolsong used fuel store approved, World Nuclear News (10 January 2020).

[17] MINISTERIO DE INDUSTRIA, TURISMO Y COMERCIO, Sixth General Radioactive Waste Plan (6th GRWP), Ministerio De Industria, Turismo Y Comercio, Madrid (2006).

[18] FEDERAL ASSEMBLY OF THE SWISS CONFEDERATION, Nuclear Energy Act of 21 March 2003, RS3 732.1, Federal Assembly of the Swiss Confederation, Bundesamt für Bauten und Logistik BBL, Bern (2003).

[19] SWISS FEDERAL DEPARTMENT OF ENERGY, Sectoral plan for deep geological repositories - conceptual part, Department of Environment, Transportation, Energy and Communication, SFOE, Bern (2008).

[20] EIDGENÖSSISCHES NUKLEARSICHERHEITSINSPEKTORAT, Joint Convention on the Safety of Spent Fuel Management and on the Safety of Radioactive Waste Management, Sixth National Report of Switzerland in Accordance with Article 32 of the Convention, Brugg (2017).

[21] UNITED STATES DEPARTMENT OF ENERGY, Sixth national report for the joint convention on the safety of spent fuel management and on the safety of radioactive waste management, USDOE, Washington D.C. (2017).

[22] UNITED STATES NUCLEAR REGULATORY COMMISSION, Safety Evaluation Report Related to Disposal of High-Level Radioactive Wastes in a Geologic Repository at Yucca Mountain, Nevada, Rep. NUREG-1949, USNRC, Washington DC (2015).

[23] UNITED STATES NUCLEAR REGULATORY COMMISSION, Supplement to the U.S. Department of Energy's Environmental Impact Statement for a Geologic Repository for the Disposal of Spent Nuclear Fuel and High-Level Radioactive Waste at Yucca Mountain, Nye County, Nevada, Rep. NUREG-2184, USNRC, Washington DC (2016).

[24] JOHNSON, L.H., MCGINNES, D.F., Partitioning of radionuclides in Swiss power reactor fuels, Technical Report 02-07, Nagra, Wettingen (2002).

[25] STANDRING, P.N., “The Long-term Storage of Advanced Gas-Cooled Reactor (AGR) Fuel”, Storage of Spent Fuel from Power Reactors – Proceedings of a symposium held in Vienna, 9–13 November 1998, IAEA-TECDOC-1089, IAEA, Vienna (1999).

[26] HAMBLEY, D., "Examination of Long Stored AGR Fuel Cladding", Poster A0139 presented at TopFuel 2015: Reactor Fuel Performance, 13–17 September 2015, Zurich, Switzerland.

[27] PHUAH, C.H., Corrosion of thermally-aged Advanced Gas-Cooled Reactor fuel cladding, PhD Thesis, Imperial College, London (2012).

[28] NORRIS, D., BAKER, C., TITCHMARSH, J., Radiation induced sensitisation of stainless steels, Proc. Symp. Radiation Induced Sensitisation of Stainless Steels, Berkley National Laboratories, United Kingdom (1986) 86.

[29] NORRIS, D., BAKER, C., TITCHMARSH, J., A study of radiation sensitisation of 20/25/Nb steel by compositional profile measurements at grain boundaries, Proc. Int. Conf. on materials for nuclear reactor core applications, British Nuclear Energy Society, **1** (1987) 277.

[30] TAYLOR, C., The formation of sensitised microstructures during the irradiation of CAGR fuel pin cladding, Proc. Symp. on Radiation Induced Sensitisation of Stainless Steels, Berkeley Nuclear Laboratory, United Kingdom, (1986) 60–73.

[31] HAMBLEY, D.I., "Technical Basis for Extending Storage of the UK's Advanced Gas-Cooled Reactor Fuel", Proc. Global 2013: International Nuclear Fuel Cycle Conference – Nuclear Energy at a Crossroads, Paper 7722, American Nuclear Society, La Grange Park, IL (2013).

[32] INTERNATIONAL ATOMIC ENERGY AGENCY, Safety of Nuclear Power Plants: Design, IAEA Safety Standards Series No. SSR-2/1, IAEA, Vienna (2012).

[33] MUTELLE H. et al, "A new research program on accidents in spent fuel pools: the DENOPI project", Proc. Water Reactor Fuel Performance Meeting (WRFPM), Sendai, Japan, 14–17 September 2014, Paper No. 100071 (2014).

[34] WAS, G.S., Fundamentals of Radiation Materials Science, Springer-Verlag, Berlin, Heidelberg (2007).

[35] FLEUROT, J., et al., Synthesis of spent fuel pool accident assessments using severe accident codes, Ann. of Nucl. Energy, 74 (2014) 58–71.

[36] EINZIGER, R.E., STRAIN, R.V., Oxidation of Spent Fuel at Between 250 and 400°C, Rep. EPRI-NP-4524, EPRI, Palo Alto, CA (1986).

[37] EINZIGER, R.E., STRAIN, R.V., Behavior of Breached Pressurized Water Reactor Spent-Fuel Rods in an Air Atmosphere between 250 and 360°C, Nucl. Technol., 75 (1986).

[38] HANSON, B.D., Clad Degradation - Dry Unzipping, ANL-EBS-MD-000013, Civilian Radioactive Waste Management Service - Management and Operations, Las Vegas, NV (2000).

[39] HANSON, B.D., et al., Fuel-in-air FY07 summary report, Rep. PNNL-17275, PNNL, Richland, WA (2008).

[40] FERRY C., et al., Synthesis on the spent fuel long term evolution, Rapport CEA-R-6084, CEA Saclay, Gif-Sur-Yvette (2005).

[41] BOUFFIOUX P., et al., Hydride reorientation in M5® cladding and its impact on mechanical properties, Proc. 2013 LWR Fuel Performance Meeting TopFuel 2013, 15–

19 September 2013, Charlotte, NC, American Nuclear Society, La Grange Park, IL (2013) 879–886.

[42] INSTITUT DE RADIOPROTECTION ET DE SÛRETÉ NUCLÉAIRE, Revue Actis n°26 2017, IRSN, Fontenay-aux-Roses (2017) (in French).

[43] GUILBERT-BANTI S., et al., Influence of hydrogen on the oxygen solubility in Zircaloy-4, J. Nucl. Mater. 469 (2016) 228–236.

[44] ELLS, C.E., Influence of Hydrogen on the behaviour of zirconium alloys in CANDU reactors, The Metallurgical Society of Canadian Institute of Metals, Annual Volume (1978) 32–44.

[45] DOMIZZI, G., Influencia del hidrógeno sobre aleaciones base circonio, PhD thesis, Universidad Nacional de San Martín, Buenos Aires (2002) (in Spanish).

[46] DOMIZZI, G., VIGNA, G., BERMUDEZ, S., OVEJERO-GARCÍA, J., Hydride distribution around a blister in Zr-2.5Nb pressure tubes, J. Nucl. Mat. **275** (1999) 255–267.

[47] SAUX, M. LE, BESSON, J., CARASSOU, S., A model to describe the mechanical behavior and the ductile failure of hydrided Zircaloy-4 fuel claddings between 25°C and 480°C, J. Nucl. Mater. **466** (2015) 43–55.

[48] DESQUINES, J., DROUAN, D., PHILIPPE, M., A new model on radial hydride precipitation in Zircaloy-4 claddings under decaying stress and temperature transient, Proc. Int. Conf on the Management of Spent Fuel from Nuclear Power Reactors 2015, IAEA, Vienna (2019).

[49] DALLONGEVILLE, M., ISSARD, H., LEONI, E., ZEACHANDIRIN, A., Transport of spent fuel after dry storage, Nuclear Engineering International, July 2014, 23–25.

[50] ZEACHANDIRIN, A., DALLONGEVILLE, M., PURCELL, P., CORY, A., Description of Fuel Integrity Project Methodology Principles, Packaging, Transport, Storage & Security of Radioactive Material 22 4 (2011) 184–191.

[51] HONG, J-D., KIM, E., YANG, Y-S., KOOK, D-H., Mechanical Property Degradation of Unirradiated Zircaloy-4 Cladding After Creep Deformation, Nucl. Technol., **203** 3 (2018) 282–292.

[52] HONG, J-D., KIM, E., KIM, S. G., YANG, Y-S., KOOK, D-H, Zircaloy-4 cladding degradation tests under simulated dry storage conditions - creep and delayed hydride cracking, Presented at International High-Level Radioactive Waste Management Meeting 2019, April 14-18, 2019, Knoxville Convention Center, Knoxville, TN.

[53] REY, J.M., "Resultados y lecciones aprendidas del Proyecto de I+D sobre Integridad del material de vaina irradiado con hidruración severa en condiciones de almacenamiento y transporte", CSN R&D Annual Meeting (2018).

[54] MARTIN RENGEL, M.A., RUIZ, J., et al., "Ring compression testing of prehydrided PWR cladding with hydride blisters", Global 2019 International Nuclear Fuel Cycle Conference / Top Fuel 2019 Light Water Reactor Fuel Performance Conference, American Nuclear Society, La Grange Park, IL (2019).

[55] MARTIN-RENGEL, M.A. RUIZ-HERVAIS, J., GOMEZ-SANCHEZ, F.J., RICO, A., RODRIGUEZ, J., “Determination of the Mechanical Properties of Blisters by Nanoindentation”, Proc. Top Fuel 2016, American Nuclear Society, La Grange Park, IL (2016).

[56] INTERNATIONAL ATOMIC ENERGY AGENCY, Regulations for the Safe Transport of Radioactive Material, 2018 Edition, IAEA Safety Standards Series No. SSR-6 (Rev.1), IAEA, Vienna (2018).

[57] KALININA, E., et al., “I+D para estudiar las vibraciones del combustible nuclear gastado durante su transporte”, ESTRATOS Magazine, No. 121. January 2019 48–56 (in Spanish).

[58] FERNÁNDEZ, F.J., et al, “Dry cask monitoring at José Cabrera NPP”, Presented at EPRI ESCP Winter 2016 Meeting, 29 November – 1 1 December 2016, Charlotte, NC.

[59] NATIONALE GENOSSENSCHAFT FÜR DIE LAGERUNG RADIOAKTIVER ABFÄLLE, The Nagra research, development and demonstration (RD&D) plan for the disposal of radioactive waste in Switzerland, Technical Report 16-02, Nagra, Wettingen (2016).

[60] EIDGENÖSSISCHES NUKLEARSICHERHEITSINSPEKTORAT, Reaktorkern, Brennelemente und Steuerelemente: Auslegung und Betrieb., ENSI Guidelines G20, ENSI, Brugg (2015) (in German).

[61] VLASSOPOULOS E., et al., "Destructive tests for determining mechanical integrity of spent nuclear fuel rods", Proc. 16th Int. High-Level Radioactive Waste Management Conf. (IHLRWMC 2017), April 9-13, 2017, Charlotte, NC, American Nuclear Society, La Grange Park, IL (2017).

[62] GONG, W., MILLE, M., ZUBLER, R., BERTSCH, J., Anisotropic influence of hydrides on Zircaloy fatigue, Global 2019 International Nuclear Fuel Cycle Conference / Top Fuel 2019 Light Water Reactor Fuel Performance Conference, American Nuclear Society, La Grange Park, IL (2019).

[63] VALANCE, S., BERTSCH, J., Hydrides reorientation investigation of high burnup PWR fuel cladding, J. Nucl. Mater. **464** (2015) 371–381.

[64] VALANCE, S., et al, Hydrogen relocation kinetics within zircaloy cladding tubes, Presented at TopFuel 2015: Reactor fuel performance, 13–17 September 2015, Zurich, Switzerland.

[65] GONG, W., TRTIK, P., ZUBLER, R., BERTSCH, J., Stress induced hydrogen redistribution in zircaloy measured by high resolution neutron imaging, Presented at 2017 Water reactor fuel performance meeting, 10–14 September 2017, Jeju, Korea.

[66] GONG, W., TRTIK, P., VALANCE, S., BERTSCH, J., Hydrogen diffusion under stress in zircaloy: High resolution neutron radiography and finite element modelling, J. Nucl. Mater. **508** (2018) 459–464.

[67] COLLDEWEIH, A.W., GONG, W., ZUBLER, R., BERTSCH, J., TRTIK, P., Influence of cracking direction during DHC of zircaloy-2 cladding, Presented at TopFuel 2019, 22–27 September 2019, Seattle, CA.

[68] ALYOKHINA, S., GOLOSHCHAPOV, V., KOSTIKOV, A., MATSEVITY, Y., Simulation of thermal state of containers with spent nuclear fuel: multistage approach, Int. J.Energy Res. **39** 14 (2015) 1917–1924.

[69] ALYOKHINA, S., KOSTIKOV, A., Unsteady heat exchange at the dry spent nuclear fuel storage, Nucl. Eng Technol. **49** (2017) 1457–1462.

[70] ALYOKHINA, S., KAPUZA, S., KOSTIKOV, A., Solar Radiation Influence on the Spent Nuclear Fuel Dry Storage Container, Voprosy Atomnoj Nauki i Tekhniki **114** 2 (2018) 57–62.

[71] ALYOKHINA, S., Thermal Analysis of Certain Accident Conditions of Dry Spent Nuclear Fuel Storage, Nucl. Eng Techol., **50** 5 (2018) 717–723.

[72] HAMBLEY, D., "Dry Storage of Irradiated Stainless Steel Clad Fuel", Proc. Global 2015: Nuclear fuel cycle for a low-carbon future, Société Française d'Énergie Nucléaire, Paris (2015) Paper 5099.

[73] WISS, T., et al, Evolution of spent nuclear fuel in dry storage conditions for millennia, J. Nucl. Mat. **451** (2014) 198–206.

[74] RAYNAUD, P., EINZIGER, R., Cladding stress during extended storage of high burnup spent nuclear fuel, J. Nucl. Mater. **464** (2015) 304–312.

[75] WALTERS, W.S., DURHAM, P., HODGE, N., The adsorption of water from a carbonaceous deposit layer on the surface of stainless steel representing spent AGR nuclear fuel cladding, J. Nucl. Sci. Technol. **55** (2017) 374–385.

[76] ELECTRIC POWER RESEARCH INSTITUTE, High Burnup Dry Storage Cask Research and Development Project Final Test Plan, Revision 0, EPRI, Palo Alto, CA (2014).

[77] BRYAN, C.R., JAREK, R.L., FLORES, C., LEONARD, E., Analysis of Gas Samples Taken from the High Burnup Demonstration Cask, Rep. SAND2019-2281, Sandia National Laboratories, Albuquerque, NM (2019).

[78] UNITED STATES NUCLEAR REGULATORY COMMISSION, Standard Review Plan for Renewal of Specific Licenses and Certificates of Compliance for Dry Storage of Spent Nuclear Fuel, Rep. NUREG-1927 Rev. 1, USNRC, Rockville, MD (2016).

[79] CENTER FOR NUCLEAR WASTE REGULATORY ANALYSES, Extended Storage and Transportation: Evaluation of Drying Adequacy, CNRWA, San Antonio, TX (2013).

[80] ELECTRIC POWER RESEARCH INSTITUTE, High-Burnup Used Fuel Dry Storage System Thermal Modeling Benchmark: Round Robin Results, Rep. EPRI-3002013124, EPRI, Palo Alto, CA (2020).

[81] MAHERAS, S. et al., Preliminary Evaluation of Removing Used Nuclear Fuel from Shutdown Sites, Rep. SFWD-IWM-2017-000024, PNNL-22676 (Rev. 10), PNNL, Richland, WA (2017).

[82] AREVA FEDERAL SERVICES, Initial Site-Specific De-Inventory Report for Big Rock Point, Rep. RPT-3014537-002, Areva Federal Services, Richland, WA (2017).

[83] AREVA FEDERAL SERVICES, Initial Site-Specific De-Inventory Report for Connecticut Yankee, Rep. RPT-3014538-002, Areva Federal Services, Richland, WA (2017).

[84] AREVA FEDERAL SERVICES, Initial Site-Specific De-Inventory Report for Humboldt Bay, Rep. RPT-3015142-004, Areva Federal Services, Richland, WA (2017).

[85] AREVA FEDERAL SERVICES, Initial Site-Specific De-Inventory Report for Kewaunee, Rep. RPT-3019262-000, Areva Federal Services, Richland, WA (2017).

[86] AREVA FEDERAL SERVICES, Initial Site-Specific De-Inventory Report for Maine Yankee, Rep. RPT-3016127-002, Areva Federal Services, Richland, WA (2017).

[87] AREVA FEDERAL SERVICES, Initial Site-Specific De-Inventory Report for Trojan, Rep. RPT-3016128-002, Areva Federal Services, Richland, WA (2017).

[88] INTERNATIONAL ATOMIC ENERGY AGENCY, Storage of Spent Nuclear Fuel, IAEA Safety Standards Series No. SSG-15 (Rev. 1), IAEA, Vienna (2020).

[89] SARRÓ, I.M., Biofouling on austenitic stainless steels in spent nuclear fuel pools, Mater. Corros. **54** (2003) 535–540.

[90] TIŠÁKOVÁ, L., et al., Bioaccumulation of 137Cs and 60Co by bacteria isolated from spent nuclear fuel pools, J. Radioanal. Nucl. Chem. **295** (2013) 737–748.

[91] ELECTRIC POWER RESEARCH INSTITUTE, Evaluation of Boral® Coupons from Zion Spent Fuel Pool, Rep. EPRI-3002008195, EPRI, Palo Alto, CA (2016).

[92] ELECTRIC POWER RESEARCH INSTITUTE, Evaluation of BORAL® Panels from Zion Spent Fuel Pool and Comparison to Zion Coupons, EPRI-3002008196, EPRI, Palo Alto, CA (2016).

[93] AKKURT, H., FEUERSTEIN, S., HARRIS, M., BAKER, S., "Overview of Zion Comparative Analysis Project for Assessment of Boral Neutron Absorber Material Performance and Monitoring in Spent Fuel Pools," Proc. of International Criticality Nuclear Safety Conference (ICNC 2015), Charlotte, NC, September 2015, ANS, La Grange Park, IL (2015).

[94] AKKURT, H., WONG, E., "Industrywide global efforts toward long term monitoring of neutron absorber materials in spent fuel pools", Proc. Int. Conf. on Management of Spent Fuel from Nuclear Power Reactors 2019, IAEA, Vienna (2020).

[95] ELECTRIC POWER RESEARCH INSTITUTE, Roadmap for the Industrywide Learning Aging Management Program (i-LAMP): For Neutron Absorber Materials in Spent Fuel Pools, Rep. EPRI-3002013122 EPRI, Palo Alto, CA (2018).

[96] AKKURT, H., "Overview of EPRI Research on Evaluation of Long Term Performance of Neutron Absorber Material Performance in Spent Fuel Pools" Proc. 17th International High-Level Radioactive Waste Management Conference, (IHLRWMC 2019), Knoxville, TN, Curran Associates Red Hook, NY (2019).

[97] AKKURT, H., QUIGLEY, A., HARRIS, M., "Accelerated Corrosion Tests to Evaluate the Long-Term Performance of BORAL® in Spent Fuel Pools", Proc. 19th Int. Symp. Packaging and Transportation of Radioactive Materials, PATRAM 2019, 4–9 August, 2019, New Orleans, LA, Curran Associates, Red Hook, NY (2019).

[98] ELECTRIC POWER RESEARCH INSTITUTE, Evaluation of the Impact of Neutron Absorber Material Blistering and Pitting on Spent Fuel Pool Reactivity, Rep. EPRI-3002013119, EPRI, Palo Alto, CA (2018).

[99] ELECTRIC POWER RESEARCH INSTITUTE, Extended storage collaboration program international subcommittee report, International perspectives in technical data gaps associated with extended transportation of used nuclear fuel, Rep. EPRI-1026481, EPRI, Palo Alto, CA (2012).

[100] ELECTRIC POWER RESEARCH INSTITUTE, Extended Storage Collaboration Program (ESCP): Progress Report and Review of Gap Analyses, Rep. EPRI-1022914, EPRI, Palo Alto, CA (2011).

[101] ELECTRIC POWER RESEARCH INSTITUTE, Failure Modes and Effects Analysis (FMEA) of Welded Stainless Steel Canisters for Dry Cask Storage Systems, Rep. EPRI-3002000815, EPRI, Palo Alto, CA (2013).

[102] ELECTRIC POWER RESEARCH INSTITUTE, Flaw Growth and Flaw Tolerance Assessment for Dry Cask Storage Canisters, Rep. EPRI-3002002785, EPRI, Palo Alto, CA (2014).

[103] ELECTRIC POWER RESEARCH INSTITUTE, Literature Review of Environmental Conditions and Chloride-Induced Degradation Relevant to Stainless Steel Canisters in Dry Cask Storage Systems, Rep. EPRI-3002002528, EPRI, Palo Alto, CA (2014).

[104] ELECTRIC POWER RESEARCH INSTITUTE, Calvert Cliffs Stainless Steel Dry Storage Canister Inspection, Rep. EPRI-1025209, EPRI, Palo Alto, CA (2014).

[105] WALDROP, K., Dry Storage Canister Inspections to Inform Aging Management Efforts, Proc. 15th Int. High-Level Radioactive Waste Management Conf. (IHLRWM 2015), 12-16 April 2015, Charleston, NC, American Nuclear Society, La Grange Park, IL (2015).

[106] ELECTRIC POWER RESEARCH INSTITUTE, Diablo Canyon Stainless Steel Dry Storage Canister Inspection, Rep. Rep. EPRI-3002002822, EPRI, Palo Alto, CA (2016).

[107] ELECTRIC POWER RESEARCH INSTITUTE, Susceptibility Assessment Criteria for Chloride-Induced Stress Corrosion Cracking (CISCC) of Welded Stainless Steel Canisters for Dry Cask Storage Systems, Rep. EPRI-3002005371, EPRI, Palo Alto, CA (2015).

[108] ELECTRIC POWER RESEARCH INSTITUTE, Aging Management Guidance to Address Potential Chloride-Induced Stress Corrosion Cracking of Welded Stainless Steel Canisters, Rep. EPRI-3002008193, EPRI, Palo Alto, CA (2017).

[109] THOMAS, R.N., et al., Permeability of observed three dimensional fracture networks in spent fuel pins, J. Nucl. Mater. **510** (2018) 613–622.

[110] RONDINELLA, V., et. al., Measurement of gas permeability along the axis of a spent fuel rod, Proc. TopFuel 2015: Reactor Fuel Performance, Sep 13–17, 2015, Zurich, Switzerland, European Nuclear Society, Brussels (2015).

[111] SANDIA NATIONAL LABORATORIES, Data Analysis of ENSA/DOE Rail Cask Tests, Rep. SFWD-SFWST-2018-000494, SNL, Albuquerque, NM (2018).

[112] ASSOCIATION OF AMERICAN RAILROADS, Standard S-2043, Performance Specification for Trains Used to Carry High-Level Radioactive Material (2017).

[113] SVENSK KÄRNBRÄNSLEHANTERING AB, RD&D Programme 2019, Programme for research, development and demondatration of methods for the management and disposal of nuclear waste, TR-19-24, SKB, Stockholm (2019) 117–179.

[114] VLASSOPOULOS E., et al., Investigation of the properties and behaviour of spent nuclear fuel under conditions relevant for interim dry storage, handling and transportation: experimental setup optimisation and cold test campaign, NAGRA Arbeitsbericht NAB 16-67, March 2017.

[115] ARBORELIUS J., et al., The Effect of Duplex Cladding Outer Component Tin Content on Corrosion, Hydrogen Pick-up and Hydride Distribution at Very High Burnup, Zirconium in the Nuclear Industry: Fourteenth Int. Symp., (RUDLING P., KAMMENZIND B., Eds), ASTM International, West Conshohocken, PA (2004).

[116] PSHENICHNIKOV A., STUCKERT J., WALTER M., Microstructure and mechanical properties of Zry-4 cladding hydrogenated at temperatures typical for loss-of-coolant accident (LOCA) conditions, Nucl. Eng. Des. **283** (2015), 33–39,

[117] RONDINELLA V.V., WISS T., PAPAIOANNOU D., NASYROW R., Studies on nuclear fuel evolution during storage and testing of used fuel response to impact loadings, Proc. PSAM11 ESREL 2012, 25–29 June 2012, Helsinki, Finland 8 vols, Curran Associates, Red Hook, NY (2012) 3171–3179.

[118] NASYROW R., et al., Bending Test Device for Mechanical Integrity Studies of Spent Nuclear Fuel Rods, Proc. PATRAM 2016 Kobe (Japan), Institute of Nuclear Materials Management, Mount Laurel, NJ (2016).

[119] VLASSOPOULOS E., et al., Mechanical Integrity of Used Nuclear Fuel: From Experimental to Numerical Studies, Proc. 2018 Reactor Fuel Performance Meeting TopFuel 2018, Paper No. A0129, 30 September – 4 October 2018, Prague, Czech Republic, European Nuclear Society, Brussels, Belgium (2018).

[120] RONDINELLA, V.V., NASYROW, R., PAPAIOANNOU, D. VLASSOPOULOS, E., CAPPIA, F., et al, “Mechanical integrity studies on spent nuclear fuel rods”, Proc. Proc. 16th International High-Level Radioactive Waste Management Conference (IHLRWMC 2017) 9–13 April 2017, Charlotte, NC, Curran Associates, Red Hook, NY (2017) 734–740.

ANNEX – RESEARCH PROJECTS WITHIN THE SPAR-IV CRP

A-1. MATERIALS DEGRADATION ASSESSMENT OF POWER REACTORS SPENT FUEL DURING LONG INTERIM DRY STORAGE

COUNTRY: Argentina

CHIEF SCIENTIFIC INVESTIGATOR: G. Domizzi

AGREEMENT NUMBER: 20912

COMPANY: CNEA

BACKGROUND: During the course of the coordinated research project 'Demonstrating performance of spent fuel and related storage system components during very long term storage', the probability of cladding degradation occurring in the Atucha-I NPP ASECQ facility was evaluated. Several different mechanisms were considered, namely oxidation, fission product induced stress corrosion cracking, mechanical failure and hydrogen effects. Of all of these, only the latter remained as a concern. Whenever hydrogen concentration in zircaloy exceeds the terminal solid solubility for precipitation (TSSP), hydrides may precipitate. This is indeed the case for Atucha-I spent fuel, where end-of-life pick up may range between 100 and 200 wt ppm. Hydrogen concentration could be higher if ingress of water into the pin has happened due to any type of failure, Even the in-reactor deterioration or limited removal of the cladding external oxide is enough to produce an increase.

A thorough data review led to the conclusion that the hydrogen effect is only relevant if radial hydrides are produced (55 ppm is critical). Hydrides in the normal precipitation plane in the absence of stresses do not generate ductility reduction below 700 ppm, whereas the maximum expected hydrogen concentration would be around 200 ppm. Expected in-storage stresses are lower than the 100 MPa needed to re-orient hydrides. However, there is a chance for reorientation due to the stress fields originated by the presence of flaws, among them, rims and blisters. These would not break under the low stress expected fields, but they do generate hydride reorientation and act as initiators for DHC cracks. During dry storage, fuel temperatures will initially increase, bringing a higher amount of hydrogen in solution out of existing hydrides, to slowly decrease later; this constitutes the optimal situation to make DHC cracks to grow, what could end up producing a pin failure, a non-acceptable situation for this facility. It is important, then, to fully evaluate if this can happen.

OBJECTIVES: To determine whether spent fuel failure due to DHC is possible during long term dry storage, due to hydride reorientation produced by the stress field generated by hydride blisters present in the spent fuel element cladding. If this mechanism can be proven to occur, then the work is expected to generate sufficient data to establish the threshold conditions for the onset of this phenomenon, in order to decide whether it can occur in the specific case of the ASECQ Facility of Atucha-I NPP.

RESEARCH APPROACH: An experimental programme is being conducted, with the purpose of evaluating the possibility of having DHC cracks generated during dry storage at the Atucha-I ASECQ Facility, out of cladding surface defects such as hydride blisters or rims. Once the reorientation feasibility is confirmed, efforts will be concentrated on establishing threshold conditions (applied stress, blister/rim size, temperature, hydrogen concentration, cooling speed etc.) in order to compare them with the facility working values. From this evaluation, it will be possible to decide whether fuel integrity may be jeopardized by this phenomenon.

Experiments are performed using sections of Zircaloy-4 cladding, previously hydrided (using a gaseous atmosphere loading method) to several concentrations, ranging from 100–250 wt ppm. Hydride blisters are grown on the sections using a cold finger attached to the surface, thus producing a cold spot to which the hydrogen may migrate until the concentration is high enough to produce a massive hydride precipitation. One of the tasks is to optimize the cold finger, with respect to material, size and other aspects. In some other samples, a ring of palladium (1–2 μm in thickness) will be electrodeposited prior to H_2 charging, in order to produce a hydride rim (50 μm in depth) on the outer side of the tube.

After blister/rim formation, a Hydride Reorientation Test (HRT) will be performed, consisting of a pressurized tube test at temperature for various periods of time, ranging from a few weeks to a few months or rupture of the specimens, whichever happens first. Finally, the specimens will be sectioned and metallographically analysed looking for the presence of radial hydrides. Some blisters will be cut without HRT in order to compare the aspect with those that were subjected to HRT. Test parameters will be adjusted in order to obtain clear DHC evidence, then they will be gradually modified to approach storage conditions; internal pressure 80 bar, test temperature 180–200°C.

A-2. CHARACTERIZATION OF HYDRIDE CONTENT AS A FUNCTION OF ACCUMULATED NEUTRON FLUX AND OPERATING TEMPERATURE IN THE PCA-S ALLOY (ZRY-4 WITH LOW TIN CONTENT)

COUNTRY: Argentina

CHIEF SCIENTIFIC INVESTIGATOR: P. Vizcaino

AGREEMENT NUMBER: 20549

COMPANY: CNEA

BACKGROUND: The effects of neutron radiation on the microstructure and hydrogen behaviour in zirconium alloys has been one of the main activities of the group for 25 years. Characterization of Zircaloy-4 and Zr-2.5 Nb alloys from neutron irradiated nuclear components was and still is one of the aims of the Zirconium Alloys Technology Department. The study of the degradation of the mechanical properties of structural materials such as fuel channels helps to understand the conditions at which the spent fuel starts degrading after long periods in dry storage installations.

Two research lines have been developed over the past 15 years:

1. Effects of the neutron irradiation on the terminal solid solubility;

2. Effects of the neutron irradiation on the microstructure.

One of the main tasks of our laboratory is the evaluation of the microstructural degradation processes of the zirconium alloys in service. Many publications on the topic are available.

RESEARCH APPROACH: The aim of the project is to characterize the degradation level of a zirconium alloy at different stages of its life in service. The knowledge of microstructural parameters such as:

- Hydrogen content;
- Hydride distribution in the bulk alloy;
- Hydride orientation;
- Oxide layer thickness;
- Internal stresses due to neutron irradiation plus fission products gas release;
- Dislocation density, type of dislocations;
- Other microstructural transformations.

The initial approach is to characterize the evolution of hydrogen content as a function of the time in service at similar temperature conditions, the hydride distribution along the width of the channel for the different in-service conditions, and similar analyses for the oxide layer thickness.

PUBLICATIONS

The following papers were published during the course of the project and fully document the findings:

1. VICENTE ALVAREZ, M.A., SANTISTEBAN, J.R., VIZCAÍNO, P., FLORES, A.V., BANCHIK, A.D., ALMER. J., Hydride reorientation in Zr2.5Nb studied by synchrotron X-ray diffraction, Acta Mater. **60** (2012) 6892–6906.

2. VIZCAÍNO, P., SANTISTEBAN, J.R., VICENTE ALVAREZ, M.A., BANCHIK, A.D., ALMER. J., Effect of crystallite orientation and external stress on hydride precipitation and dissolution in Zr2.5%Nb, J. Nucl. Mater. **447** (2014) 82–93.

3. VICENTE ALVAREZ, M.A., SANTISTEBAN, J.R., VIZCAÍNO, P., RIBARIK, G., UNGAR, T., Quantification of dislocations densities in zirconium hydride by X-ray line profile analysis, Acta Mater. **117** (2016) 1–12.

4. VICENTE ALVAREZ, M.A., SANTISTEBAN, J.R., DOMIZZI, G., ALMER, J., J. Acta Mat., Phase and texture analysis of a hydride blister in a Zr–2.5%Nb tube by synchrotron X-ray diffraction, Acta Mater **59** (2011) 2210–2220.

5. VIZCAÍNO, P., FLORES, A. V., BOZZANO, P. B., BANCHIK, A. D., VERSACI, R. A., RÍOS, R. O. XVI ASTM Int. Symp. of the zirconium in the Nuclear Industry. Chengdu, Sichuan Province, P.R. China, May 9–13, 2010.

6. VICENTE ALVAREZ, M. A., SANTISTEBAN, J. R., DOMIZZI, G., OKASINSKI, J., ALMER, J., Elastic strain tensor of zirconium hydrides in Zr2.5%Nb pressure tubes by synchrotron X-ray diffraction J. Appl. Cryst. **52** (2019) 1128–1143

7. VIZCAINO, P., FLORES, A. V., VICENTE, M. A., SANTISTEBAN, J. R., DOMIZZI, G., TOLLEY, A., CONDÓ, A., ALMER, J., XIX ASTM International Symposium of the zirconium in the Nuclear Industry. Manchester, United Kingdom, May 20–23, 2019. *Accepted for publication as a STP (Selected Technical Paper) of the Symposium.*

A-3. CONTRIBUTION TO THE EVALUATION OF STORAGE SYSTEM AND USED FUEL DURING STORAGE

COUNTRY: France

CHIEF SCIENTIFIC INVESTIGATOR: H. Issard

AGREEMENT NUMBER: 20544

COMPANY: Orano TN

RESEARCH APPROACH: Gathering information on the experience of spent fuel and storage system components performance in Orano TN storage systems. Evaluation of potential degradation of spent fuel and cask materials under storage conditions.

A-4. SPENT WWER-440 FUEL PERFORMANCE UNDER LONG-TERM STORAGE CONDITIONS

COUNTRY: Hungary

CHIEF SCIENTIFIC INVESTIGATOR: F. Takáts

AGREEMENT NUMBER: 20361

COMPANY: TS Enercon

BACKGROUND: Hungary presently operates 4 units of the Paks NPP. There are spent fuel storage pools at each reactor and a Modular Vault Dry Storage (MVDS) adjacent to the plant. In the beginning of the plant's operation, spent fuel was transported to the Soviet Union (later Russia) for reprocessing, but this practice was stopped in the 1990s.

Spent fuel is removed from the pools after about 5 years of cooling, while the design lifetime of the MVDS is 50 years. Behaviour of the spent fuel both in wet and dry conditions is an important aspect of the reliable operation of the plant. Various monitoring programmes are in place, but Hungary is also benefitting from studying international spent fuel storage experience.

Because of the above, a continuation of the IAEA's SPAR research programme provides a review of the results from monitoring and research activities on a wider scale, and could help address the implication of fuel design changes on storage requirements.

RESEARCH APPROACH: Looking to capture data on both wet and dry storage aspects at Paks NPP.

- Wet storage: collection and systematic evaluation of data on both spent fuel and pool components.
- Dry storage: collection and systematic evaluation of data of spent fuel data gathered during:
    - Transfer from the AR pool to MVDS;
    - Measurements during the drying process (e.g. crud release);
    - Measurements of spent fuel conditions during storage;
    - In the event of a transfer back to the AR pool, rewetting experience.

A-5. RODS AND ASSEMBLY BASED NUCLEAR FUEL INTEGRITY EVALUATION FOR DRY STORAGE AND TRANSPORTATION

COUNTRY: Republic of Korea

CHIEF SCIENTIFIC INVESTIGATOR: D. Kook

AGREEMENT NUMBER: 20703

COMPANY: KAERI

BACKGROUND: The Republic of Korea is transitioning its fuel into dry storage due to delays to the repository plan. Spent fuel characterization and integrity evaluation are essential for the dry storage licensing process to obtain public confidence in the safety of long-term operations. For the first 5 years, R&D will be focused on the lower burnup fuel range, of which 80% of the current spent fuel inventory is in. After this, successive R&D will be focussed on higher burnup fuels. The project balances the work scope on both fuel rod and assembly testing. Collaboration and communication with experts involved will be a useful contribution to this research.

RESEARCH APPROACH: The primary objective of the research is to characterize domestic spent fuel. The secondary objective is to anticipate the safety of long term spent fuel dry storage by several single effect tests and DrySim6 evaluation. The anticipated outcomes are spent fuel characterization data and methodologies to ensure spent fuel integrity during storage and handling.

A-6. WWER-440 WET STORAGE FACILITY STRUCTURAL MATERIALS PERFORMANCE IN JASLOVSKÉ BOHUNICE

COUNTRY: Slovakia

CHIEF SCIENTIFIC INVESTIGATOR: M. Brezina

AGREEMENT NUMBER: 20561

COMPANY: VUJE

BACKGROUND: Surveillance samples have been kept in the spent fuel interim storage (SFIS) pool in Jaslovské Bohunice and monitored on an annual basis. The samples are used to infer the current conditions of the SFIS pool lining and the ATABOR steel used to fabricate the compact racks in use. An additional area of work is characterization of biofilms formed on the surface of the SFIS pools.

RESEARCH APPROACH: Corrosion behaviour of the pool and rack materials is estimated by analysis of surveillance samples. This analysis includes the determination of corrosion rates and analysing any localised corrosion attack on the prepared samples.

The biofilms recovered along with the samples will also be analysed.

A-7. SPENT FUEL MECHANICAL BEHAVIOUR DURING LONG TERM STORAGE AND TRANSPORTATION

COUNTRY: Spain

CHIEF SCIENTIFIC INVESTIGATOR: M. Navarro

AGREEMENT NUMBER: 20456

COMPANY: ENRESA

BACKGROUND:

According to the 6th General Radioactive Waste Plan (GRWP) in force, the strategy document for radioactive waste management in Spain, spent fuel will have to be gathered in a Centralized Temporary Storage (CTS) for some decades prior to any further decision. A 7th GRWP is being drafted with similar views, but including a revised NPP shutdown schedule, with revised SNF inventory, accordingly. ENRESA is actively supporting, alone or with other partners, a number of R&D programmes on interim dry storage and transportation, mostly concerned about high burnup fuel issues, fuel-with-defects management, and ageing management.

OBJECTIVE:

- Review of spent fuel data relevant for future storage in Spain;
- Perform destructive and non-destructive examinations on irradiated and non-irradiated fuel rods relevant to Spanish spent fuel management, which includes long term storage and transportation to a CTS.

RESEARCH APPROACH:
Among the programmes initiated in the last few years (already finished or about to be finished), the following ones are highlighted and presented within SPAR-IV:

- Mechanical testing on irradiated spalled fuel rods and un-irradiated surrogate samples to support safe management of spalled fuel and its classification as undamaged fuel;
- Participation in international projects in support of safe transportation of spent fuel: Multi-modal transportation test (truck, rail and ship) of a transport cask with dummy assemblies to verify normal conditions of transport;
- Dry cask temperature monitoring on site, in support of ageing management plans.

RESULTS

Spent fuel management is an important issue for fuel cycle costs. Any method for optimizing the storage and transport of spent fuel produces increasing profits to nuclear industry. Many of the limits in the regulatory guidance related to spent fuel management (i.e. storage and transportation systems) have not followed the evolution of increasing fuel burnup discharge, new materials, and new designs.

Spanish SNF strategy considers the transportation of SNF to a Centralized Temporary Storage (CTS) Facility for long term storage prior to direct disposal, avoiding keeping a relatively large number of facilities at NPP sites to store SNF, to optimize SNF management. Therefore,

transport and storage regulations are both considered in the design and licensing of systems used in Spain.

One particular issue present in a number of fuel assemblies operated in Spanish PWRs is spalling of Zry-4 cladding oxide. Indeed, at medium-to-high burnup, Zry-4 can develop relatively thick oxide layers that can spall off the cladding, creating a cold spot in the cladding beneath. This cold spot might mobilize hydrogen within the cladding due to temperature gradients, increasing hydrogen concentration at the cold spot and precipitating in the form of thick zirconium hydrides, called blisters. Due to the known brittle behaviour of hydrogen precipitates, blisters can affect cladding behaviour, decreasing the remaining thickness able to withstand stresses that could arise under off-normal storage or transport conditions (i.e. accident conditions). A project involving CSN (nuclear regulatory body), Enusa (fuel supplier) and Enresa (waste management organization), with the support of Spanish utilities, included a combined set of mechanical tests and analysis of irradiated samples and unirradiated surrogate samples with the aim of characterizing spalled cladding behaviour. With the analysis performed in parallel, a group of fuel assemblies was accepted as undamaged to be included among the contents of a storage and transportation system used at a Spanish site. It is planned to go on working to increase the number of spalled fuel assemblies undergoing this analysis so that more of them can be classified as undamaged.

Apart from characterizing the SNF behaviour, it is important to characterize the SNF systems used for its management (storage and/or transportation). For this reason, Enresa has also supported projects in relation to transport conditions and ageing management of systems used in Spain. For the former, Enresa has actively participated in an international multi-modal transport test to assess normal conditions of transport by land (truck and rail) and sea (ship) led by US laboratories and with participation of other US, Korean and Spanish partners. An instrumented cask loaded with surrogate fuel assemblies was sent for testing in realistic normal conditions. Data was obtained for transport and handling operations and compared with irradiated fuel properties. For the latter, a temperature monitoring system based on optical fibres was tested at a Spanish ISFSI. The feasibility of the system was verified. Thermal profiles were obtained and compared with models of the storage system.

A-8. SPENT FUEL INVESTIGATIONS AT DRY STORAGE CONDITIONS FOR SAFE TRANSPORT AND ENCAPSULATION IN GEOLOGICAL REPOSITORY

COUNTRY: Switzerland

CHIEF SCIENTIFIC INVESTIGATOR: S. Caruso

AGREEMENT NUMBER: 22482

COMPANY: NAGRA

BACKGROUND: Experimental investigations are being undertaken at JRC Karlsruhe on mechanisms potentially affecting the physical/chemical state and the mechanical integrity of spent nuclear fuel and cladding during transport and handling, along with the possible consequences of loss of integrity due to rod failure and the release of radionuclides.

RESEARCH APPROACH: The main scientific goal is to develop the capability to assess the impact of potential deterioration mechanisms on fuel and spent fuel storage components, in the context of spent fuel handling and transport operations for final disposal. Particular attention will be given to a comprehensive identification and characterization of the material released in consequence of the breaking of a fuel rod with attention to decontamination issues.

The experimental campaign includes bending and fracture tests on LWR spent fuel rods. Relevant macroscopic and microstructure properties of spent fuel and cladding are studied, including the characterization of amount and particle size distribution of the fuel released during the impact tests. In addition to Nagra, JRC and École polytecnique fédérale de Lausanne (EPFL) are collaborating, with indirect support from Areva and Gösgen NPP.

A-9. THE DEVELOPMENT OF A DATABASE FOR NUMERICAL ESTIMATION OF TEMPERATURES INSIDE STORAGE CASKS WITH SPENT NUCLEAR FUEL

COUNTRY: Ukraine

CHIEF SCIENTIFIC INVESTIGATOR: S. Alyokhina

AGREEMENT NUMBER: 20605

COMPANY: A.M. Pidgorny Institute of Mechanical Engineering Problems

BACKGROUND: Thermal processes play a key role during all periods of spent fuel storage. There is no effective methodology for the physical measurement or numerical calculation of temperatures inside a storage cask containing spent nuclear fuel. In the first case, it is not possible to organize an effective measuring system that will give detailed information about the temperature of the fuel rods for a large number of storage casks without the risk of depressurization. In the latter, a large number of intensive calculations are required, which does not enable online monitoring of cask temperatures or to be able to take into account all outer influences. This project is based on the development of a multi-stage methodology of thermal state calculation that considerably decreases the calculation time. This methodology is planned for usage at Project calculation and includes solving of the direct and inverse heat transfer problems.

RESEARCH APPROACH: The overall objective of the project is the development of an information base for the numerical estimation of thermal state of storage casks and the nuclear fuel inside at various operating conditions. It is necessary to collect the main thermal data (for example, the maximum temperatures in each fuel assembly, the maximum temperatures on the cask surface, temperatures pattern inside storage cask, etc.) for typical storage casks with spent fuel assemblies of different types of power reactors. The effective safety assessment and development of spent fuel management programmes require scientific analysis of storage systems and their components at any operational conditions. So, the thermal analysis has to be made for typical casks storage conditions which include normal operation (the natural convection cooling without additional external influences) and accident conditions. Analysis and generalization of all storage conditions and their transformation to the thermal conditions will be carried out. For some operational conditions, it will require solving of the inverse heat transfer problems because there are no known temperatures and heat transfer coefficients for storage cask surfaces. Finally, the thermal data will be collected for typical construction of storage casks under various operating conditions. On the basis of this information, the thermal stress calculations, numerical estimation of degradation mechanisms and control of ageing processes will be possible to do without additional thermal simulation. The results of Project will allow to organize effective surveillance and monitoring programmes of spent fuel storage facilities.

A-10. CONDITION MONITORING RELEVANT TO LONG-TERM WET STORAGE OF ADVANCED GAS-COOLED REACTOR FUEL

COUNTRY: United Kingdom

CHIEF SCIENTIFIC INVESTIGATOR: D. Hambley

AGREEMENT NUMBER: 20849

COMPANY: NNL

BACKGROUND: The AGR fuel storage regime will transition from interim storage followed by reprocessing, to long term storage followed by disposal. The research focuses on issues related to long-term wet storage and preparation of the fuel for direct disposal.

The research objectives are:

- To determine whether or how modern operating conditions (increased burnup, fuel shuffling, reactor rating changes) affect AGR fuel's susceptibility to corrosion during wet storage;

- To determine how, if the fuel fails during wet storage, water ingress will occur and affect subsequent drying.

This research will show whether modern operating conditions have changed the total volume or axial position of fuel susceptible to intergranular attack. This can inform decisions relating to the packaging of fuel for storage. The results will also indicate the total quantity of water that is to be dried and how drying occurs. The modelling results will aid decisions on techniques for drying the fuel for disposal.

RESEARCH APPROACH: The research objectives will be fulfilled by:

- Characterization using microscopy to investigate location, extent and degree of radiation-induced segregation (RIS). These results will be compared to reactor operating conditions and investigation of historic fuel to determine how modern operating conditions may alter the susceptibility of AGR cladding to intergranular attack.

- The total water carryover and subsequent drying of pins that have failed during storage will be measured.

- Modelling techniques will be developed to model water ingress and flow through pellets.

A-11. DEVELOPMENT OF INTERIM STORAGE FOR SPENT AGR FUEL

COUNTRY: United Kingdom

CHIEF SCIENTIFIC INVESTIGATOR: S. Clarke

AGREEMENT NUMBER: 20684

COMPANY: Sellafield Ltd

BACKGROUND: The proposed research is intended to support the underpinning for wet interim storage of advanced gas-cooled reactor (AGR) fuel awaiting geological disposal. There are two key aspects to the work:

- Hot cell characterization of irradiated fuel post irradiation and post storage;
- Full scale corrosion testing of irradiated fuel using an in-pond test rig to study the margins to the planned storage water chemistry and assess the storage performance of higher irradiated fuel.

RESEARCH APPROACH: To develop the technical underpinning of AGR interim wet storage, the following aspects will be addressed:

- Increase confidence in the storage regime by establishing the condition of spent AGR fuel after 25 years storage in sodium hydroxide dosed conditions and establish acceptable margins in pool water chemistry (in terms of pH and chloride concentration);
- Characterization of long stored failed fuel and establish its evolution over 25 years of storage;
- Demonstration of wet storage of higher burnup fuel and establish the characteristics of fuel cladding in terms of effects of increased time at elevated temperature and increased neutron dose on radiation-induced segregation.

A-12. US INDUSTRY SPENT NUCLEAR FUEL MANAGEMENT (R&D AND OPERATING EXPERIENCE) – CONTRIBUTIONS TO SPAR PHASE IV

COUNTRY: United States of America

CHIEF SCIENTIFIC INVESTIGATOR: K. Waldrop

AGREEMENT NUMBER: 20448

COMPANY: Electric Power Research Institute (EPRI)

BACKGROUND: In the USA, it is highly likely that commercial spent nuclear fuel will need to be stored for many decades until either reprocessing or a final disposal site becomes available. The use of dry storage is now in widespread use: about one third of the USA spent fuel inventory is now stored in dry, inert atmosphere systems. Currently available information has enabled several utilities to obtain license extensions for up to 60 years for spent fuel with assembly-average burnup less or equal to 45 GWd/tU. A confirmatory project for spent fuel with assembly-average burnup greater than 45 GWd/tU is presently being conducted at the Dominion's North Anna site under sponsorship by the US Department of Energy (DOE) and EPRI. Based on the expected successful completion of this project, the US Nuclear Regulatory Commission (USNRC) has recently granted a conditional license extension to 60 years for some systems containing spent fuel with burnup greater than 45 GWd/tU. However, given the persistent uncertainty with regard to the availability of other options for managing spent fuel, it may be necessary to store spent fuel for longer than 60 years. The R&D projects that are part of the proposed SPAR-IV CRP will emphasize the technologies that need to be considered for extended storage, such as ageing management of storage system structures, systems and components and long term spent fuel (with emphasis on cladding) performance.

RESEARCH APPROACH: Problems to be addressed during the project include:

- Chloride induced stress corrosion cracking (CISCC) is a potential degradation mechanism for austenitic stainless-steel canisters currently used in dry cask storage systems. Overall objectives for research on this topic are:
    - Assessment of the potential for CISCC to lead to confinement breach;
    - Prevention of through-wall CISCC cracks in canisters.
- Collection of high burnup fuel performance confirmatory data. Overall objectives for this tope are:
    - Thermal benchmarking;
    - Fuel integrity monitoring during dry system loading operations (including fuel drying) and initial storage period.

A-13. US INDUSTRY SPENT NUCLEAR FUEL MANAGEMENT (R&D AND OPERATING EXPERIENCE) – CONTRIBUTIONS TO SPAR PHASE IV

COUNTRY: United States of America

CHIEF SCIENTIFIC INVESTIGATOR: B. Bevard

AGREEMENT NUMBER: 23525

COMPANY: Oak Ridge National Laboratory (ORNL)

BACKGROUND: In the USA, it is highly likely that commercial spent nuclear fuel will need to be stored for many decades until either reprocessing or a final disposal site becomes available. The use of dry storage is now in widespread use: about one third of the USA spent fuel inventory is now stored in dry, inert atmosphere systems. Currently available information has enabled several utilities to obtain license extensions for up to 60 years for spent fuel with assembly-average burnup less or equal to 45 GWd/tU. A confirmatory project for spent fuel with assembly-average burnup greater than 45 GWd/tU is presently being conducted at the Dominion's North Anna site under sponsorship by the US Department of Energy (DOE) and EPRI. Based on the expected successful completion of this project, the US Nuclear Regulatory Commission (USNRC) has recently granted a conditional license extension to 60 years for some systems containing spent fuel with burnup greater than 45 GWd/tU. However, given the persistent uncertainty with regard to the availability of other options for managing spent fuel, it may be necessary to store spent fuel for longer than 60 years. The R&D projects that are part of the proposed SPAR-IV CRP will emphasize the technologies that need to be considered for extended storage, such as ageing management of storage system structures, systems and components and long term spent fuel (with emphasis on cladding) performance.

RESEARCH APPROACH: Spent Nuclear Fuel (SNF) degradation during drying, long term storage, and transport are key issues where data to support modelling and licensing is insufficient. Determining the SNF mechanical and thermal properties and how those properties change over time is critical for supporting extended periods of interim dry storage prior to final disposal in a repository. Also, understanding dry storage canister performance during extended interim storage is also critical for this activity.

Overall objectives:

(a) understand baseline SNF mechanical properties;

(b) determine what can affect SNF during drying and extended storage (and transportation);

(c) determine SNF mechanical/thermal properties as SNF ages in dry storage;

(d) understand how these changes can be modelled;

(e) determine potential impacts on Interim Storage Facilities;

(f) determine canister weld mechanical properties to support understanding of stress corrosion cracking.

LIST OF ABBREVIATIONS

AECL	Atomic Energy Canada Limited
AFR	away from reactor
AGR	advanced gas cooled reactor
AMP	ageing management programme
AR	at reactor
BADGER	boron-10 areal density gage for evaluating racks
BEFAST	behaviour of spent fuel assemblies in storage
BWR	boiling water reactor
CEA	Commissariat à l'Énergie Atomique et aux Énergies Alternatives
CFD	computational fluid dynamics
CISCC	chloride induced stress corrosion cracking
CNEA	Comisión Nacional de Energía Atómica
CRP	coordinated research project
CSFSF	centralized spent fuel storage facility
CSN	Consejo de Seguridad Nuclear
CTS	centralized temporary storage
DHC	delayed hydride cracking
DPC	dual purpose cask
DSS	dry storage system
EDF	Électricité de France
EPRI	Electric Power Research Institute
ENRESA	Empresa Nacional de Residuos Radiactivos, S.A.
ENSA	Equipos Nucleares S.A.
EPFL	École polytechnique fédérale de Lausanne
EPR	european pressurized water reactor
FBG	Fibre Bragg grating
FDC	final disposal container
FMEA	failure modes and effect analysis
GCR	gas cooled reactor
GRWP	general radioactive waste plan
HAW	higher activity waste
HLW	high level waste
HRT	hydride reorientation treatment
IGA	intergranular attack
IRSN	Institut de Radioprotection et de Sûreté Nucléaire
ISFS	interim spent fuel store
ISFSF	independent spent fuel storage facility
ISFSI	independent spent fuel storage installation
KAERI	Korean Atomic Energy Research Institute
LWR	light water reactor
MEB	multi element bottle
MOX	mixed oxide fuel
MVDS	modular vault dry store
Nagra	Nationale Genossenschaft für die Lagerung radioaktiver Abfälle
NNL	National Nuclear Laboratory
NPP	nuclear power plant
OECD-NEA	Organisation for Economic Cooperation and Development – Nuclear Energy Agency
PCT	peak cladding temperature

PHWR	pressurized heavy water reactor
PSR	periodic safety review
PWR	pressurized water reactor
R&D	research and development
RCM	research coordination meeting
RCT	ring compression test
RIS	radiation induced segregation
SCC	stress corrosion cracking
SEM	scanning electron microscope
SFA	spent fuel assembly
SFP	spent fuel pool
SNF	spent nuclear fuel
SPAR	spent fuel performance assessment and research
TEM	transmission electron microscope
TR&S	Thorp Receipt and Storage
TSC	transport and storage cask (Switzerland)
TSSD	terminal solid solubility dissolution
TSSP	terminal solid solubility precipitation
TTCI	Transportation Technology Center, Inc.
UOX	uranium oxide
USDOE	United States Department of Energy
USNRC	United States Nuclear Regulatory Commission
WWER	water water energetic reactor
VSC	ventilated storage container

CONTRIBUTORS TO DRAFTING AND REVIEW

Alyokhina, S.	A.M. Pidgorny Institute, Ukraine
Bevard, B.	Oak Ridge National Laboratory (ORNL), United States of America
Brezina, M.	VUJE, Slovakia
Caruso, S.	Nationale Genossenschaft für die Lagerung radioaktiver Abfälle (Nagra), Switzerland
Clarke, S.	Sellafield Limited, United Kingdom
Domizzi, G.	Comisión Nacional de Energía Atómica (CNEA), Argentina
Dus, J.	Eidgenössisches Nuklearsicherheitsinspektorat (ENSI), Switzerland
Einziger, R.	Nuclear Waste Technology Review Board (NWTRB), United States of America
Fernandez Lopez, J.	Empresa Nacional de Residuos Radiactivos, S.A. (Enresa), Spain
Gastl, C.	International Atomic Energy Agency
González Espartero, A.	International Atomic Energy Agency
Hambley, D.	National Nuclear Laboratory (NNL), United Kingdom
Hillier, A.	Sellafield Limited, United Kingdom
Issard, H.	Orano TN, France
Kook, D.	Korean Atomic Energy Research Institute (KAERI), Republic of Korea
Machiels, A.	Electric Power Research Institute (EPRI), United States of America
McManniman, L	International Atomic Energy Agency
Papaioannou, D.	Joint Research Centre Karlsruhe, European Commission
Petzova, J.	VUJE, Slovakia
Rowley, J.	Sellafield Limited, United Kingdom
Standring, P.N.	Sellafield Limited, United Kingdom
Takats, F.	TS Enercon, Hungary
Vizcaino, P.	Comisión Nacional de Energía Atómica (CNEA), Argentina
Vlassopoulos. E.	Nationale Genossenschaft für die Lagerung radioaktiver Abfälle (Nagra), Switzerland
Waldrop, K.	Electric Power Research Institute (EPRI), United States of America

Zencker, U.	Bundesanstalt für Materialforschung und -prüfung (BAM), Germany

Research Coordination Meetings

Vienna, Austria: 15–19 August 2016

Seoul, Republic of Korea: 9–13 April 2018

Buenos Aires, Argentina: 7–10 October 2019

Consultants Meetings

Vienna, Austria: 3–6 November 2015, 14–17 March 2017, 5–8 February 2019, 2–5 June 2020

IAEA
International Atomic Energy Agency

No. 26

ORDERING LOCALLY

IAEA priced publications may be purchased from the sources listed below or from major local booksellers.

Orders for unpriced publications should be made directly to the IAEA. The contact details are given at the end of this list.

NORTH AMERICA

Bernan / Rowman & Littlefield

15250 NBN Way, Blue Ridge Summit, PA 17214, USA
Telephone: +1 800 462 6420 • Fax: +1 800 338 4550

Email: orders@rowman.com • Web site: www.rowman.com/bernan

REST OF WORLD

Please contact your preferred local supplier, or our lead distributor:

Eurospan Group

Gray's Inn House
127 Clerkenwell Road
London EC1R 5DB
United Kingdom

Trade orders and enquiries:

Telephone: +44 (0)176 760 4972 • Fax: +44 (0)176 760 1640
Email: eurospan@turpin-distribution.com

Individual orders:

www.eurospanbookstore.com/iaea

For further information:

Telephone: +44 (0)207 240 0856 • Fax: +44 (0)207 379 0609
Email: info@eurospangroup.com • Web site: www.eurospangroup.com

Orders for both priced and unpriced publications may be addressed directly to:

Marketing and Sales Unit
International Atomic Energy Agency
Vienna International Centre, PO Box 100, 1400 Vienna, Austria
Telephone: +43 1 2600 22529 or 22530 • Fax: +43 1 26007 22529
Email: sales.publications@iaea.org • Web site: www.iaea.org/publications

International Atomic Energy Agency
Vienna